

Effective Fine Structure Constant

by

©Reefat

A Dissertation submitted to the School of Graduate Studies in partial fulfillment of
the requirements for the degree of

M.Sc.

Department of Physics and Physical Oceanography

Memorial University of Newfoundland

September 2019

St. John's

Newfoundland

Abstract

In this thesis, we use the dispersive approach to calculate the effective fine structure constant. In this calculation, a truncated self-energy and triangle topology is considered up to Next-to-Next to Leading Order (NNLO). We have used the dispersive approach for two-loop self energy to evaluate a NNLO (two loop) contributions and a result obtained is rather compact expressions using only two loop Passarino-Veltman function basis. For the triangle topology, we have used a bulk approximation technique. The numerical result was obtained using the LoopTools and ColliersLink packages in Mathematica.

Acknowledgements

I would like to gratefully acknowledge all the people who have been supporting and inspiring me throughout my life, especially while I was working on this thesis.

My deepest gratitude to my thesis supervisors, Dr. Aleksandrs Aleksejevs, Dr. Ivan Booth and Dr. Svetlana Barkanova whose constant guidance and enthusiasm kept me motivated to explore this challenging topic which I, at the beginning was vaguely acquainted with. Their instructions along with the courses that they taught shaped my knowledge and skills to accomplish this task.

With due respect, I would also like to acknowledge the faculty members of the Mathematics and Physics and Physical Oceanography Department for their lessons, guidance and various supports during the past years in Memorial University of Newfoundland. I am eternally grateful to Dr. Mahbub Majumdar and Dr. Khurshed Alam Kabir for his teachings and lessons during my college years.

I am greatly thankful for my parents who gave me hope and courage. Lastly, I am thankful to all the new people, especially Catherine, Shi hao, Junayed and Sheldon, I met here in Newfoundland who gave me the mental strength and support to cope in this new place. For these, I can walk on paths that are less traveled by. I hope, by what this journey offers, I can give back something that the world can cherish.

Table of Contents

Abstract	2
Acknowledgments	3
List of Tables	7
List of Figures	9
1 Introduction	10
1.1 The Standard Model	11
1.2 Fermions	13
1.2.1 Leptons	13
1.2.2 Quarks	14
1.3 Bosons	15
1.3.1 Gauge Bosons	15
1.3.2 Higgs Boson	16
1.4 Limitations of the Standard Model	16
1.5 Physics Beyond the Standard Model (BSM)	18
1.6 Precision Frontier	20
1.7 Mathematica	21

2	Theoretical Background	22
2.1	Feynman Diagrams: A General Overview	22
2.2	Feynman rules for QED	25
2.3	Passarino-Veltman Function	30
2.3.1	One-point and two-point scalar function	31
2.3.2	Vector Boson Self-Energy (QED only)	36
2.3.3	Three-point function	39
2.4	Renormalization of QED	41
2.4.1	Motivation for renormalization	41
2.4.2	Renormalization of ϕ^3 theory	42
2.4.3	Vacuum Polarization in Quantum Electrodynamics	44
2.5	One particle irreducible contribution(1P1)	51
2.6	Effective Feynman Propagator	52
2.7	The Dispersion Approach	54
2.7.1	Self-energy sub-loop dispersion representation	54
2.8	Renormalization in the Dispersion Approach	56
3	Results	59
3.1	Next to Leading Order (NLO) Correction	59
3.2	Next-to-the-Next Leading Order (NNLO) Correction	61
3.2.1	Two-loop self-energy topologies	63
3.2.2	Two-loop triangle topologies	66
3.3	Results	70
4	Conclusion	73
4.1	Summary of Results	73
4.2	Mathematica	73

4.3 Future Work	74
A Mathematica Notebook of the Calculations	76
Bibliography	107

List of Tables

1.1	The four fundamental forces and their corresponding gauge-bosons . .	15
3.1	The contributions of the Leptons in two-loop vacuum polarization function	65
3.2	The contributions of the Leptons and Quarks in two-loop vacuum polarization function	66
3.3	The contributions of all two-loop graphs in two-loop vacuum polarization function	66
3.4	The contributions of both NLO and NNLO in vacuum polarization function	67
3.5	Table showing the mean value for the Dirac form factor	69
3.6	Relative correction to the effective fine structure constant with NNLO contributions	71

List of Figures

1.1	The Standard Model of Particle Physics [10]	12
1.2	A pie-chart showing the matter contribution in the universe [12] . . .	17
1.3	Three frontiers of Physics [5]	19
2.1	General topology of a one-loop self energy diagram	24
2.2	General topology of a first order correctio to one-loop self-energy diagram	24
2.3	Feynman diagram for electron-muon scattering	28
2.4	One-loop N-point topology	30
2.5	Fermion self-energy diagram	31
2.6	Truncated vector boson self-energy diagram with incoming momentum k and mass m_1 and m_2	36
2.7	A general triangle topology with p_i are the incoming momenta and m_i represents the masses of the off-shell particles	39
2.8	One-loop Feynman diagram for ϕ^3 theory	42
2.9	A generic t-channel scattering diagram	43
2.10	A generic scalar bubble diagram	44
2.11	Feynman rules for counter-term Lagrangian	47
2.12	Photon self-energy diagram	48
2.13	Fermion self-energy diagram	49
2.14	One-Particle irreducible contribution (1PI)	52

2.15	Feynman diagram for Effective propagator	52
2.16	Examples of self-energy subloops	56
3.1	Feynman diagrams generated using FEYNARTS	60
3.2	One-loop level correction for the fine structure constant	62
3.3	Two-loop self-energy topologies ($\gamma \mapsto \gamma$)	63
3.4	Two-loop self-energy topologies ($\gamma \mapsto \gamma$)	64
3.5	Two-loop triangle topologies ($\gamma \mapsto \gamma$)	68
3.6	A general insertion for two-loop triangle topology	69
3.7	Dirac form-factor in eq: 3.2	70
3.8	Dirac form-factor in eq: 3.3	70
3.9	Dirac form-factor in eq: 3.4	70
3.10	Dirac form-factor in eq: 3.5	70
3.11	A triangle topology after substituting the insertion	71
3.12	Plot of the Effective Fine Structure Constant upto NNLO correction .	72

Chapter 1

Introduction

In quantum electrodynamics (QED) the coupling constant, α , the Thompson limit is the low energy limit known as the fine structure constant tells us about the strength of any electromagnetic interaction. Usually, it is considered as a constant and has been measured to have a numerical value of $\frac{1}{137}$. However, from renormalization theory we know that α is not really a constant; rather it is a function that depends on the total amount of momentum associated with the interaction. As a result, the strength of the coupling constant varies significantly with the energy of the associated particles (significantly in the GeV scale energy). In this thesis, we tried to calculate, theoretically, the correction of the fine structure constant. We evaluated the effective fine structure constant at different energies and have shown the sub-percent level correction to the Thomson limit.

In order to fully understand the underlying processes of how the effective fine structure constant is calculated, in this thesis, we will have to know about the Standard model of particle physics. Throughout this chapter, there will be a discussion of our understanding of the Standard model and its possibilities and limitations. Also, there will be a description of the software and the related packages that we have used for

modeling and calculating our results. All the physical theories associated with the calculations are discussed in-depth in the following chapter. We discussed the details of our results in the chapter after that. Finally, we concluded by discussing the possible uses of the calculations and the future directions of similar kind of calculations.

1.1 The Standard Model

An ancient Greek philosopher, Democritus, who lived around 460 B.C. summed up some philosophical views of the world and proposed the idea of atom - everything in the world is constructed by "something" which cannot be broken-down further. He believed that there are many different types of atoms which either attract each other or repel. Due to limitations of scientific knowledge at the time, he could not theorize about subatomic particles; yet, it was a milestone. In 1897, J.J. Thomson discovered the electron while studying the properties of the cathode ray which lead to the investigation of the subatomic particles. Consequently, the theories and discoveries of thousands of physicists since the 1930s have helped us gain a remarkable insight into the fundamental structure of matter. All of these developments in the field of particle physics lead physicist to propose the Standard model.

The Standard model of particle physics is one of the most successful theories of subatomic particles. It is capable of describing all interactions that subatomic particles undergo with the exception of gravity. Most of the theoretical development of the Standard model was concluded in the 1970s. It has been successful in explaining almost all experimental results and precisely predicted a wide variety of phenomena over the last decades. As a result, it is considered as one of the most well-tested physical theories of subatomic particles.

There are three generation of subatomic particles in the Standard model. They

Three generations of matter (fermions)					
	I	II	III		
mass →	2.4 MeV/c ²	1.27 GeV/c ²	171.2 GeV/c ²	0	? GeV/c ²
charge →	$\frac{2}{3}$	$\frac{2}{3}$	$\frac{2}{3}$	0	0
spin →	$\frac{1}{2}$	$\frac{1}{2}$	$\frac{1}{2}$	1	0
name →	u up	c charm	t top	γ photon	H Higgs boson
Quarks	4.8 MeV/c ²	104 MeV/c ²	4.2 GeV/c ²	0	
	$-\frac{1}{3}$	$-\frac{1}{3}$	$-\frac{1}{3}$	0	
	$\frac{1}{2}$	$\frac{1}{2}$	$\frac{1}{2}$	1	
	d down	s strange	b bottom	g gluon	
Leptons	<2.2 eV/c ²	<0.17 MeV/c ²	<15.5 MeV/c ²	91.2 GeV/c ²	
	0	0	0	0	
	$\frac{1}{2}$	$\frac{1}{2}$	$\frac{1}{2}$	1	
	ν_e electron neutrino	ν_μ muon neutrino	ν_τ tau neutrino	Z⁰ Z boson	
	0.511 MeV/c ²	105.7 MeV/c ²	1.777 GeV/c ²	80.4 GeV/c ²	
	-1	-1	-1	±1	
	$\frac{1}{2}$	$\frac{1}{2}$	$\frac{1}{2}$	1	
	e electron	μ muon	τ tau	W[±] W boson	
				Gauge bosons	

Figure 1.1: The Standard Model of Particle Physics [10]

could either be fermions or bosons. They all have an intrinsic property called the spin. Any subatomic particles that have half-integer spin (e.g. $\frac{1}{2}$ or $\frac{3}{2}$) are classified as fermions. On the other hand, any subatomic particles that have an integer spin (e.g. 1 or 2) are known as bosons. It is believed that all of the known universe is only made up of the first generation of fermions and bosons and that is widely supported by astrophysical data. Generally, fermions are associated with matter and bosons are force carriers in an interaction that the fermions participate. In a way, fermions are that "something" which the ancient Greek philosophers thought to be indestructible. All the fermions and bosons currently known and described by the Standard model are shown in figure 1.1.

1.2 Fermions

All quantum particles in nature have an associated intrinsic angular momentum like property which is known as the spin. Fermions are defined as particles with half integer spin (e.g. $\frac{1}{2}, \frac{3}{2}$). Moreover, fermions obey Pauli Exclusion Principle, which states that no two identical and bounded fermions can simultaneously occupy the same quantum state. For instance, for the electrons in an atom, to exist in the same orbital, they must have different spin values, typically known as spin up($+\frac{1}{2}$) or spin down($-\frac{1}{2}$). However, bosons does not exhibit the Pauli Exclusion Principle. According to the Standard model of particle physics, all fermions can be classified further as quarks and leptons, see figure 1.1. On the other hand, bosons include fundamental particles such as photons, gluons, and W and Z bosons which are force-carrying gauge bosons, Higgs boson and the hypothetical graviton of quantum gravity.

1.2.1 Leptons

Leptons, shown in figure 1.1, are fundamental particles in the Standard model that have half-integer spin and are classified to be fermions.

Fermions have several intrinsic properties such as electric charge, spin, and mass. They interact via electromagnetic interactions (exchange of photons), weak interactions (exchange of W^+, W^- and Z^0) or gravity (exchange of gravitons)¹. However, they do not take part in strong interactions-exchange of gluon. There are three generations of leptons which can either be charged or neutral and the mass of the leptons increases with the generation.

The charged leptons are electron, muon, and tau, and the neutral ones are electron neutrino, muon neutrino, and the tau neutrino. All three generations of neutrinos have

¹No experimental verification yet.

a very small mass and they only interact via the weak interaction. In fact, a single neutrino could travel through millions of kilometers of a material, like steel, without even being detected. As a consequence of this, neutrinos were discovered much later than other leptons in the Standard model. In 1930, Wolfgang Pauli proposed an undetectable particle which transferred energy when he was trying to explain missing energy in nuclear β -decay [3]. In 1956, Clyde Cowan and Fred Reines confirmed the existence of neutrinos via their experiment [4].

The second and third generation of charged leptons share similar properties to that of electrons. However, they are much more massive than electrons; consequently, they are very unstable because of spontaneous decay. Muon and tau leptons tend to decay into less massive particles in less than a microsecond.

1.2.2 Quarks

Quarks are fermionic particles in the Standard model having half-integer spin.

The existence of quarks was independently proposed by Murray Gell-Mann and George Zweig in 1963 [6] and in 1968 was experimentally verified at Stanford Linear Accelerator Center. The scattering of electron beams into liquid hydrogen revealed that protons and neutrons consist of even smaller particles- quarks [16].

Quarks interact via the strong interaction and form composite particles. Due to a phenomena called the color confinement, quarks are never found in isolation. Quarks are found in bound states known as hadrons. All the different types of quarks are shown in figure 1.1. The top quark is the most massive quark in the Standard model. It is 186 times the mass of a proton. Due to the uncertainty principle, the massive top quarks have much shorter life due to having higher energy and their tendency of spontaneous decay to be in a lower quantum state which prevents them from interacting with other quarks and form hadrons. Examples of hadrons include

Pion (π) and Kaon (K). Hadrons can be classified further into Baryons and Mesons.

Like leptons, the mass of quarks also increases with generation, i.e. the second generation of quarks are heavier than the first generation. Despite the mass difference between the generations, the interaction within each generation remain identical. They also have another property called the flavor. Each flavor of quarks also has three different color charges. In addition, all the quarks in the Standard model have their associated anti-quarks which have the same mass but opposite electrical charge.

1.3 Bosons

Fundamental particles are either bosons or fermions. Bosons are the particles that has integer spin. Unlike fermions, they do not obey Pauli Exclusion Principle which means bosons with same energy can occupy the same quantum state, thus allowing the bosons to be the mediator of any interaction.

Force	Relative Strength	Range (m)	Mediator	Theory
Strong	1	10^{-15}	Gluon	Chromodynamics
Electromagnetic	$\frac{1}{137}$	∞	Photon	Electrodynamics
Weak	10^{-6}	10^{-18}	W^+, W^- & Z^0	Flavordynamics
Gravitational	10^{-42}	$\frac{1}{r^2}$	Graviton ²	Geometrodynamics

Table 1.1: The four fundamental forces and their corresponding gauge-bosons

1.3.1 Gauge Bosons

There are four fundamental forces of nature. In order to quantize them gauge bosons were introduced in the Standard model. In classical field theory there is no need of a mediator particle for interactions to occur. On the contrary, in quantum field theory, any interactions are explained by the exchange of mediator particles of a particular theory. These mediator particles are the gauge bosons. In the classical view, inter-

actions occur at a single point and there is no need of a mediator particle. At low energies, the classical model of field theory gives us an accurate approximation. However, at high energies this model fails and eventually is replaced by the intermediate vector boson theory.

1.3.2 Higgs Boson

The Higgs boson plays an important role in the Standard model of particle physics. Unlike gauge bosons, the Higgs boson is the carrier of the Higgs field which is included in the theory as a mass gaining field. Only inside the Higgs field, all fundamental particles in the SM can get their respective masses. The idea of the Higgs particle was proposed around the 1960s- by three different working groups but it was only discovered in 2012 at CERN.

1.4 Limitations of the Standard Model

The Standard model of particle physics, as discussed above is the most successful theory that is capable of explaining a lot of the physical phenomena around us. However, there are a lot of observations that cannot be explained by the current version of the Standard model.

At first, let us take the example of the mass of the neutrinos. From experimental evidence, we have come to know that neutrinos have a non-vanishing mass, though their exact mass is yet to be discovered. In addition, we also know that they are abundant in nature. Consequently, we may expect them to contribute a fair share of the mass of the universe. As a result, they may play a significant role in the evolution of the universe. Moreover, experimental evidence suggests that there are interactions of both neutrinos and anti-neutrinos. We also know that neutrinos do not have charge;

therefore, the notion of having an anti-particle is controversial. Neutrino-oscillations is also a phenomena that has been observed but cannot be explained by the theory nor can they be explained by the Standard model.

The universe consists of ordinary matter which is made up from the sub-atomic particles existing in the Standard model [1.1](#). Scientists have estimated that the ordinary matter in the observable universe only accounts for roughly 4.9% of the total matter and energy. However, from astrophysical observations, the accelerating expansion of the universe, we know that there must be other kinds of matter and energy in the universe and their rough estimation is shown in figure [1.2](#). We also know that the Standard model of particle physics does not recognize the existence of dark matter or dark energy. Therefore, we can safely say that the Standard model of particle physics is not complete.

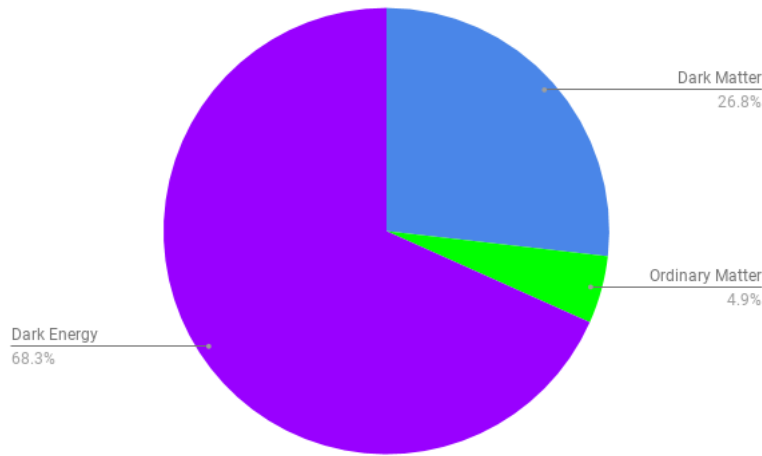


Figure 1.2: A pie-chart showing the matter contribution in the universe [12]

In addition, the existence of the hypothetical graviton is yet to be confirmed by experimental evidences. Moreover, at certain instances, the most successful theory of gravity, General Relativity, is incompatible with the Standard model.

Lastly, the matter-antimatter asymmetry is also a major drawback of the Standard

model. The universe is mostly made up of matter; however, from the predictions of the Standard model we expect them to be created in equal amounts just after the inflation in the early universe. From astrophysical observations, however, we know they are in disproportionate ratio; however, there is no mechanism in the Standard model to describe this.

We can clearly say that the Standard model is not a complete theory and in order to explain all the physical phenomena we observe, we need a theory that explains physics beyond the Standard model.

1.5 Physics Beyond the Standard Model (BSM)

The limitations of the Standard model (as discussed in the section 1.4) lead physicists to look for physics beyond the Standard model. Some of the theories that try to explain the limitations of the Standard model include various extensions to the theory such as Supersymmetry, String theory, M-theory, and a lot of mathematical models including extra dimensions. However, not all of these theories can be simultaneously correct. In the near future, physicists hope to find enough experimental evidence to support one of these theories that will be able to explain all of the observed physical phenomena.

Generally, there are three different ways of probing the physics beyond the Standard model; the Energy Frontier, the Cosmic Frontier and the Precision/ Intensity Frontier, shown in figure 1.3. The Energy frontier uses high-energy colliders, like the Large Hadron Collider (LHC) and others, to probe physics of the Standard model and beyond. They tend to look for the origin of mass which is partly revealed by the discovery of the Higgs boson. In addition, they look for the matter-anti-matter asymmetry, dark matter, unification of the forces, and new physics beyond the standard

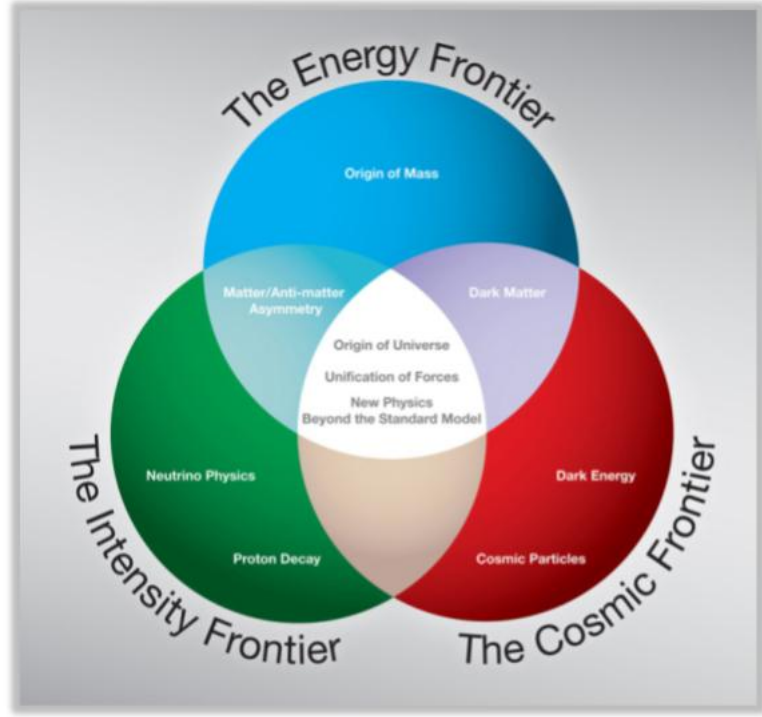


Figure 1.3: Three frontiers of Physics [5]

model.

The Cosmic Frontier is another way of unraveling all the unknown physical phenomena that is yet to be discovered. The people working in this frontier use underground experiments and ground-based and space-based telescopes to collect astronomical data. One such example would be Laser Interferometer Gravitational-Wave Observatory (LIGO) which recently discovered gravitational waves. Generally, they look for cosmic particles, try to get data that suggests the existence of dark energy, and consequently look for physics beyond the Standard model.

The Precision or the Intensity Frontier is the other group which tries to probe physics beyond the Standard model using intense particle beams and precise calculations of the cross-sections involved in the scattering process for a physical phenomena.

1.6 Precision Frontier

A number of theories describing the early universe predicted that there are many other particles which disappeared at the time after inflation. However, it is believed that those particles are now indirectly present as interaction carriers, and can be probed through precision measurements at low momentum transfer. In order to access the scale of the new physics at multi-TeV level, we need to push one or more experimental parameters such as asymmetry [2] to extreme precision. Few of the ongoing theoretical research to probe at these high precise level includes precision neutrino scattering, weak-electromagnetic interference (such as opposite parity transitions in heavy atoms), and parity-violating electron scattering.

From a theoretical perspective, the precise calculation can be achieved by extending the perturbation expansion of the scattering matrix element. However, the calculation of such a scattering matrix is highly involved. Since electroweak (EW) interactions usually have different mass-propagators and higher-order tensor Feynman integrals, even a two-loop EW calculation can become increasingly complicated. If we consider EW interactions, it is sometimes very challenging and even impossible to find analytical results beyond the one-loop level. This has lead us to use various approximations or purely numerical methods.

In this thesis, however, I have considered only quantum electrodynamics and kept my calculations only up to two-loop levels. In addition to various approximations, I have used several numerical methods and the Dispersion approach [1] to calculate the effective fine structure constant. I have intensively used MATHEMATICA for the purpose of my numerical calculations.

1.7 Mathematica

In this thesis, we have used Mathematica as the main language to code our calculations. In addition, we have extensively used three publicly available packages-FEYNARTS, FORMCALC and LOOPTOOLS [7] [8]. FEYNARTS was used to generate all the necessary Feynman diagrams. FEYNARTS is also capable of generating multi-loop topologies such as the vertex, box, etc.

FORMCALC uses an algorithm that has all the Feynman rules built-in for calculating the scattering matrix of a single Feynman diagram. In addition, it is also capable of combining all the scattering matrices of several Feynman diagrams. At the end of a calculation, the amplitude is given in Passarino-Veltman basis. Passarino-Veltman basis are discussed in more detail in chapter 2.3. However, FORMCALC only performs tree-level calculations and the algorithm is unable to calculate the scattering matrices for two-loop level topologies. Furthermore, FORMCALC has a built-in renormalization procedure for one-loop or tree-level topologies. For the purpose of doing two-loop topologies we used the renormalization scheme developed for EW in the paper [1]. However, we had to modify the renormalization scheme, shown in 2.8, because we have only considered quantum electrodynamics.

LOPTTOOLS is used in the last part of the calculation. It calculate all the numerical integration of the scattering matrices. It is a very powerful numerical tool to do Feynman integrals for one-loop topologies. However, it cannot perform two-dimensional Feynman integrals. We used the dispersion approach and converted the two-dimensional Feynman integrals to one-dimensional Feynman integrals. As a result, we were able to calculate our final result using LOOPTOOLS. Furthermore, there are some parameters in our Mathematica notebook that can also be used to test the divergences from FORMCALC and also the numerical stability of LOOPTOOLS.

Chapter 2

Theoretical Background

This chapter provides a general overview of the quantum field theories that are relevant for the understanding of the calculations.

2.1 Feynman Diagrams: A General Overview

One of the most important parts of any calculation in quantum field theory is the calculation of the S-matrix. This calculation involves a large number of convoluted integrals. However, upon close inspection, a repeated pattern appears in such calculations. These repeated patterns can be depicted by Feynman diagrams which are a general graphical representation that describes the interactions of the fundamental particles in the Standard model. The diagrams can be used to construct amplitudes for different scattering processes. One can easily associate field theories such as Quantum Electrodynamics (QED), Electroweak, etc. with Feynman diagrams in order to extract mathematical information that a Feynman diagram holds. Moreover, the diagrams can be associated to arbitrary mathematical fields such as the ϕ^4 , ϕ^3 , etc. in order to model different physical phenomena.

The Feynman rules are generally derived from the Lagrangian of the theory. For

instance, ϕ^4 with the Lagrangian

$$\mathcal{L} = \frac{1}{2}(\partial_\mu\phi)^2 - \frac{1}{2}m^2\phi^2 - \frac{\lambda}{4!}\phi^4 \quad (2.1)$$

has the following space-time Feynman rules:

For each external point: 1

For each vertex: $(-i\lambda)$

For each propagator: $D_F(x - y)$

where $D_F(x - y)$ is the two-point correlation function, sometimes called the two-point Green's function in ϕ^4 theory. For the purpose of defining the correlation we use the Dirac notation from quantum physics. We introduce $\langle\Sigma|$ to denote the ground state of the interacting theory. However, this is not the same ground state, $\langle 0|$, as in a free theory. We introduce T as a time-ordering symbol and also the fields $\phi(x)$ and $\phi(y)$. We know that in free theory [15], the propagator is defined as

$$\begin{aligned} D_F(x - y) &= \langle 0| T\phi(x)\phi(y) |0\rangle_{\text{free}} \\ &= \int \frac{d^4p}{(2\pi)^4} \frac{ie^{-ip\cdot(x-y)}}{p^2 - m^2 + i\epsilon} \end{aligned} \quad (2.2)$$

where p is the four-momentum associated with the interaction. Then, using the Hamiltonian of ϕ^4 theory as in [15]

$$H = H_0 + H_{\text{int}} = H_{\text{Klein-Gordon}} + \int d^3x \frac{\lambda}{4!}\phi^4(x) \quad (2.3)$$

and writing the correlation function of ϕ^4 theory as a power series of λ while ensuring that the Hamiltonian is a unitary operator. The last term in equation (2.3) is the coupling constant that shows up in the vertex. Using these rules, we can easily

construct all the S-matrices for the interaction. Finally, by adding them together and dividing by the symmetry factor we will get probability amplitude. When the interaction $\phi^4(x)$ is substituted by the QED interaction term we can derive same kind of Feynman rules for QED.

For the purpose of this thesis, we focused on two different types of Feynman diagrams; namely the one-loop self energy diagram and two-loop self energy diagram. A general topology of those types are shown in figure 2.1 and figure 2.2. Finally, using a computer algebra package like FormCalc [7] [9] we can insert associated fermion fields to the topology and then get the S-matrix of any fields associated with these kinds of topology.

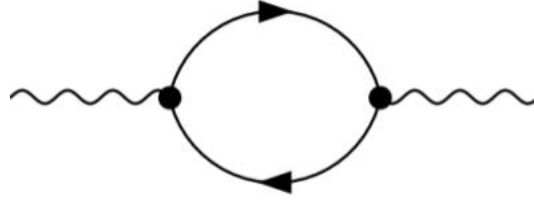


Figure 2.1: General topology of a one-loop self energy diagram

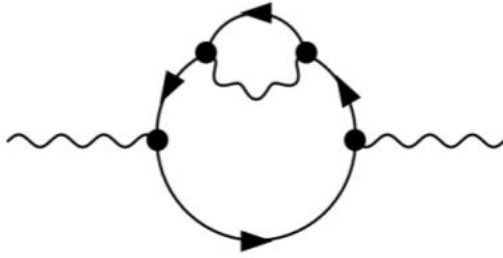


Figure 2.2: General topology of a first order correction to one-loop self-energy diagram

One of our primary goal is to calculate the Vacuum Polarization function, $\hat{\Pi}(Q^2)$ where Q^2 is the momentum squared associated with the interaction. The vacuum polarization function is directly related to the effective fine structure constant as

follows (derivation shown in section 2.6):

$$\alpha(Q^2) = \frac{\alpha(0)}{1 - \Delta\alpha(Q^2)} \quad (2.4)$$

$$= \frac{\alpha(0)}{1 - \hat{\Pi}(Q^2)} \quad (2.5)$$

where $\alpha(0)$ is the coupling constant for QED at $Q^2 = 0$ and $\alpha(Q^2)$ is the effective coupling constant at momentum Q^2 .

2.2 Feynman rules for QED

The Lagrangian of QED which as

$$\mathcal{L}_{\text{QED}} = i\bar{\psi}\not{\partial}\psi - \bar{\psi}m\psi - \frac{1}{4}(F_{\mu\nu})^2 - e\bar{\psi}\gamma_\mu A^\mu\psi \quad (2.6)$$

where

$$F_{\mu\nu} = \partial_\mu A_\nu - \partial_\nu A_\mu$$

$$\not{\partial} = \partial_\mu \gamma^\mu$$

γ_μ are the Dirac matrices

ψ are the spinor field associated with the particle fields

A_μ is the four- potential of the electromagnetic field generated by the particles

m is the mass of the particle associated

e is the coupling constant in the theory.

The above Lagrangian can be used to derive the Feynman rules for QED using functional derivatives of the path integral. In order to do so we have to apply the functional

derivative of the path integral on the Lagrangian to get S and then use $\Pi = iS^{-1}$ to derive the propagator and $\Gamma = iS$ to get the coupling. This is a rather involved task. However, as shown in *Introduction to Elementary Particles* [6], we can use a set of Feynman rules, similar to the ϕ^4 -theory in previous section, to derive the desired scattering matrix. In general, to get the scattering matrix of a QED interaction we have to use the following steps from a given Feynman diagram:

- Notations: It is customary to label the momenta of incoming and outgoing particles as p_1, p_2, \dots, p_n and the internal momenta as q_1, q_2, \dots, q_n . It is also required to use an arrow in order to trace the direction of the momenta.
- External lines: A particle associated with the interaction is denoted by an external line and there is a corresponding Dirac spinor (for a fermion) or a polarization vector (for a vector boson)

$$\text{Particles : } \begin{cases} \text{Incoming: } u \\ \text{Outgoing: } \bar{u} \end{cases}$$

$$\text{Anti-particles : } \begin{cases} \text{Incoming: } \bar{u} \\ \text{Outgoing: } u \end{cases}$$

$$\text{Photons : } \begin{cases} \text{Incoming: } \epsilon_\mu \\ \text{Outgoing: } \epsilon_\mu^* \end{cases}$$

- Coupling: At each vertex, a coupling Γ^μ is introduced which is given by

$$\Gamma^\mu = ig\gamma^\mu \quad (2.7)$$

where g is the strength of the coupling. It represents the coupling strength of the participating particles. It may depend on the spin of the particles for parity violating interactions(weak interactions).

- Propagators: For each internal line or particle, the following terms should be introduced:

$$\text{For Fermions: } \Pi = \frac{i\not{q} + m}{q^2 - m^2}, \text{ where } \not{q} = q_\mu \gamma^\mu$$

$$\text{For Bosons: } \Pi^{\mu\nu} = \frac{ig^{\mu\nu}}{q^2 - m^2}$$

where q and m are the momentum and the mass of the internal particle. The particle that does not belong to external lines is assumed to be off-shell particles. Off-shell particles are those particles that are spontaneously formed during pair production and do not obey energy-momentum conditions of the Dirac equation.

- Conservation of energy and momenta: For each vertex, a Δ -function is needed to ensure the conservation of energy and momentum which is given by

$$\Delta = (2\pi)^4 \delta^4(k_1 + k_2 + k_3)$$

where k_i is the momentum of the corresponding particle and the sign of k_i is determined by the direction of the momentum of the particle.

- Integration over internal momenta: For each internal particle, the integration I of the internal momenta is:

$$I = \frac{d^4 q_j}{(2\pi)^4}$$

- Finally, we have to assemble all the terms together and rewrite the delta function as:

$$\Delta = (2\pi)^4 \delta^4(p_i + p_2 + \dots - p_n)$$

and after multiplying the whole expression by i we derive the amplitude \mathcal{M} .

As an example, we can choose electron-muon scattering as shown in figure 2.3, and use the steps of the Feynman rules to get the amplitude \mathcal{M} .

The external particles are the incoming electron (p_1, m_1) , incoming muon (p_2, m_2) ,

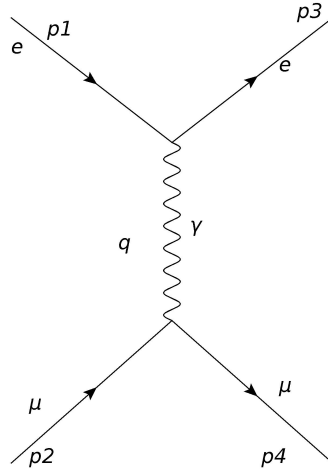


Figure 2.3: Feynman diagram for electron-muon scattering

the outgoing electron (p_3, m_3) and the outgoing muon (p_4, m_4) , where the kinematic information p_i, m_i is known. Now, according to Feynman rules:

1. The Dirac spinors are:

- $u_e(p_1, m_1)$
- $\bar{u}_e(p_3, m_3)$
- $u_m(p_2, m_2)$
- $\bar{u}_m(p_4, m_4)$

2. The coupling for the vertices are: $ig_e\gamma^\mu$ and $ig_m\gamma^\nu$

3. The propagator is: $\frac{-ig_{\mu\nu}}{q^2}$

4. The delta function and the integration term is: $\delta^4(p_1 - p_3 - q)\delta^4(p_2 - p_4 + q)\frac{d^4q}{(2\pi)^4}$

Now, when we assemble everything we get:

$$\mathcal{M} = (2\pi)^4 \int [\bar{u}_e(p_3, m_3)(ig_e\gamma^\mu)u_e(p_1, m_1)] \frac{-ig_{\mu\nu}}{q^2} [\bar{u}_m(p_4, m_4)(ig_e\gamma^\nu)u_m(p_2, m_2)] \times \delta^4(p_1 - p_3 - q)\delta^4(p_2 - p_4 + q)d^4q \quad (2.8)$$

Simplifying the integration and the delta function we get:

$$\mathcal{M} = \frac{-ig_e}{(p_1 - p_3)^2} [\bar{u}_e(p_3, m_3)(ig_e\gamma^\mu)u_e(p_1, m_1)] [\bar{u}_m(p_4, m_4)(ig_e\gamma_\mu)u_m(p_2, m_2)] \quad (2.9)$$

Since, the kinematic information is known, the numerical value can easily be calculated.

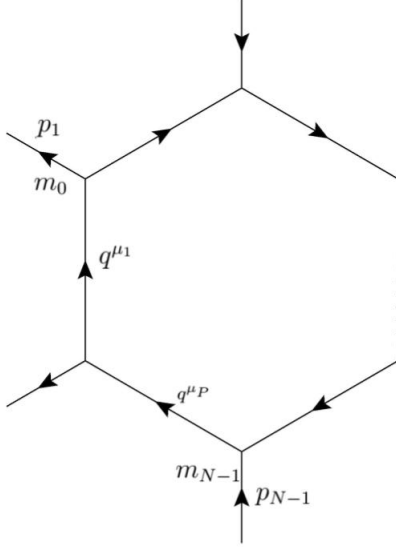


Figure 2.4: One-loop N-point topology

2.3 Passarino-Veltman Function

For calculating the amplitude in Feynman diagrams at tree level(one-loop) Veltman and 't Hooft introduced basic one-loop integrals, namely scalar 1-point, 2-point, 3-point and 4-point integrals [18]. An example of such one-loop tensor N-point integral is shown in figure 2.4 and has the following general form

$$T^{N,\mu_1\ldots\mu_P}(p_1, \ldots, p_{N-1}, m_0, \ldots, m_{N-1}) = \frac{(2\pi\mu)^{4-D}}{i\pi^2} \int d^D q \frac{q^{\mu_1} \ldots q^{\mu_P}}{N_0 N_1 \ldots N_{N-1}} \quad (2.10)$$

where

$$N_k = (q + p_k)^2 - m_k^2 + i\eta, \quad (p_0 = 0)$$

and $i\eta$ for $\eta > 0$ denotes an infinitesimal small imaginary part, μ is a mass parameter and D is the non-integer dimension of the spacetime defined as $D = 4 - \epsilon$. Then Passarino and Veltman provided a systematic method which allowed us to reduce all tensor integrals with up to four-loop internal propagators to these basic integrals [13].

These functions are often recognized as Passarino-Veltman functions. In the following sections, I will show explicit examples of a few of the Passarino-Veltman functions that can be derived from a given Feynman diagram.

2.3.1 One-point and two-point scalar function

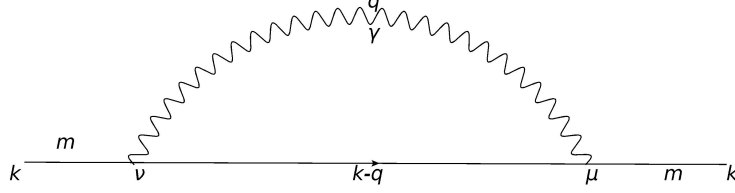


Figure 2.5: Fermion self-energy diagram

The truncated amplitude for figure 2.5 is

$$\begin{aligned}\Sigma_{ff}(q^2) &= -ie^2 \int d^4q \gamma_\nu \frac{\not{k} - \not{q} + m}{[(k-q)^2 - m^2]} q^{\gamma_\mu} \frac{g^{\mu\nu}}{q^2} \\ &= \underbrace{2ie^2 \int d^4q \frac{\not{k}}{[(k-q)^2 - m^2]q^2}}_{I_1} - \underbrace{2ie^2 \int d^4q \frac{\not{q}}{[(k-q)^2 - m^2]q^2}}_{I_2}\end{aligned}\quad (2.11)$$

where k , q and m are shown in figure 2.5 and the limit of integration is taken from $+\infty$ to $-\infty$. In most cases, this kind of integration is divergent. In order to evaluate, we will set the dimension of the integration to be D instead of 4 and introduce a pre-factor $\frac{\mu^{4-D}}{2\pi^D}$. Thus, I_1 becomes

$$I_1 = \frac{\mu^{4-D}}{2\pi^D} \int d^Dq \frac{1}{[(k-q)^2 - m^2]q^2}\quad (2.12)$$

and using the Feynman trick

$$\frac{1}{ab} = \int_0^1 dz \frac{1}{[az + b(1-z)]^2}\quad (2.13)$$

where z is the Feynman parameter, I_1 takes the form

$$I_1 = \frac{\mu^{4-D}}{2\pi^D} \int_0^1 dz \int d^D q \frac{1}{[(q - kz)^2 - k^2 z^2 + (k^2 - m^2)]^2} \quad (2.14)$$

and now we can chose $q - kz \mapsto q$ without changing the integration which gives us

$$I_1 = I_1 = \frac{\mu^{4-D}}{2\pi^D} \int_0^1 dz \int d^D q \frac{1}{[q^2 - k^2 z^2 + (k^2 - m^2)]^2} \quad (2.15)$$

Then, we use the following Feynman master integral [15]

$$\int \frac{d^D q}{2\pi^D} \frac{1}{(q^2 - \Pi)^2} = \frac{i}{(4\pi)^{D/2}} \frac{\Gamma(2 - \frac{D}{2})}{\Gamma(2)} \left(\frac{1}{\Pi} \right)^{2 - \frac{D}{2}} \quad (2.16)$$

where

$$\begin{aligned} \Gamma(z) &= \int_0^\infty t^{z-1} e^{-t} dt \\ &= \frac{1}{z} - \gamma + \theta(z) \end{aligned} \quad (2.17)$$

and $\gamma \approx 0.5772$ (known as Euler Mascheroni constant) give us

$$I_1 = \frac{i\mu^{4-D}}{4\pi^D} \int_0^1 dz \frac{\Gamma(2 - \frac{D}{2})}{\Gamma(2)} \left(\frac{1}{q^2 - k^2 z^2 + (k^2 - m^2)} \right)^{2 - \frac{D}{2}} \quad (2.18)$$

. Now,

$$\begin{aligned} \Gamma\left(2 - \frac{D}{2}\right) &= \frac{2}{4 - D} - \gamma + \theta\left(\frac{4 - D}{2}\right) \\ &= \frac{2}{\epsilon} - \gamma + \theta(\epsilon) \end{aligned} \quad (2.19)$$

with $\epsilon = 4 - D$ and

$$\mu^{4-D} = (\mu^2)^{\frac{4-D}{2}} = 1 - \frac{\epsilon}{2} \ln \left(\frac{1}{\mu^2} \right) + \theta(4 - D) \quad (2.20)$$

and

$$\left(\frac{1}{k^2 z^2 - (k^2 - m^2)z} \right)^{\frac{\epsilon}{2}} = 1 - \frac{\epsilon}{2} \ln (k^2 z^2 - k^2 z + m^2 z) \quad (2.21)$$

where $\epsilon \mapsto 0$ when $D = 4$ which is known as the limit of dimensional regularization.

The dimensional regularization confines the divergence of I_1 and gives us

$$I_1 = \frac{\mu^2}{(4\pi)^2 k^2} \left(\frac{2}{\epsilon} - \gamma + \frac{2k^2}{\mu^2} + \frac{m^2}{\mu^2} \ln \frac{m^2}{\mu^2} + \frac{k^2 - m^2}{\mu^2} \ln \frac{k^2 - m^2}{\mu^2} \right) \quad (2.22)$$

. By using similar methods, we derived

$$I_2 = \frac{\not{k}}{(4\pi)^2} \left[\frac{1}{\epsilon} \frac{\gamma}{2} + \frac{m^2}{2k^2} - \frac{m^4}{2k^4} \ln \frac{m^2}{\mu^2} - \left(\frac{1}{2} - \frac{m^4}{2k^4} \right) \ln \frac{m^2 - k^2}{\mu^2} \right] \quad (2.23)$$

. Using the results for I_1 and I_2 we get the truncated amplitude to be

$$\begin{aligned} \Sigma_{ff}(k) = ie^2 \frac{2ie^2 \mu^2}{(4\pi)^2 k^2} & \left(\frac{2}{\epsilon} - \gamma + \frac{2k^2}{\mu^2} + \frac{m^2}{\mu^2} \ln \frac{m^2}{\mu^2} + \frac{k^2 - m^2}{\mu^2} \ln \frac{k^2 - m^2}{\mu^2} \right) \\ & - \frac{2ie^2 \not{k}}{(4\pi)^2} \left(\frac{1}{\epsilon} - \frac{\gamma}{2} + \frac{m^2}{2k^2} - \frac{m^4}{2k^4} \ln \frac{m^2}{\mu^2} - \left(\frac{1}{2} - \frac{m^4}{2k^4} \right) \ln \frac{m^2 - k^2}{\mu^2} \right) \end{aligned} \quad (2.24)$$

. Now, equation (2.24) can be rewritten in the Passarino-Veltman basis using a one-point Passarino-Veltman function defined as

$$\begin{aligned} A_0(m^2) &= \int \frac{d^4 q}{q^2 - m^2} \\ &= m^2 \left[\frac{1}{\epsilon} - \ln \frac{m^2}{\mu^2} + 1 - \gamma + \ln(4\pi) \right] \end{aligned} \quad (2.25)$$

where m is the mass parameter in the figure, the scalar two-point function is defined

as

$$B_0(p^2, m_1^2, m_2^2) = \frac{\mu^{4-D}}{i\pi^2} \int d^D q \frac{1}{(q^2 - m_1^2) [(q+p)^2 - m_2^2]} \quad (2.26)$$

and a general B-function is defined as

$$B_{\nu_1, \nu_2, \dots, \nu_N} = \frac{\mu^{4-D}}{i\pi^2} \int d^D q \frac{q_{\nu_1, \nu_2, \dots, \nu_N}}{(q^2 - m_1^2) [(q+p)^2 - m_2^2]} \quad (2.27)$$

where k, q, m_1 and m_2 are shown in figure 2.5. From the figure 2.5, using the Feynman rules for QED the following amplitude can be defined

$$\begin{aligned} M &= \int d^4 q \left[\bar{u}(k) (ie\gamma_\mu) \frac{\not{k} - \not{q} + m}{[(k-q)^2 - m^2]} (ie\gamma_\nu) u(k) \right] \frac{ig^{\mu\nu}}{q^2} \\ &= -i(4\pi\alpha) \left[\bar{u}(k) \int d^4 q \frac{\gamma_\mu (\not{k} - \not{q} + m) \gamma^\mu}{[(k-q)^2 - m^2] q^2} u(k) \right] \end{aligned} \quad (2.28)$$

. Now, from equation (2.28) we can separate the following integrals

$$I_1 = -2\not{k} \int d^4 q \frac{1}{\mathcal{D}} \quad (2.29)$$

$$I_2 = - \int d^4 q \frac{\gamma_\mu \not{q} \gamma^\mu}{\mathcal{D}} \quad (2.30)$$

$$I_3 = 4m \int d^4 q \frac{1}{\mathcal{D}} \quad (2.31)$$

where $\mathcal{D} = [(k-q)^2 - m^2] q^2$. With careful inspection we see that we can write equation (2.29) and equation (2.31) using the scalar B-function in equation (2.26) as

$$I_1 = -2\not{k} B_0[k^2, 0, m^2] \quad (2.32)$$

$$I_3 = 4m B_0[k^2, 0, m^2] \quad (2.33)$$

also, taking the trace of the matrices $\text{Tr}[\gamma_\mu \gamma_\alpha \gamma^\mu \equiv -2\gamma_\alpha]$ we get

$$I_2 = 2\gamma_\alpha B^\alpha[k^2, 0, m^2] \quad (2.34)$$

. Then by using tensor reduction defined as

$$B_\alpha[k^2, m_1^2, m_2^2] = k_\alpha B_1 \otimes k^\alpha \quad (2.35)$$

and contracting both side of of equation (2.54) with k_α we evaluate B_1 which is

$$\int d^4q \frac{(q \cdot k)}{\mathcal{D}} = -k^2 B_1 \quad (2.36)$$

where $(q \cdot k) = \frac{1}{2} [(k - q)^2 - m^2] + m^2 - k^2 - q^2$ which gives us

$$\begin{aligned} & \frac{1}{2} \int d^4q \frac{[(k - q)^2 - m^2] + m^2 - K^2 - q^2}{\mathcal{D}} \\ &= \frac{1}{2} \left\{ \underbrace{\int d^4q \frac{1}{q^2}}_{A_0[0]} + m^2 \underbrace{\int d^4q \frac{1}{\mathcal{D}}}_{B_0[k^2, 0, m^2]} - k^2 \underbrace{\int d^4q \frac{1}{\mathcal{D}}}_{B_0[k^2, 0, m^2]} - \underbrace{\int d^4q \frac{1}{[(k - q)^2 - m^2]}}_{A_0[m^2]} \right\} \end{aligned} \quad (2.37)$$

. After collecting everything together and since $A_0[0]$ converges to zero we get

$$B_1 = \frac{1}{2k^2} [A_0[m^2] + (k^2 - m^2)B_0[k^2, 0, m^2]] \quad (2.38)$$

and

$$\begin{aligned} M &= i(4\pi\alpha)\bar{u}(k) \left[4mB_0[k^2, 0, m^2] \right. \\ &\quad \left. - 2\not{k} \left[B_0[k^2, 0, m^2] + \frac{1}{2k^2} [A_0[m^2] + (k^2 - m^2)B_0[k^2, 0, m^2]] \right] \right] u(k) \end{aligned} \quad (2.39)$$

Although the value of M in equation 2.39 can be calculated manually, it is a

laborious task. In this thesis, I used the FORMCALC package in Mathematica to do this calculation.

2.3.2 Vector Boson Self-Energy (QED only)

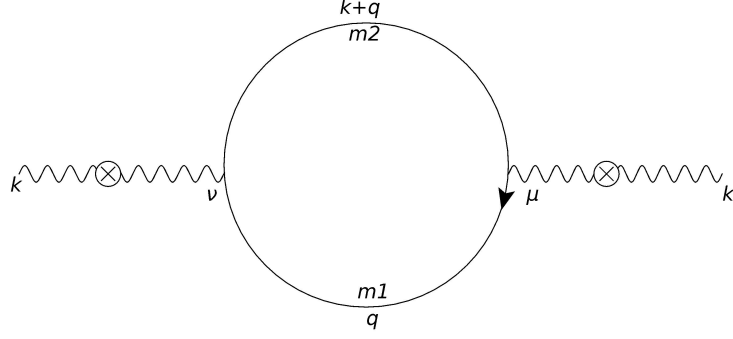


Figure 2.6: Truncated vector boson self-energy diagram with incoming momentum k and mass m_1 and m_2

In figure 2.6, the photon is off-shell and the amplitude is a second-rank tensor. Using the Feynman rules for QED, the amplitude works out to be

$$\Pi_{\mu\nu} = \text{Tr} \left[\int d^4q (ie\gamma_\nu) \frac{\not{q} + m_1}{q^2 - m_1^2} (ie\gamma_\mu) \frac{\not{k} + \not{q} + m_2}{[(k+q)^2 - m_2^2]} \right] \quad (2.40)$$

. Now, expanding the numerator and defining the following denominator as

$$\mathcal{D}_1 = q^2 - m_1^2 \quad (2.41)$$

$$\mathcal{D}_2 = (k+q)^2 - m_2^2 \quad (2.42)$$

we get

$$\Pi_{\mu\nu} = (-4\pi\alpha) \text{Tr} \left[\int d^4q \left[\gamma_\nu \not{q} \gamma_\mu + \gamma_\nu \not{q} \gamma_\mu \not{q} + \gamma_\nu \not{q} \gamma_\mu m_2 + m_1 \left(\gamma_\nu \gamma_\mu (\not{k} + \not{q} + m_2) \right) \right] \frac{1}{\mathcal{D}_1 \mathcal{D}_2} \right] \quad (2.43)$$

. After taking the trace of all the matrices we obtain the following form

$$\Pi_{\mu\nu} = (-4\pi\alpha) \int d^4q \left[\text{Tr}[\gamma_\nu \not{q} \gamma_\mu \not{k}] + \text{Tr}[\gamma_\nu \not{q} \gamma_\mu \not{q}] + 4m_1 m_2 g_{\mu\nu} \right] \frac{1}{\mathcal{D}_1 \mathcal{D}_2} \quad (2.44)$$

. Now, we can use the following one-point and two-point Passarino-Veltman functions:

$$A_0[m_2^2] + m_1^2 B_0 = \int d^4q \left(\frac{k^2 - m_1^2 - m_2^2}{\mathcal{D}_1 \mathcal{D}_2} \right) \quad (2.45)$$

$$B_\nu[k^2, 0, m^2] = \int d^4q \left(\frac{k_\nu}{\mathcal{D}_1 \mathcal{D}_2} \right) \quad (2.46)$$

$$B_{\mu\nu}[k^2, m_1, m^2] = \int d^4q \left(\frac{k_\mu k_\nu}{\mathcal{D}_1 \mathcal{D}_2} \right) \quad (2.47)$$

$$B_\alpha[k^2, 0, m^2] = \int d^4q \left(k^\alpha \frac{k^2}{\mathcal{D}_1 \mathcal{D}_2} \right) \quad (2.48)$$

$$B_0[k^2, 0, m^2] = \int d^4q \left(\frac{1}{\mathcal{D}_1 \mathcal{D}_2} \right) \quad (2.49)$$

Using the above one-point and two-point functions we can write equation (2.40) as

$$\begin{aligned} \Pi_{\mu\nu} = & (-16\pi\alpha) [k_\mu B_\nu + k_\nu B_\mu + 2B_{\mu\nu} - g_{\mu\nu} k^\alpha B_\alpha + g_{\mu\nu} m_1 m_2 B_0] \\ & + (16\pi\alpha) [A_0(m_2^2) + m_1 B_0] g_{\mu\nu} . \end{aligned} \quad (2.50)$$

In the equation (2.50), there are some two-point functions which are not numerically stable and are therefore not suitable for numerical integration; therefore, we tend to use tensor decomposition, such as

$$B_\mu = k_\mu B_1 \quad (2.51)$$

$$B_{\mu\nu} = g_{\mu\nu} B_{00} + k_\mu k_\nu B_{11} \quad (2.52)$$

. Substituting equation (2.51) and equation (2.52) in equation (2.50) we get

$$\begin{aligned}
\Pi_{\mu\nu} &= -(16\pi\alpha) \left[2k_\mu k_\nu B_1 + 2(g_{\mu\nu} B_{00} + k_\mu k_\nu B_{11}) - g_{\mu\nu} k^2 B_1 + g_{\mu\nu} m_1 m_2 B_0 \right. \\
&\quad \left. - g_{\mu\nu} (A_0(m_2^2) + m_1^2 B_0) \right] \\
&= -(16\pi\alpha) \left[g_{\mu\nu} \{ 2B_{00} - k^2 B_1 - A_0(m_2^2) - m_1^2 B_0 + m_1 m_2 B_0 \} + k_\mu k_\nu \{ 2(B_1 + B_{11}) \} \right]
\end{aligned} \tag{2.53}$$

and with a tensor reduction such as

$$B_\nu[k^2, m_1^2, m_2^2] = k_\nu B_1 \otimes k^\nu \tag{2.54}$$

$$B_{\mu\nu}[k^2, m_1^2, m_2^2] = g_{\mu\nu} B_{00} + k_\mu k_\nu B_{11} \otimes \begin{pmatrix} g^{\mu\nu} \\ k^\mu k^\nu \end{pmatrix} \tag{2.55}$$

we use equation (2.54) and (2.55) to get the following relations between two-point functions

$$B_1 = \frac{1}{2k^2} \{ A_0(m_1^2) - A_0(m_2^2) - (k^2 - m_2^2 + m_1^2) B_0 \} \tag{2.56}$$

$$g^{\mu\nu} B_{\mu\nu} = 4B_{00} + k^2 B_{11} \tag{2.57}$$

$$B_{11} = \frac{1}{3} \left\{ A_0(m_2^2) + m_1^2 B_0 - \frac{1}{2} [A_0(m_2^2) - (k^2 - m_2^2 + m_1^2) B_1] \right\} \tag{2.58}$$

$$B_{00} = \frac{1}{3k^2} \left\{ 2 [A_0(m_2^2) - (k^2 - m_2^2 + m_1^2) B_1] - A_0(m_2^2) - m_1^2 B_0 \right\} \tag{2.59}$$

. Furthermore, if we set $m_1 = m_2 = m$ we get

$$B_1 = -\frac{1}{2} B_0 \tag{2.60}$$

$$B_{00} = \frac{1}{3} \left(\frac{1}{2} A_0 + m^2 B_0 - \frac{1}{4} k^2 B_0 \right) = \frac{1}{12} (2A_0 + B_0(k^2 - 4m^2)) \tag{2.61}$$

$$B_{11} = \frac{1}{3k^2} (A_0 + B_0(k^2 - m^2)) \tag{2.62}$$

. Finally, we can write equation (2.40) as

$$\Pi_{\mu\nu} = -(16\pi\alpha) \left(g_{\mu\nu} \left\{ -\frac{2}{3}A_0 + \frac{1}{3}B_0(k^2 + 2m^2) \right\} - \frac{k_\mu k_\nu}{k^2} \left\{ -\frac{2}{3}A_0 + \frac{1}{3}B_0(k^2 + 2m^2) \right\} \right) \quad (2.63)$$

2.3.3 Three-point function

In figure 2.7 there is a generic triangle insertion. In our calculation, however, we will only consider virtual particles that are possible according to QED. In figure 2.7,

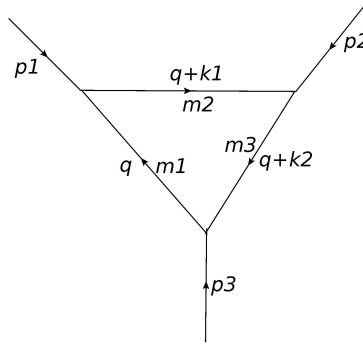


Figure 2.7: A general triangle topology with p_i are the incoming momenta and m_i represents the masses of the off-shell particles

$k_1 = p_1$ and $k_2 = p_1 + p_2$. The amplitude for a general triangle topology such as in figure 2.7 is given as

$$C_{\mu_1, \mu_2, \dots, \mu_N} = \frac{\mu^{4-D}}{i\pi^{D/2}} \int d^D q \frac{q_{\mu_1}, q_{\mu_2}, \dots, q_{\mu_N}}{[q^2 - m_1^2] [(q + k_1)^2 - m_2^2] [(q + k_2)^2 - m_3^2]} \quad (2.64)$$

where m_1 , m_2 and m_3 are the masses of the vertex shown in figure 2.7, and their respective momentum is as shown in figure 2.7. By doing some algebra in equation (2.64), we will try to get a similar structure to the master integral in appendix of [15].

For that purpose, we will use the Feynman trick which is

$$\begin{aligned}\frac{1}{ABC} &= \int dx dy dz \delta(x+y+z-1) \cdot \frac{1}{[Ax+By+Cz]^3} \\ &= \int_0^1 dx \int_0^{1-x} dy \cdot \frac{1}{[Ax+By+(1-x-y)C]^3}\end{aligned}\quad (2.65)$$

and then define

$$\mathcal{D} \equiv (1-x-y) [q^2 - m_1^2] + [(q+p_1)^2 - m_2^2] x + [(q+p_1+p_2)^2 - m_3^2] y \quad (2.66)$$

. Then using equation (2.65) and defining

$$A \equiv [q^2 - m_1^2] \quad (2.67)$$

$$B \equiv [(q+k_1)^2 - m_1^2] \quad (2.68)$$

$$C \equiv [(q+k_2)^2 - m_3^2] \quad (2.69)$$

$$l = q + p_1(x+y) + p_2 y \quad (2.70)$$

$$\Delta = p_1^2 (x+y)^2 + 2(p_1 \cdot p_2) y (x+y) + p_2^2 y^2 + m_1^2 (\bar{x} - y) - x p_1^2 + m_2^2 x - p_{12} y + y m_3^2 \quad (2.71)$$

where $\bar{x} = 1-x$ and $p_{12} = (p_1 + p_2)^2$ we get a similar structure to the master integral in the appendix of the book "An Introduction To Quantum Field Theory" [15] which is

$$\int \frac{d^D l}{(2\pi)^D} \cdot \frac{1}{(l^2 - \Delta)^n} = \frac{(-1)^n i}{(4\pi)^{D/2}} \frac{\Gamma(n - \frac{D}{2})}{\Gamma(n)} \left(\frac{1}{\Delta}\right)^{n - \frac{D}{2}} \quad (2.72)$$

where $n = 3$ and $\Gamma(n) = (n-1)!$ which finally gives us

$$\begin{aligned}C_0 &= \int_0^1 dx \int_0^{1-x} dy (-i) \frac{(4\pi)^{D/2}}{(4\pi)^{d/2}} (-i) \frac{\Gamma(1)}{3} \left(\frac{1}{\Delta}\right)^1 \\ &= -\frac{1}{2} \int_0^1 dx \int_0^{1-x} dy \left(\frac{1}{\Delta}\right)\end{aligned}\quad (2.73)$$

. In the limiting case $D \mapsto 4$ the poles cancel analytically which in turns makes C_0 a convergent integral.

2.4 Renormalization of QED

In order to understand the renormalization of Quantum Electrodynamics we will start with a toy model, namely ϕ^3 theory, and then proceed from there. This helps us to understand the the logical sequence that underlies the process of renormalization.

2.4.1 Motivation for renormalization

The core idea behind the renormalization in quantum field theory [17] is-"Observables are finite and in-principle calculable functions of other observables." Regularization serves to isolate the infinite terms appearing in the loop integrals and renormalization is the procedure that absorbs these infinite terms in the bare parameters of the theory to generate the physical and measurable parameters of the theory. There could be divergences which appear in the intermediate steps of the calculations, such as calculating a loop graphs, but after regularization the infinities will disappear.

In general, tree level amplitudes are mathematically rational polynomials and we do not have any functions which result in infinity; this is not the case for a loop diagram. For instance, if we consider the toy model ϕ^4 theory we find that the expression for the correlation function involves terms like $\ln\left(\frac{s}{s_0}\right)$ which give rise to infinities. Expressing the correlation function at the scale s in terms of the correlation function at a different scale s_0 gives a finite prediction.

2.4.2 Renormalization of ϕ^3 theory

The Lagrangian for ϕ^3 theory is

$$\mathcal{L} = -\frac{1}{2}\phi(\square + m^2)\phi + \frac{g}{3!}\phi^3 \quad (2.74)$$

. We will consider a off-shell one-loop Feynman diagram as in figure 2.8, and by using

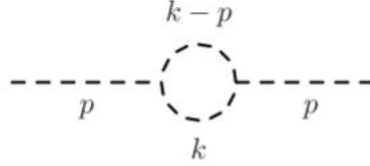


Figure 2.8: One-loop Feynman diagram for ϕ^3 theory

the Feynman rules for ϕ^3 theory as in [15] we get

$$i\mathcal{M}_{\text{loop}}(p) = \frac{1}{2}(ig)^2 \int \frac{d^4k}{(2\pi)^4} \frac{i}{(k-p)^2 - m^2 + i\epsilon} \frac{i}{k^2 - m^2 + i\epsilon} \quad (2.75)$$

where \mathcal{M} is the amplitude. Then we use the following Feynman trick [17]

$$\frac{1}{AB} = \int_0^1 \frac{dx}{[A + (B-A)x]^2} \quad (2.76)$$

where x is the Feynman parameter. In addition we use the shift $k^\mu \mapsto k^\mu + p^\mu(1-x)$ and Pauli-Villars regularization

$$\int \frac{d^4k}{(2\pi)^4} \frac{1}{(k^2 - \Delta + i\epsilon)^2} = -\frac{i}{16\pi^2} \ln \frac{\Delta}{\Lambda^2} \quad (2.77)$$

where Λ is a fictitious scalar mass that obeys fermionic statistics and $\Delta = m^2 - p^2 x(1-x)$. Finally, by completing the integration we get

$$\mathcal{M}_{\text{loop}}(p) = \frac{g^2}{32\pi^2} \left[2 - \ln \frac{-p^2}{\Lambda^2} \right] \quad (2.78)$$

. By redefining $\Lambda^2 \mapsto \Lambda^2 e^{-2}$ and assuming p^μ is spacelike we get

$$\mathcal{M}_{\text{loop}}(p) = -\frac{g^2}{32\pi^2} \ln \frac{Q^2}{\Lambda^2} \quad (2.79)$$

where Q^2 is a physical scale which is related to Casimir force [17]. We can see that $\ln Q^2$ is the regulator that will generate the physical prediction from the loop. Now,

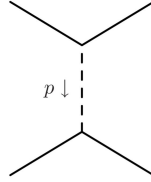


Figure 2.9: A generic t-channel scattering diagram

we use equation (2.79) as a insertion into a tree level diagram as in figure 2.9, i.e. we calculate the amplitude for the topology in figure 2.10 and use the conditions $p^2 < 0$ and $Q^2 = -p^2$ with $Q > 0$ resulting in

$$M(Q) = M^0(Q) + M^1(Q) = \frac{g^2}{Q^2} \left(1 - \frac{1}{32\pi^2} \frac{g^2}{Q^2} \ln \frac{Q^2}{\Lambda^2} + \mathcal{O}(g^4) \right) \quad (2.80)$$

. Let us now substitute $\tilde{g} \equiv \frac{g^2}{Q^2}$, to make it a dimensionless quantity at some fixed Q_0 which gives us the renormalization condition for this diagram which is

$$\tilde{g}_R^2 = M(Q_0) \quad (2.81)$$

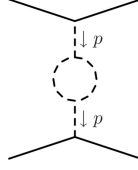


Figure 2.10: A generic scalar bubble diagram

The renormalization condition defines the coupling in terms of an observable which reduces the possibilities of the renormalization condition to be only one parameter in a quantum theory. Finally, substituting \tilde{g}_R^2 in to the matrix element gives us a prediction for the matrix element at the scale of Q in terms of the matrix element at the scale of Q_0 which is

$$M(Q) = \tilde{g}_R^2 + \frac{1}{32\pi} \tilde{g}_R^2 \ln \frac{Q_0^2}{Q^2} + \dots \quad (2.82)$$

Thus, we get the renormalized amplitude for ϕ^3 theory which is given by equation 2.82. The amplitude can be measured at one Q and then it can be used to make non-trivial prediction at another value of Q .

2.4.3 Vacuum Polarization in Quantum Electrodynamics

The Lagrangian of QED is given as

$$\mathcal{L}_{\text{QED}} = i\bar{\psi}\not{\partial}\psi - \bar{\psi}m\psi - \frac{1}{4}(F_{\mu\nu})^2 - e\bar{\psi}\gamma_\mu A^\mu\psi \quad (2.83)$$

where where

$$F_{\mu\nu} = \partial_\mu A_\nu - \partial_\nu A_\mu$$

$$\not{\partial} = \partial_\mu \gamma^\mu$$

γ_μ are the Dirac matrices

ψ are the spinor field associated with the particle fields

A_μ is the four- potential of the electromagnetic field generated by the particles

m is the mass of the particle associated

e is the coupling constant in the theory.

. The counter-term Lagrangian will give us the the Feynman rules for that can be used to get the renormalized amplitude. In order to get the derive the the Feynman rules for the renormalized amplitude we start with the construction of the Lagrangian for the counter-terms:

$$\mathcal{L}_{\text{QED}}^0 = \bar{\psi}_0 \left(i\not{\partial} - e_0 \not{A}_0 - m_0 \right) \psi_0 - \frac{1}{4} (F_{\mu\nu}^0)^2 \quad (2.84)$$

where

$$\psi_0 \mapsto \sqrt{z_\psi} \psi \quad \text{with } z_i = 1 + \delta z_i,$$

$$e_0 \mapsto z_e e,$$

$$A_\mu^0 \mapsto \sqrt{z_\gamma} A_\mu \quad \text{and}$$

$$m_0 \mapsto z_m m$$

. Thus, we have

$$\begin{aligned}
\hat{\mathcal{L}}_{\text{QED}} &= (1 + \delta z_\psi) \bar{\psi} \left(i \not{\partial} - (1 + \delta z_e) e + (1 + \delta z_\gamma)^{1/2} \not{A} - (1 + \delta z_m) m \right) \\
&\quad \psi - \frac{1}{4} (F_{\mu\nu})^2 (1 + \delta z_\gamma) \\
&= (1 + \delta z_\psi) \bar{\psi} \left(i \not{\partial} - (1 + \delta z_e) e + (1 + \frac{1}{2} \delta z_\gamma) \not{A} - (1 + \delta z_m) m \right) \\
&\quad \psi - \frac{1}{4} (F_{\mu\nu})^2 (1 + \delta z_\gamma) \\
&= \bar{\psi} \left(i \not{\partial} - i e \not{A} - m \right) \psi - \frac{1}{4} (F_{\mu\nu})^2 \\
&\quad \delta z_\psi \bar{\psi} (i \not{\partial} - e \not{A} - m) \psi + \bar{\psi} (-\delta z_e) e \not{A} \psi \\
&\quad \bar{\psi} \left(-\frac{1}{2} \delta z_\gamma \right) e \not{A} \psi + \bar{\psi} (-\delta z_m) m \psi - \frac{1}{4} (F_{\mu\nu})^2 \delta z_\gamma \\
&= \mathcal{L} + \delta \mathcal{L}
\end{aligned} \tag{2.85}$$

where $\delta \mathcal{L}$ is the counter-term Lagrangian. The counter terms help us to get rid of the infinities that arises in the amplitude and is given by

$$\begin{aligned}
\delta \mathcal{L} &= \delta z_\psi \bar{\psi} (i \not{\partial} - e \not{A} - m) \psi + \bar{\psi} (-\delta z_e) e \not{A} \psi \\
&\quad \bar{\psi} \left(-\frac{1}{2} \delta z_\gamma \right) e \not{A} \psi + \bar{\psi} (-\delta z_m) m \psi - \frac{1}{4} (F_{\mu\nu})^2 \delta z_\gamma
\end{aligned}$$

. The Feynman rules for the counter-term Lagrangian $\delta \mathcal{L}$ are then derived as follows

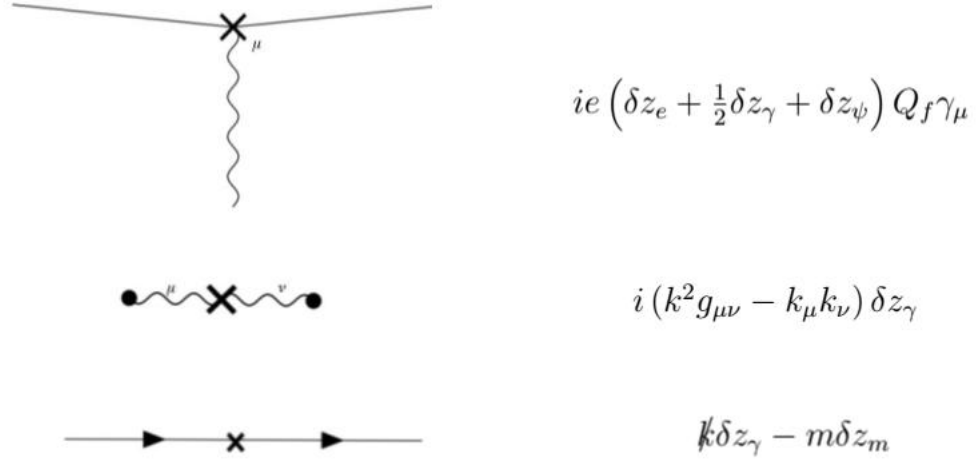


Figure 2.11: Feynman rules for counter-term Lagrangian

Then by using the following renormalization conditions

$$1. \quad \hat{\Sigma}_{\gamma\gamma}(0) = 0 \quad (2.86)$$

$$2. \quad \frac{\partial \hat{\Sigma}_{\gamma\gamma}}{\partial k^2} \Big|_{k^2=0} = 0 \quad (2.87)$$

$$3. \quad \hat{\Sigma}_{ff}(m) = 0 \quad (2.88)$$

$$4. \quad \frac{\partial \hat{\Sigma}_{ff}(k^2)}{\partial \not{k}} \Big|_{\not{k}=m} = 0 \quad (2.89)$$

$$5. \quad \hat{\Gamma}_{ff}^\gamma(k^2) \Big|_{k^2=0} = -ie Q_f \gamma_\mu \quad (2.90)$$

where $\hat{\Sigma}_{\gamma\gamma}$ is the truncated photon self-energy amplitude, $\hat{\Sigma}_{ff}$ is the truncated fermion self-energy graph and $\hat{\Gamma}_{ff}^\gamma$ is the vertex correction to the fermion current. They are

defined as:

$$\hat{\Sigma}_{\gamma\gamma}(k^2) = k^2 \hat{\Pi}(k^2) \quad (2.91)$$

$$\hat{\Pi}_{\mu\nu}(k^2) = i \left(g_{\mu\nu} - \frac{k_\mu k_\nu}{k^2} \right) \hat{\Sigma}_{\gamma\gamma}(k^2) \quad (2.92)$$

$$\hat{\Sigma}_{ff}(k) = \not{k} \hat{\Sigma}_V(k^2) + m \Sigma_S(k^2) \quad (2.93)$$

$$\hat{\Gamma}_\mu = -ieQ_f \gamma_\mu + ieQ_f \left(\gamma_\mu \hat{F}_1(k^2) + \frac{i}{2m} \sigma_{\mu\alpha} k^\alpha \hat{F}_2(k^2) \right) \quad (2.94)$$

and F_1 and F_2 are the Dirac and Pauli form factors respectively. Using the Feynman rules for counter-term Lagrangian and using the renormalization condition, the renormalized amplitude will be derived for the photon self-energy diagram and the fermion self energy diagram.

Renormalization of photon self-energy

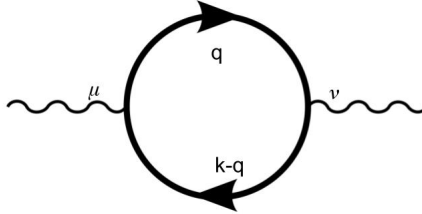


Figure 2.12: Photon self-energy diagram

The amplitude of the photon self-energy in figure 2.12 has the following form

$$\begin{aligned} \hat{\Pi}_{\mu\nu} &= i \left(g_{\mu\nu} - \frac{k_\mu k_\nu}{k^2} \right) \Sigma_{\gamma\gamma}(k^2) + i \left(g_{\mu\nu} - \frac{k_\mu k_\nu}{k^2} \right) \delta z_\gamma k^2 \\ &= i \left(g_{\mu\nu} - \frac{k_\mu k_\nu}{k^2} \right) \left(\Sigma_{\gamma\gamma}(k^2) + k^2 \delta z_\gamma \right) \end{aligned} \quad (2.95)$$

and

$$\hat{\Sigma}_{\gamma\gamma}(k^2) = \Sigma_{\gamma\gamma}(k^2) + k^2 \delta z_\gamma \quad (2.96)$$

. Then, by using using the renormalization conditions we get

$$\delta z_\gamma = -\frac{\partial \Sigma_{\gamma\gamma}(k^2)}{\partial k^2} \Big|_{k^2=0} \quad (2.97)$$

and finally

$$\hat{\Sigma}_{\gamma\gamma}(k^2) = \Sigma_{\gamma\gamma}(k^2) - k^2 \frac{\partial \Sigma_{\gamma\gamma}}{\partial k^2} \Big|_{k^2=0} \quad (2.98)$$

$$\hat{\Pi}(k^2) = \Pi(k^2) - \Pi(0) \quad (2.99)$$

which is the renormalized amplitude for a photon self-energy graph.

Renormalization of fermion self-energy

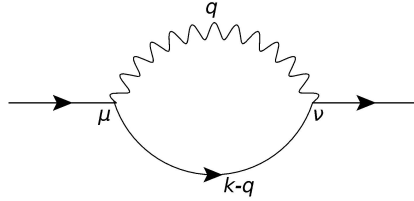


Figure 2.13: Fermion self-energy diagram

The amplitude of the fermion self-energy graph [2.13](#) has the following structure

$$\hat{\Sigma}_{ff}(k) = \not{k} \Sigma_V(k^2) + m \Sigma_S(k^2) + (\not{k} - m) \delta z_\psi - m \delta z_m \quad (2.100)$$

By using the renormalization conditions we get

$$\begin{aligned} \hat{\Sigma}_{ff}(m) &= m \Sigma_V(m^2) + m \Sigma_S(m^2) - m \delta z_m = 0 \\ &= \Sigma_V(m^2) + \Sigma_S(m^2) - \delta z_m = 0 \end{aligned} \quad (2.101)$$

which gives us

$$\delta z_m = \Sigma_V(m^2) + \Sigma_S(m^2)$$

. Then using the renormalization conditions we get

$$\begin{aligned}\delta z_\psi &= \Sigma_V(m^2) - 2m^2 \left(\frac{\partial \Sigma_V}{\partial k^2} + \frac{\partial \Sigma_S}{\partial k^2} \right) \Big|_{k^2=m^2} \\ &= - \frac{\partial \Sigma_{ff}}{\partial k} \Big|_{k=m}\end{aligned}$$

Finally, we get the renormalized amplitude as

$$\hat{\Sigma}_{ff}(k) = k \Sigma_V(k^2) + m \Sigma_S(k^2) - (k - m) \frac{\partial \Sigma_{ff}}{\partial k} \Big|_{k=m} \quad (2.102)$$

.

Renormalization of Vertex

Rewriting the equation (2.94)

$$\hat{\Gamma}_\mu(k^2) = -ieQ_f \gamma_\mu + ieQ_f \left(\gamma_\mu \hat{F}_1(k^2) + \frac{i}{2m} \sigma_{\mu\alpha} k^\alpha \hat{F}_2(k^2) \right) \quad (2.103)$$

we see that

$$\begin{aligned}\delta \Gamma_\mu &= ieQ_f \left(\gamma_\mu \hat{F}_1(k^2) + \frac{i}{2m} \sigma_{\mu\alpha} k^\alpha \hat{F}_2(k^2) \right) \\ &= \delta z_e + \frac{1}{2} \delta z_\gamma + \delta z_\psi\end{aligned} \quad (2.104)$$

and using Thomson limit

$$\hat{\Gamma}_\mu(0) = -ieQ_f \gamma_\mu \quad (2.105)$$

we get

$$\hat{\Gamma}_\mu(0) = -ieQ_f \gamma_\mu + ieQ_f \hat{F}_1(0) \gamma_\mu - ieQ_f \gamma_\mu \left(\delta z_e + \frac{1}{2} \delta z_\gamma + \delta z_\psi \right) \quad (2.106)$$

. Since $\hat{\Gamma}_\mu(0) = -ieQ_f\gamma_\mu$ we get

$$\hat{F}_1(0) = \delta z_e + \frac{1}{2}z_\gamma + \delta z_\psi \quad (2.107)$$

. Thus we finally obtain

$$\hat{\Gamma}_\mu(k^2) = -ieQ_f\gamma_\mu + \delta\Gamma_\mu(k^2) - \underbrace{ieQ_f\gamma_\mu\hat{F}_1(0)}_{\delta\Gamma_\mu(0)} \quad (2.108)$$

which can be written as

$$\hat{\Gamma}_\mu(k^2) = -ieQ_f\gamma_\mu + \delta\Gamma_\mu(k^2) - \delta\Gamma_\mu(0) \quad (2.109)$$

.

2.5 One particle irreducible contribution(1P1)

In equation (2.63), we see that the Lorentz structure for a vacuum polarization function is

$$\Pi_{\mu\nu} = i(k^2 g_{\mu\nu} - k_\mu k_\nu) \Pi(k^2) \quad (2.110)$$

. The contribution to the vacuum polarization function in such case is known as the one particle irreducible contribution. We see that there is a integration pre-factor associated with the vacuum polarization function which is given by $i(2\pi)^{-4 \times \text{number of loops}}$; which for one-loop gives us $\frac{i}{16\pi^4}$.

Since the photon is off-shell there is an infinite number of possible topologies. Few of these diagrams are shown in figure 2.14; however, it is not possible for us to

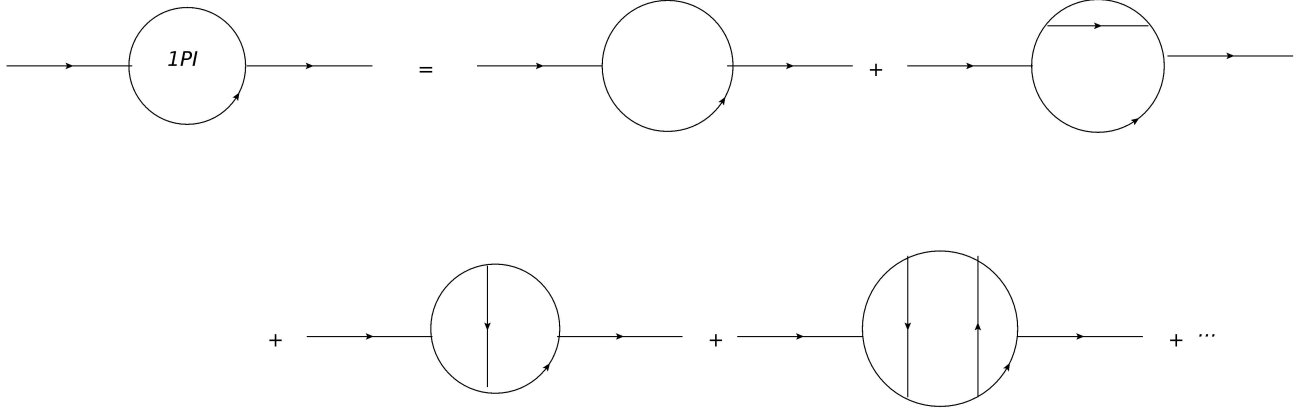


Figure 2.14: One-Particle irreducible contribution (1PI)

calculate the vacuum polarization function for an infinite number of topologies. We should consider an effective propagator for any kind of interaction taking place which is discussed in the following section.

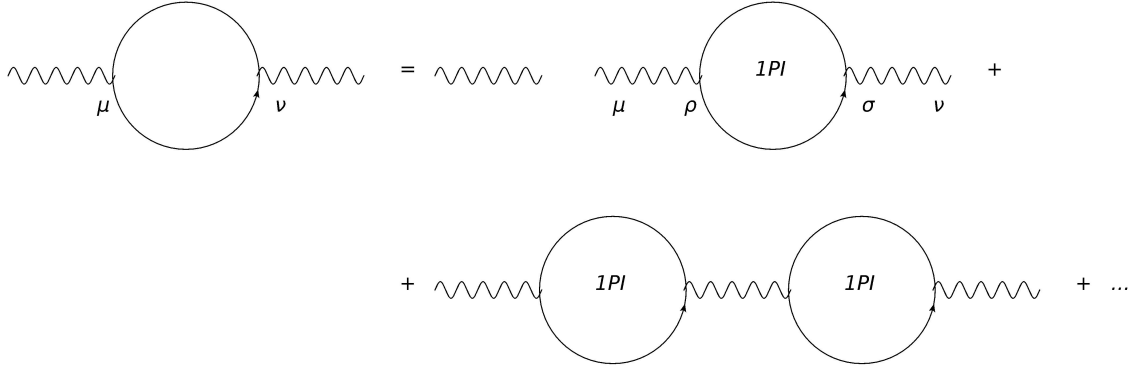


Figure 2.15: Feynman diagram for Effective propagator

2.6 Effective Feynman Propagator

In section 2.5, we have seen the amplitude for one-particle irreducible contribution. In general, we have the Feynman diagram as in figure 2.15, for any kind of interaction. The amplitude for the effective propagator is given as

$$\Pi_{\mu\nu}^{\text{eff}}(k^2) = \frac{-ig_{\mu\nu}}{k^2} + \frac{-ig_{\mu\rho}}{k^2} \left[i \left(k^2 g^{\rho\sigma} - k^\rho k^\sigma \right) \Pi(k^2) \right] \frac{-ig_{\nu\sigma}}{k^2} + \dots \quad (2.111)$$

where k^2 is the momentum of the incoming photon. Now, using

$$\begin{aligned}
& i \left(k^2 g^{\rho\sigma} - k^\rho k^\sigma \right) \frac{-i g_{\mu\nu}}{k^2} \\
&= \delta_\nu^\rho - \frac{k^\rho k_\nu}{k^2} \\
&\equiv \Delta_\nu^\rho
\end{aligned} \tag{2.112}$$

we get

$$\begin{aligned}
\Pi_{\mu\nu}^{\text{eff}}(k^2) &= \frac{-i g_{\mu\nu}}{k^2} + \frac{-i g_{\mu\rho}}{k^2} \Pi^2 \cdot \Delta_\nu^\rho + \frac{-i g_{\mu\rho}}{k^2} \Delta_\sigma^\rho \Delta_\nu^\sigma \Pi^2 + \dots \\
&= \frac{-i g_{\mu\nu}}{k^2} + \frac{-i g_{\mu\rho}}{k^2} \left(\delta_\nu^\rho - \frac{k^\rho k_\nu}{k^2} \right) [\Pi(k^2) + \Pi(k^2) + \dots]
\end{aligned} \tag{2.113}$$

which gives us the following effective propagator

$$\Pi_{\mu\nu}^{\text{eff}}(k^2) = \frac{-i}{k^2 [1 - \Pi(k^2)]} \left(g_{\mu\nu} - \frac{k_\mu k_\nu}{k^2} \right) \tag{2.114}$$

. Using gauge-invariance, Dirac equation and the fact that at zero momentum transfer the fine structure constant gives us same result as in Thomson limit, $\alpha = \frac{e^2}{4\pi}$, to deduce the vacuum polarization tensor. The effective fine structure constant turns out to be

$$\alpha(k^2) = \frac{\alpha(0)}{1 - \hat{\Pi}(k^2)} \tag{2.115}$$

where

$$\hat{\Pi}(k^2) = \Pi(k^2) - \Pi(0) \tag{2.116}$$

and

$$\Pi(k^2) = \Pi_{1\text{Loop}} + \Pi_{2\text{Loop}} + \dots \tag{2.117}$$

2.7 The Dispersion Approach

A dispersion relation [1] allows us to express a loop integral through the known imaginary part as follows:

$$L(q^2) = \frac{1}{\pi} \int_{s_0}^{\infty} ds \frac{\Im L(s)}{s - q^2 - i\epsilon} \quad (2.118)$$

where q^2 is the external momentum squared, s is the dispersion parameter and s_0 is the branch-point position on the real axis. The imaginary part $\Im L(q^2)$ can be calculated from discontinuities of the loop integral using Cutkosky rules. Cutkosky rules tell us to put internal propagators on the mass-shell in order to determine the imaginary part of a Feynman amplitude [11].

2.7.1 Self-energy sub-loop dispersion representation

A self-energy sub-loop can be used as an insertion to another self-energy, triangle or a box topology. For fermions or vector bosons, the self-energy sub-loop can be defined in form of the Lorentz covariant terms [1] as follows:

$$\Sigma_{\mu\nu}^{V-V}(q) = \left(g_{\mu\nu} - \frac{q_\mu q_\nu}{q^2} \right) \Sigma_T^{V-V}(q^2) + \frac{q_\mu q_\nu}{q^2} \Sigma_L^{V-V}(q^2) \quad (2.119)$$

$$\Sigma^f(q) = \not{q} \Sigma^f(q^2) + m_f \Sigma^f(q^2) \quad (2.120)$$

where $\Sigma_T^{V-V}(q^2)$ and $\Sigma_L^{V-V}(q^2)$ are the transverse and longitudinal parts of the diagonal and mixed vector boson self-energies. Both equations (2.119) and (2.120) can be written in terms of the Passarino-Veltman two-point tensor coefficient functions. Then, each of the two-point tensor coefficient functions $B_{i,ij,ijk}(q^2, m_\alpha^2, m_\beta^2)$ can be

replaced by the dispersion integral as

$$B_{i,ij,ijk}(q^2, m_\alpha^2, m_\beta^2) = \frac{1}{\pi} \int_{(m_\alpha+m_\beta)^2}^{\infty} ds \frac{\mathcal{I}B_{i,ij,ijk}(s, m_\alpha^2, m_\beta^2)}{s - q^2 - i\epsilon} \quad (2.121)$$

where $\mathcal{I}B_{i,ij,ijk}(s, m_\alpha^2, m_\beta^2)$ can be computed with LOOPTOOLS [8] or COLLIERSLINK [14].

In the paper [1] this has been done for electroweak case which can be applied for our case (only QED) and that gives the following for a sub-loop represented by a vector boson self-energy

$$\begin{aligned} I_{\mu_1, \mu_2, \nu_1 \dots \nu_R}^{1, M, 1} \\ = \frac{1}{\pi} \frac{\mu^{(4-D)}}{\pi(i\pi^{D/2})} \Sigma_{\alpha, \beta} \int_{(m_\alpha+m_\beta)^2}^{\infty} ds \int d^D q_2 \frac{q_{2, \nu_1} \dots q_{2, \nu_R}}{s - q_2^2 - i\epsilon} \frac{F_{\mu_1 \mu_2}(q_2, s, m_\alpha, m_\beta)}{\prod_{j=0}^M [(q_2 + k_{j, M})^2 - m_{j, M}^2]} \end{aligned} \quad (2.122)$$

where $F_{\mu_1 \mu_2}(q_2, s, m_\alpha, m_\beta)$ is defined as

$$\begin{aligned} F_{\mu_1 \mu_2}(q_2, s, m_\alpha, m_\beta) = & \left(g_{\mu_1 \mu_2} - \frac{q_{2\mu_1} q_{2\mu_2}}{q_2^2} \right) \mathcal{I}\Sigma_T^{V-V}(s, m_\alpha^2, m_\beta^2) \\ & + \frac{q_{2\mu_1} q_{2\mu_2}}{q_2^2} \mathcal{I}\Sigma_L^{V-V}(s, m_\alpha^2, m_\beta^2). \end{aligned} \quad (2.123)$$

For the sub-loop insertion from fermion self-energy we get

$$\begin{aligned} I_{\nu_1, \dots, \nu_R}^{1, M, 1} \\ = \frac{1}{\pi} \frac{\mu^{(4-D)}}{\pi(i\pi^{D/2})} \Sigma_{\alpha, \beta} \int_{(m_\alpha+m_\beta)^2}^{\infty} ds \int d^D q_2 \frac{q_{2, \nu_{F_{\mu_1 \mu_2}(q_2, s, m_\alpha, m_\beta)}} \dots q_{2, \nu_R}}{s - q_2^2 - i\epsilon} \frac{1}{\prod_{j=0}^M [(q_2 + k_{j, M})^2 - m_{j, M}^2]} \end{aligned} \quad (2.124)$$

where $G(q_2, s, m_\alpha, m_\beta)$ is given by

$$G(q_2, s, m_\alpha, m_\beta) = \left[\not{q}_2 \mathcal{I}\Sigma^f(s, m_\alpha^2, m_\beta^2) + m_f \mathcal{I}\Sigma_S^f(s, m_\alpha^2, m_\beta^2) \right]. \quad (2.125)$$

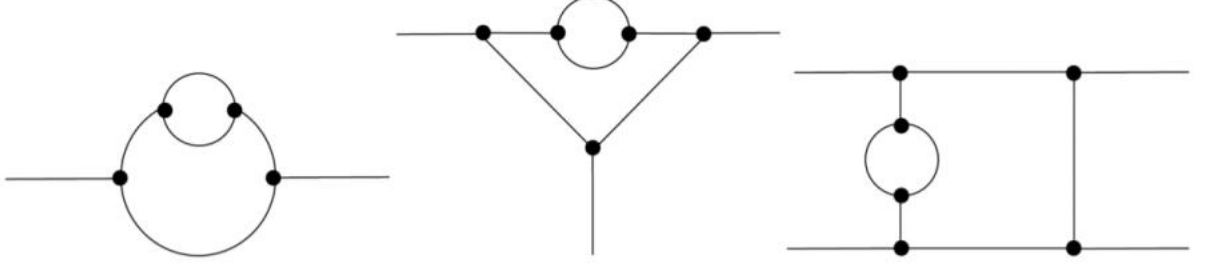


Figure 2.16: Examples of self-energy subloops

2.8 Renormalization in the Dispersion Approach

The vector boson self-energy insertion for diagrams such as in figure 2.16, has the following analytical structure for the amplitude

$$\Sigma_{ff}(k) = k \Sigma_V(k^2) + m \Sigma_S(k^2) \quad (2.126)$$

where k is the incoming momentum and m is the mass of the fermion. We know from [1] that the renormalized amplitude for fermion self-energy insertion is given by

$$\hat{\Sigma}_{ff} = \Sigma_{ff}(k) - \Sigma_{ff}(m) - \left. \frac{\partial \Sigma_{ff}}{\partial k} \right|_{k=m} (k - m) \quad (2.127)$$

and

$$\left. \frac{\partial \Sigma_{ff}}{\partial k} \right|_{k=m} (k - m) = \Sigma_V(m^2) + 2m^2 \left. \frac{\partial \Sigma_V}{\partial k^2} \right|_{k^2=m^2} + 2m^2 \left. \frac{\partial \Sigma_S}{\partial k^2} \right|_{k^2=m^2} \quad (2.128)$$

where Σ_V and Σ_S are the scalar and the vector part of the vacuum polarization function. Then we define

$$\Sigma'_V(m^2) = \left. \frac{\partial \Sigma_V}{\partial k^2} \right|_{k^2=m^2} \quad (2.129)$$

$$\Sigma'_S(m^2) = \left. \frac{\partial \Sigma_S}{\partial k^2} \right|_{k^2=m^2} \quad (2.130)$$

and finally we get

$$\begin{aligned}\hat{\Sigma}_{ff}(k) = & k\Sigma_V(k^2) + m\Sigma_S(k^2) - m\Sigma_V(m^2) - m\Sigma_S(m^2) \\ & - \left[\Sigma_V(m^2) + 2m^2\Sigma'_V(m^2) + 2m^2\Sigma'_S(m^2) \right] (k - m).\end{aligned}\tag{2.131}$$

Now, when we finally separate the vector part and the scalar part from $\hat{\Sigma}_{ff}(k)$ we get

$$\hat{\Sigma}_V(k^2) = \Sigma_V(k^2) - \Sigma_V(m^2) - 2m^2 \left[\Sigma'_V(m^2) + \Sigma'_S(m^2) \right] \tag{2.132}$$

$$\hat{\Sigma}_S(k^2) = \Sigma_S(k^2) - \Sigma_S(m^2) - 2m^2 \left[\Sigma'_V(m^2) + \Sigma'_S(m^2) \right]. \tag{2.133}$$

The last part of equation (2.133) and equation (2.132) are the UV-finite parts. We use the following dispersive representation of $\hat{\Sigma}_V(k^2)$ and $\hat{\Sigma}_S(k^2)$ [1]

$$\Sigma_{V,S}(k^2) = \frac{1}{\pi} \int_{m^2}^{\infty} \frac{\Im \Sigma_{V,S}(s)}{s - k^2 - i\epsilon} ds. \tag{2.134}$$

Also, as shown in Ref. [1] we see

$$\Sigma'_{V,S}(m^2) = \frac{1}{\pi} \int_{m^2}^{\infty} \frac{\Im \Sigma_{V,S}(s)}{(s - m^2 - i\epsilon)^2} ds \tag{2.135}$$

and by combining equation 2.134 and equation 2.135 we get

$$\begin{aligned}\hat{\Sigma}_{V,S}(k^2) = & \frac{k^2 - m^2}{\pi} \int_{m^2}^{\infty} ds \frac{\Im \Sigma_{V,S}}{(s - k^2)(s - m^2)} \\ & - \frac{2m^2}{\pi} \int_{m^2}^{\infty} ds \frac{\Im [\Sigma_V(s) + \Sigma_S(s)]}{(s - m^2)^2}\end{aligned}\tag{2.136}$$

In equation (2.136), the second part $\int_{m^2}^{\infty} ds \frac{\Im [\Sigma_V(s) + \Sigma_S(s)]}{(s - m^2)^2}$ is a convergent integral; it plays the role as a constant. The numerical evaluation is often challenging because the the numerical integration is highly unstable. However, the numerical value of $\int_{m^2}^{\infty} ds \frac{\Im [\Sigma_V(s) + \Sigma_S(s)]}{(s - m^2)^2}$ is equal to the the numerical value of the UV-finite part.

Substitution of equation (2.136) into the second-loop will result in the cancellation of $(k^2 - m^2)$ with one of the fermion propagators, where k^2 is the momentum of the insertion and m is the mass of the fermion in the insertion as shown in figure 2.16. This gives us the possibility to employ a computer-algebra approach, where the second-loop integral could be evaluated analytically, and after subtractions the dispersion integration can be carried out numerically.

Chapter 3

Results

The calculation of the effective fine structure constant using the Dyson-resummation technique involves the evaluation of many Feynman diagrams. In this thesis, I have only considered Quantum Electrodynamics (QED). For evaluating the vacuum polarization function up to one-loop level, we have used FEYNARTS and FORMCALC [7]. All the two-loop level Feynman diagrams are shown in figure 3.3, figure 3.4 and figure 3.5. These are the diagrams that gave rise to the numerically unstable Passarino-Veltman functions and an alternative representation to evaluate them had to be found. We have used the Dispersion representation explained in the paper [1].

3.1 Next to Leading Order (NLO) Correction

Since we are only considering QED, there were only nine Feynman diagrams in Next-to-Leading Order (NLO) calculations. The Feynman diagrams for NLO are shown in figure 3.1. As we have mentioned earlier, we did not evaluate these diagrams by hand. We used FEYNARTS and FORMCALC to generate the vacuum polarization function and did the numerical integration using LOOPTOOLS. Since NLO diagrams only contain one-loop, the calculated vacuum polarization function only gave one-point and

$$\gamma \rightarrow \gamma$$

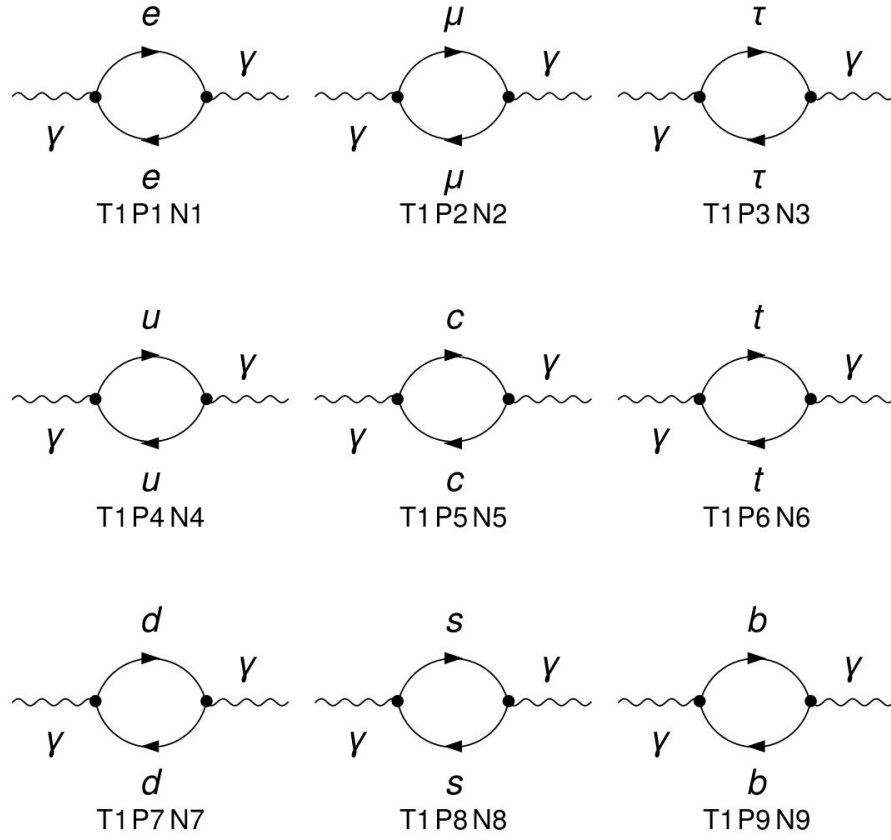


Figure 3.1: Feynman diagrams generated using FEYNARTS

two-point Passarino-Veltman functions which are numerically stable and we did not have to use the dispersion representation for them. We used the following equation to calculate the effective fine structure constant (code as shown in the Appendix):

$$\alpha_{\text{eff}} = \frac{\alpha(0)}{1 - \hat{\Pi}(k^2)} \quad (3.1)$$

where $\alpha(0)$ is the fine structure constant with no momentum transfer and $\alpha(p^2)$ is the renormalized vacuum polarization function up to one-loop level. Using the numerical results obtained from the one-loop level correction we plotted the graph in figure 3.2, this shows a clear indication of the difference in the fine structure constant at zero-momentum transfer and the effective fine structure constant.

The results shown in graph 3.2 (which has already been published in several articles) are a clear indication of the need to calculate the effective fine structure constant for high momentum transfer interaction. The distinctive kinks in the graphs are due to the threshold limit of the particles that have been considered in the loops. In the next section, we showed how we did that for Next-to-the-Next Leading Order (NNLO) interactions in QED.

3.2 Next-to-the-Next Leading Order (NNLO) Correction

For the analysis of the NNLO Feynman diagrams, the diagrams are separated into two categories: NNLO self-energy topologies and the NNLO triangle topologies. The methods used to evaluate these two categories of topologies are different and are explained in the next sub-sections.

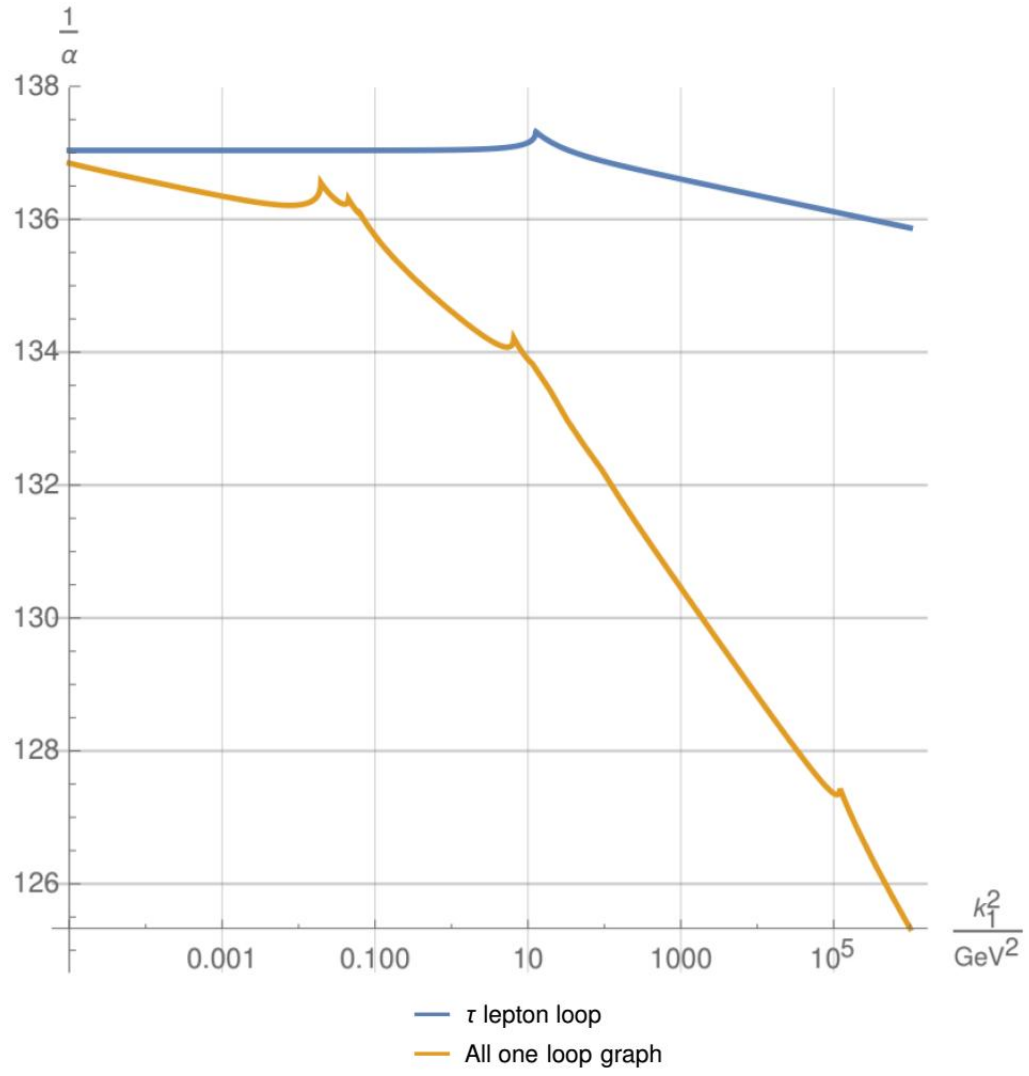


Figure 3.2: One-loop level correction for the fine structure constant

3.2.1 Two-loop self-energy topologies

$$\gamma \rightarrow \gamma$$

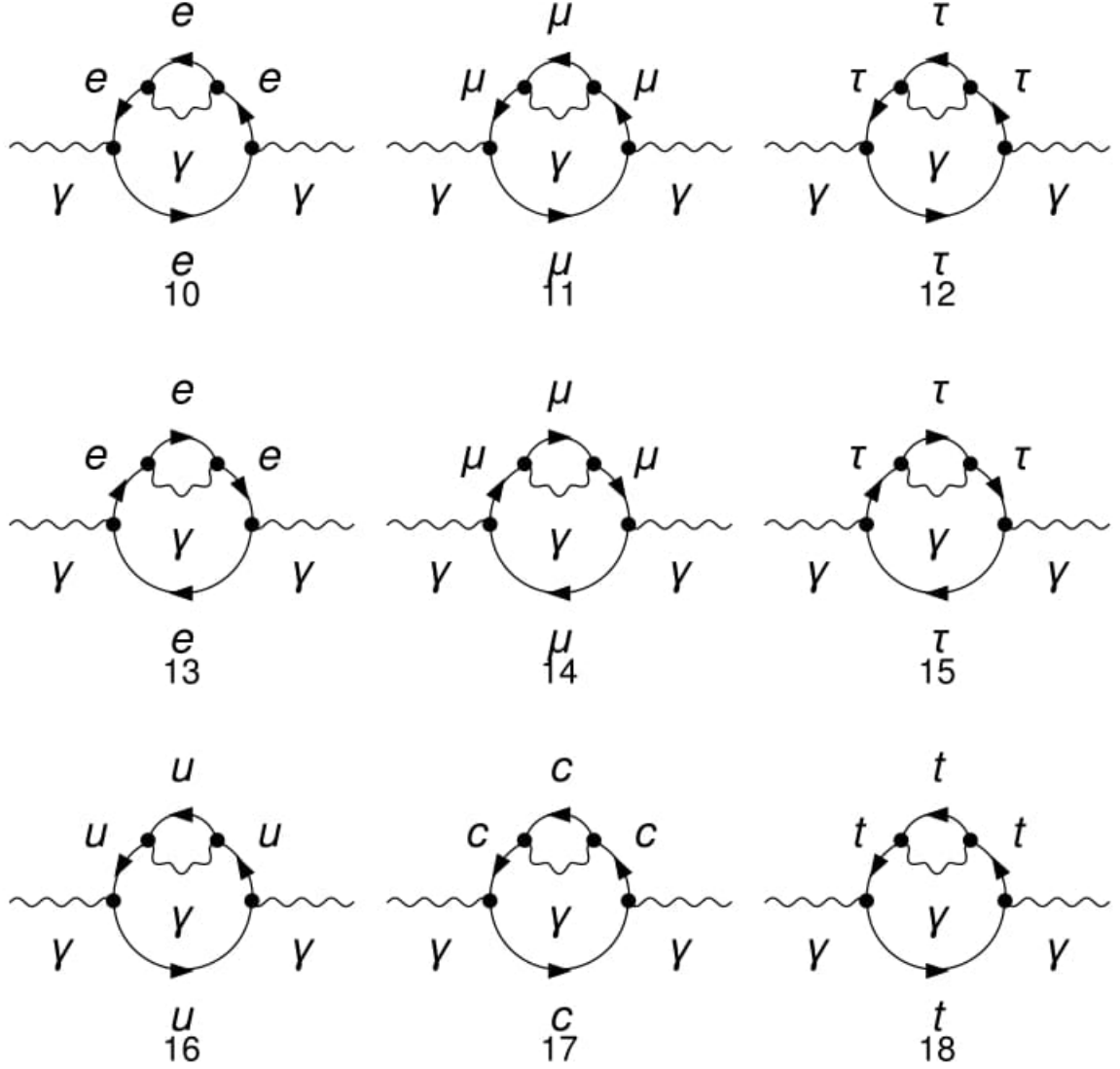


Figure 3.3: Two-loop self-energy topologies ($\gamma \mapsto \gamma$)

All the two-loop self-energy topologies for the calculation are shown in figure 3.3 and 3.4. These diagrams have been generated using FEYNARTS and FORMCALC to create the scattering matrices (S-matrix) for these topologies. In the S-matrix we see

$$\gamma \rightarrow \gamma$$

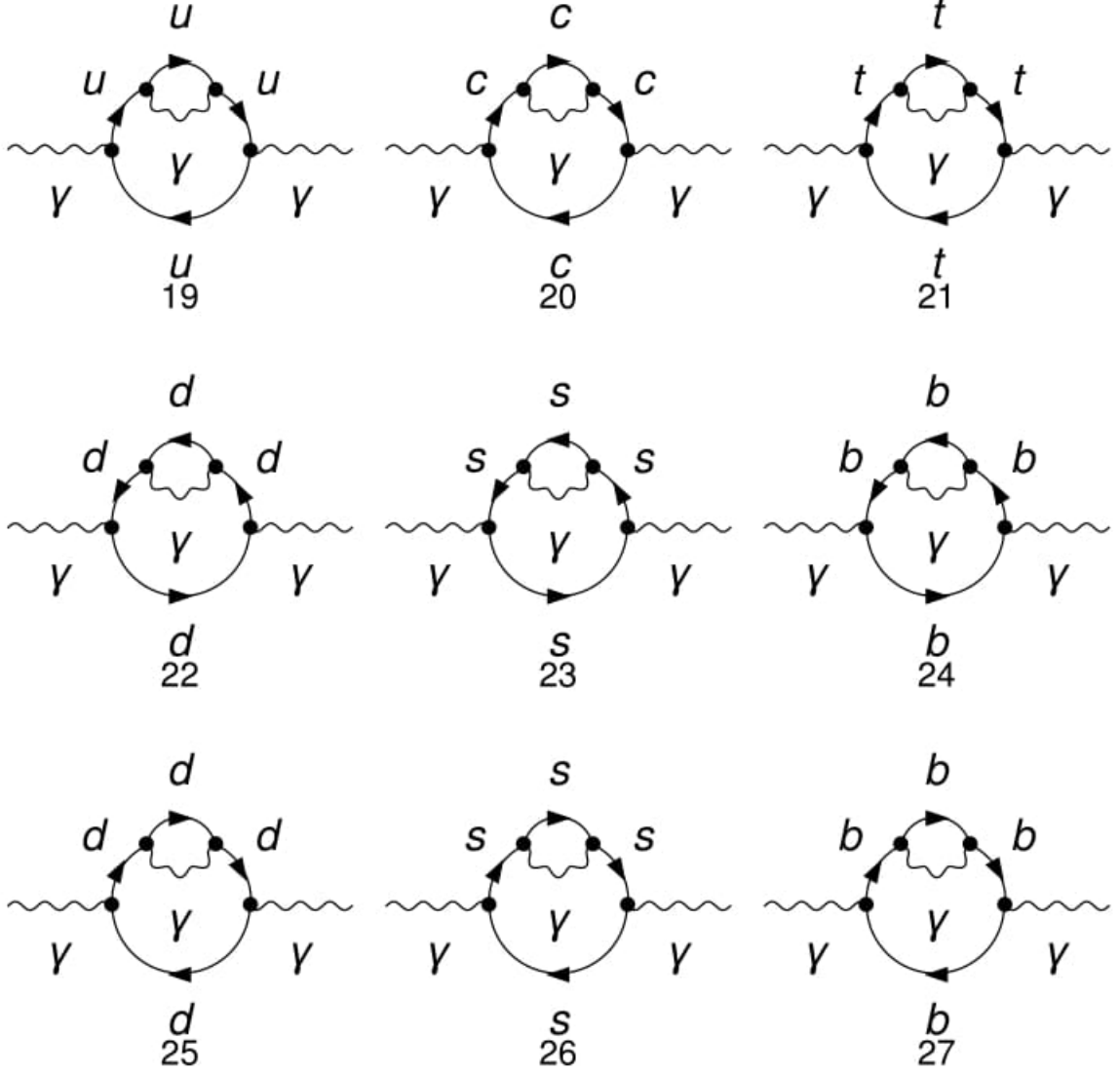


Figure 3.4: Two-loop self-energy topologies ($\gamma \mapsto \gamma$)

that each diagram has five propagators; calculating them gives us C-functions (three-point) and D-functions (four-point). However, these functions are not numerically stable and cannot be calculated using the existing numerical packages. So, we had to use the Dispersion approach as explained in earlier chapters and in the paper [1].

All the two-loop self-energy topologies have essentially the same graph except for two major differences: the mass of the leptons and quarks and the coupling constant between the leptons and quarks. The up-quarks, charm-quarks and the top-quarks have the same coupling constant because of their electric charges ($\frac{2}{3}$ the charge of an electron). The down-type quarks are the down-quarks, strange-quarks and the bottom-quarks which also has the same electric charge ($-\frac{1}{3}$ the charge of an electron). Finally, the renormalized vacuum polarization function was calculated using the method explained in section 2.8 of chapter 2. The detailed code is shown in the Appendix.

As we can see, the vacuum polarization in the denominator of equation (2.115) is the numerical quantity that contributes to the running of the fine structure constant. We have calculated the contribution of the leptons and quarks up to two-loop level in the vacuum polarization function and tabulated them. Table 3.1 shows the correction of the vacuum polarization function when only the leptonic two-loop diagrams are considered. Similarly, when we add the quark-type topologies, we see the difference in the numerical value of the vacuum polarization function in table 3.2. These tables show us the correction to the running of the fine structure which lead us to finally tabulate the effective fine structure constant.

Momentum transfer squared/ GeV^2	Vacuum polarization function correction due to Leptons
0.001	0.00012048246763488457
0.1	0.0002812312188941
10.0	0.00027932401957754776
1000.0	0.00047956039021741965
100000	0.0004535550036151077
1000000	0.0004405454537314081

Table 3.1: The contributions of the Leptons in two-loop vacuum polarization function

Momentum transfer squared/ GeV^2	Vacuum polarization function correction due to Leptons and Quarks
0.001	0.000020810356655247066
0.1	0.00027361764606209795
10.0	0.0003708261066308674
1000.0	0.0006321762510106652
100000	0.0006220256362705225
1000000	0.0007480856478050458

Table 3.2: The contributions of the Leptons and Quarks in two-loop vacuum polarization function

Similarly, we tabulated the correction in the vacuum polarization function when the triangle graphs are calculated, which is shown in table 3.3 and finally in table 3.4 shows us the correction in the vacuum polarization function when both NLO and NNLO graphs are considered.

Momentum transfer squared/ GeV^2	Vacuum polarization function correction due to all two-loops
0.001	0.0000209593893316985
0.1	0.00027338164478734966
10.0	0.00037041624847941276
1000.0	0.0006315322406318514
100000	0.000621140603685161
1000000	0.0007470983294597187

Table 3.3: The contributions of all two-loop graphs in two-loop vacuum polarization function

3.2.2 Two-loop triangle topologies

All the two-loop triangle topologies are shown in figure 3.5. Neither the dispersion approach used in evaluating the two-loop self-energy topologies could be used directly in the two-loop triangle topologies nor could we use the straightforward numerical

Momentum transfer squared/ GeV^2	Vacuum polarization function correction due to NLO and NNLO graphs
0.001	0.005004016603699983
0.1	0.00964054125350663
10.0	0.023317684755984832
1000.0	0.048653735079418794
100000	0.07122482924961453
1000000	0.08617354677478717

Table 3.4: The contributions of both NLO and NNLO in vacuum polarization function

methods for evaluating these topologies. To begin with we calculated the S-matrix of the insertion for one of the diagrams of two-loop triangle topologies. A generic topology of such insertion is shown in figure 3.6.

The CREATEAMP function in FORMCALC was then used to calculate that amplitude. All the Dirac form-factors that were in the amplitude were separated. The non-vanishing Lorentz contributions comes from the following:

$$\gamma_\mu \times C_1 \tag{3.2}$$

$$\not{k}_1 \not{k}_2 \gamma_\mu \times C_2 \tag{3.3}$$

$$k_{1\mu} m \not{k}_2 \times C_3 \tag{3.4}$$

$$k_{2\mu} m \not{k}_2 \times C_4 \tag{3.5}$$

where k_1 and k_2 are the incoming momenta shown in figure 3.6 and C_1 , C_2 , C_3 and C_4 are the coefficients associated with each form-factors. The Dirac form-factors are then plotted against the square of the momenta which is shown in figure 3.7, 3.8, 3.9 and 3.10.

From the plots in figure 3.7 we see that only one of the graphs gives us a significant numerical value. The other graphs are almost vanishing which can be ignored for

$$\gamma \rightarrow \gamma$$

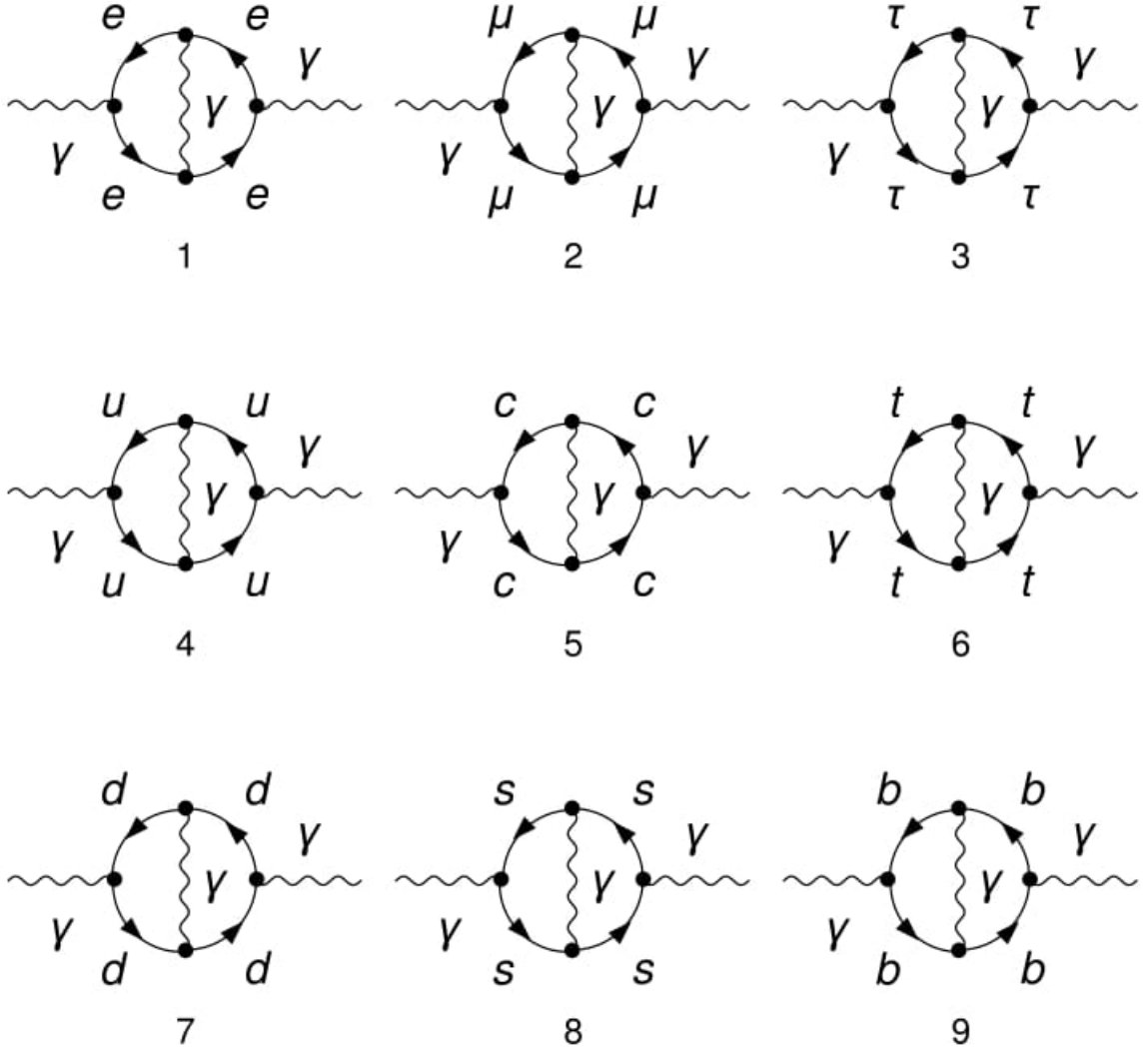


Figure 3.5: Two-loop triangle topologies ($\gamma \mapsto \gamma$)

NNLO calculations. This gives us an approximation for insertions like in figure 3.6 and we calculated all the graphs for the different masses in our QED NNLO calculations. We have plotted the graphs for leptons electrons, muons, and tau and for all the quarks, up, down, charm, strange, bottom and top. A similar kind of plot is obtained

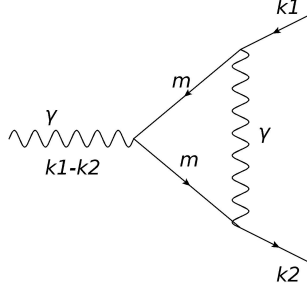


Figure 3.6: A general insertion for two-loop triangle topology

for all the different types of particles.

We used a bulk-approximation method and have taken an average value for the Dirac form-factor. The average values for all the different types of particles are shown in table 3.5.

Types of particle	Mean value of Dirac form factor
Electron	-0.000029251336819614
Muon	-0.000029251336819614
Tau	-0.0000292359781139407
Up	$8.66688281254374 \times 10^{-6}$
Down	$-1.08336034580833 \times 10^{-6}$
Charm	$8.65764030942123 \times 10^{-6}$
Strange	$-1.08331217418434 \times 10^{-6}$
Top	$5.06935613130901 \times 10^{-6}$
Bottom	$-1.08338541665249 \times 10^{-6}$

Table 3.5: Table showing the mean value for the Dirac form factor

When we substitute these numerical values into the triangle graphs, the graphs essentially become one-loop self-energy graphs with an extra numerical pre-factor. This is shown in figure 3.11, where the shaded region represents the insertion, i.e. the numerical values in the table 3.5. Finally, we used FORMCALC to get the vacuum polarizaton function and LOOPTOOLS to get the corrections for the effective fine structure constant.

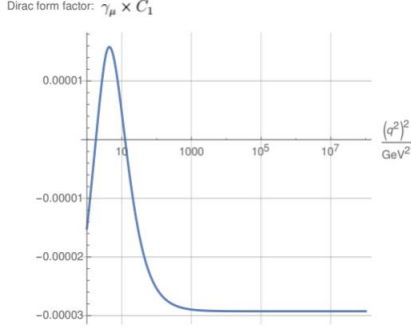


Figure 3.7: Dirac form-factor in eq: 3.2

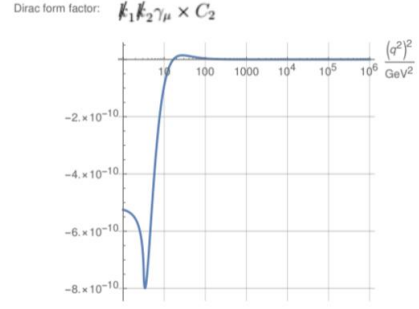


Figure 3.8: Dirac form-factor in eq: 3.3

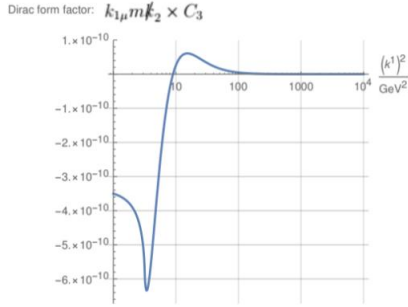


Figure 3.9: Dirac form-factor in eq: 3.4

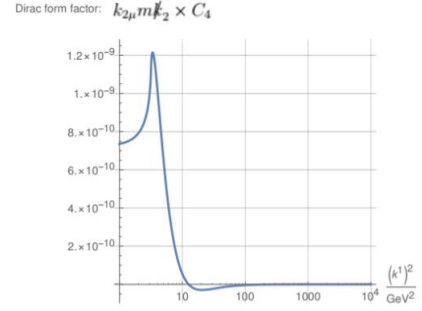


Figure 3.10: Dirac form-factor in eq: 3.5

3.3 Results

With the techniques described above we get the numerical values for the effective fine structure constant up to Next-to-the-Next to the Leading order. The percentage difference between the fine structure constant with zero momentum transfer and the effective fine structure constant is shown in table 3.6. In the table 3.6 the momentum-transferred was chosen arbitrarily.

As expected, we see a sub-percent level accuracy in our results in table 3.6. We have also plotted a graph for the inverse of the effective fine structure constant upto NNLO which is shown in figure 3.12.

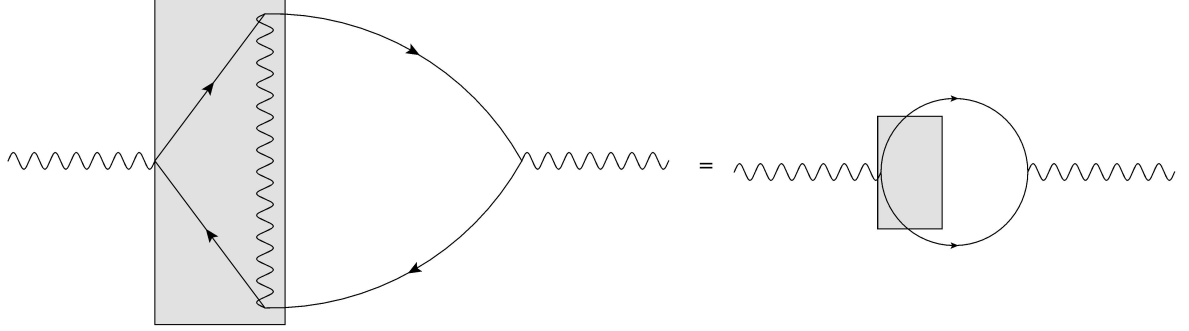


Figure 3.11: A triangle topology after substituting the insertion

Momentum transfer squared/ GeV^2	$\frac{\alpha_{\text{up to 2-Loops}} - \alpha_{\text{up to 1-Loop}}}{\alpha_{\text{zero momentum transfer}(\frac{1}{137})}} \times 100$
0.001	-0.00207361097745995
0.1	0.027290109718436373
10.0	0.038004453663620374
1000.0	0.06823448932844478
100000	0.0703759794650427
1000000	0.08739471414560551

Table 3.6: Relative correction to the effective fine structure constant with NNLO contributions

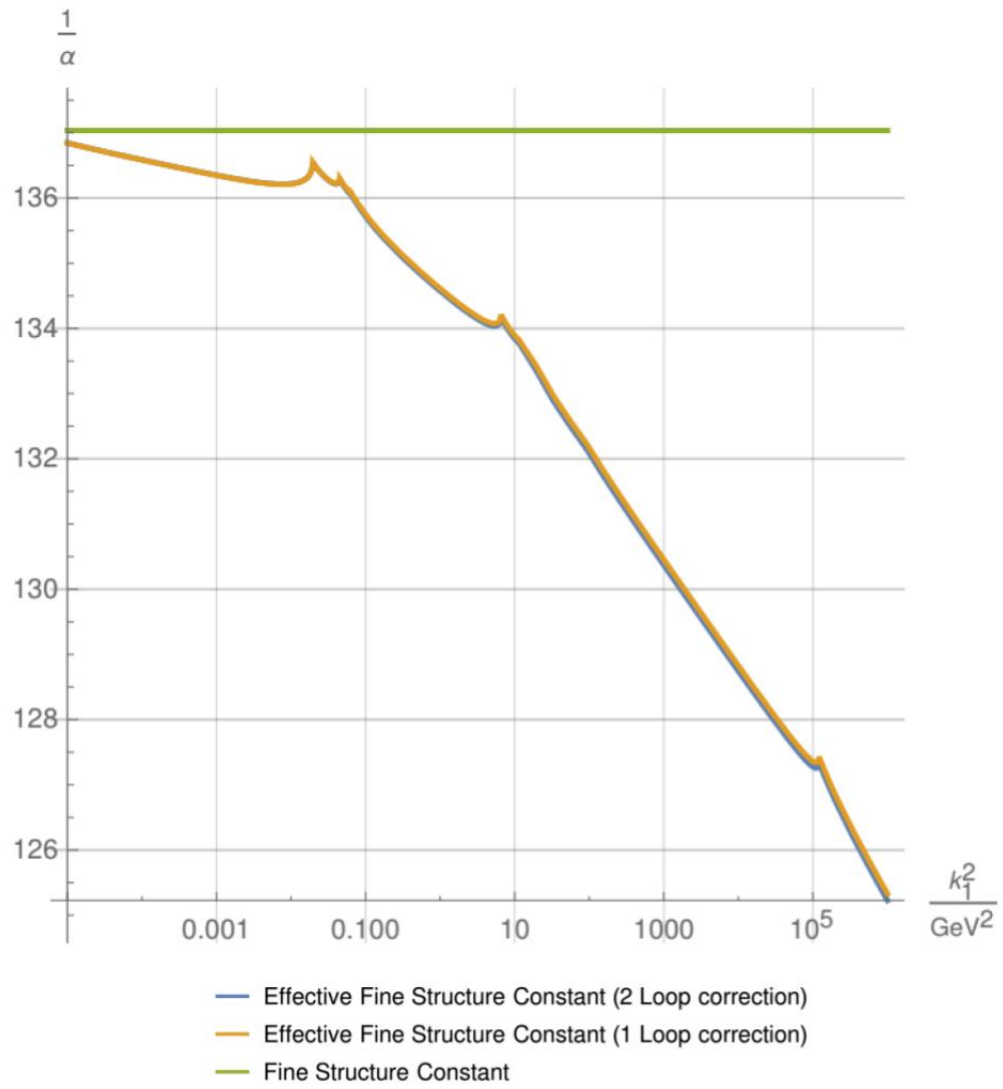


Figure 3.12: Plot of the Effective Fine Structure Constant upto NNLO correction

Chapter 4

Conclusion

4.1 Summary of Results

In chapter 2, we have seen the contribution of the Next to the Next to the Leading Order contribution and how it changes the numerical value of the fine structure constant at high momentum transfer.

The behaviour shown in the plots and the tables in 3 is the one that we were expecting. The effective fine structure constant at low momentum transfer coincides with the Bohr's approximation value of $\frac{1}{137}$.

In table 3.6 in chapter 3, we saw that the percentage accuracy for an addition of the Next to the Next to the Leading Order (NNLO) is at the sub-percent level which was also expected.

4.2 Mathematica

Mathematica provided a nice platform to calculate the theoretical predictions. All the well developed packages we used made our calculations easier and manageable allowing us to focus on the physics, rather than the tedious mathematical analysis.

The packages that were used for the calculations in this thesis are FEYNARTS, FORMCALC, LOOPTOOLS, X and COLLIERSLINK. The packages provided us with a lot of options for optimization and also provided us with tools to implement new methods for solving Feynman diagrams beyond one-loop topologies. Although we have used our own renormalization method for both Next to the Leading Order (NLO) and Next-to-the-Next to the Leading Order (NNLO), there is a built-in algorithm for the NLO topologies in FORMCALC which can be easily used to get a renormalized amplitude.

4.3 Future Work

Mathematica was very useful for the optimization of the calculations involved in the thesis. However, compared to low-level programming languages such as C++ or FORTRAN it is still much slower. In addition, even with all the packages which are publicly available we are only able to perform one-loop level calculations automatically. In order to do all the two-loop calculations we had to manually interfere with the existing functions in those packages.

In the future, I would like to look for methods and design algorithms that are able to do all these calculations automatically in Mathematica. In addition, when we consider QCD, the number of diagrams increases dramatically and the calculations become slower. In certain cases they take days, which is mainly due to the NINTEGRATE function in Mathematica not being optimized for multi-variable calculus. Also, the fact that most of the integrations involved in multi-loop level calculations are numerically unstable, does not help. One of my future targets is to design a more efficient numerical integration either in Mathematica or a low level programming language.

Futhermore, we can use tensor reduction and tensor decomposition to convert

Passarino Veltman functions as shown in paper [1]. In that case, we can convert three-loop functions and four-loop functions into more stable two-loop functions which will make our calculations of the triangle topologies and even box topologies easier and faster. Currently, I am working on this using Python 3.

Appendix A

Mathematica Notebook of the Calculations

```

In[ ]:= << FeynArts`
        << FormCalc`

FeynArts 3.10 (21 Jan 2019)
by Hagen Eck, Sepp Kueblbeck, and Thomas Hahn

FormCalc 9.6 (16 Apr 2018)
by Thomas Hahn

In[ ]:= NLOSE = CreateTopologies[1, 1 → 1, ExcludeTopologies →
      {Tadpoles, Boxes, Pentagons, Hexagons, AllBoxes, WFCorrections, Triangles}];
NLOSEfields = InsertFields[NLOSE, {V[1]} → {V[1]}, Restrictions → {QEDOnly},
      InsertionLevel → {Particles}, Model → "SM", GenericModel → "Lorentz"];

loading generic model file /home/reefat/packages1/FeynArts-3.10/Models/Lorentz.gen
> $GenericMixing is OFF
generic model {Lorentz} initialized

loading classes model file /home/reefat/packages1/FeynArts-3.10/Models/SM.mod

$CKM = False

> 46 particles (incl. antiparticles) in 16 classes
> $CounterTerms are ON
> 88 vertices
> 115 counterterms of order 1
> 6 counterterms of order 2
classes model {SM} initialized

Excluding 2 Generic, 21 Classes, and 25 Particles fields

inserting at level(s) {Particles}
> Top. 1: 0 Particles insertions
> Top. 2: 9 Particles insertions

Restoring 2 Generic, 21 Classes, and 25 Particles fields
in total: 9 Particles insertions

```

```

In[*]:= SetOptions[CreateFeynAmp, Truncated → True];
SetOptions[DeclareProcess, OnShell → False, Transverse → False];
SetOptions[CalcFeynAmp, FermionChains → VA,
  FermionOrder → None, PaVeReduce → True, SortDen → True,
  CombineDen → True, CancelQ2 → True, Dimension → D];

In[*]:= NLOSEfieldsCreate = CreateFeynAmp[NLOSEfields];

creating amplitudes at level(s) {Particles}
> Top. 1: 9 Particles amplitudes
in total: 9 Particles amplitudes

In[*]:= NLOSEfieldsCalc = CalcFeynAmp[NLOSEfieldsCreate] //. Subexpr[] //. Abbr[] //.
  Pair[k[1], k[1]] → Q2 //. Finite → 1;

preparing FORM code in /home/reefat/fc-amp-13.frm
running FORM...
ok

In[*]:= IGram[x_] =  $\frac{1}{x}$ ;

In[*]:= metricpartNLO[Q2_] = FullSimplify[
  Coefficient[NLOSEfieldsCalc[[1]], MetricTensor[Lor1, Lor2]] //. Finite → 1];

In[*]:= metricpartNLOZERO[Q2_] = FullSimplify[D[metricpartNLO[Q2], Q2]] //. Q2 → Q2Z;

In[*]:= metricpartNLOREN[Q2_] = FullSimplify[metricpartNLO[Q2] - Q2 * metricpartNLOZERO[Q2]];

In[*]:= metricpartUVREN[Q2_, BH_, BH2_] :=

$$\begin{aligned}
& -\frac{1}{288 \pi^5} i \text{Alfa} \left( -\frac{1}{\left(\frac{1}{10000} + 2 \text{BH}\right) Q2} 30000 \left( \left( \text{BH}^2 - \left(\frac{1}{10000} + \text{BH}\right)^2 + 2 Q2 \right) \right. \right. \\
& \quad \left. \text{A0} \left[ \left(\frac{1}{10000} + \text{BH}\right)^2 \right] \left( 4 \text{BH}^2 \text{BH2} \left( -\frac{\text{Alfa B0i}[d\text{bb0}, \text{BH2}, 0, \text{BH2}]}{\pi} - \frac{1}{2 \pi} \right. \right. \right. \\
& \quad \quad \left. \left. \left. \text{Alfa} \left( -\text{B0i}[d\text{bb0}, \text{BH2}, 0, \text{BH2}] - \text{B0i}[d\text{bb1}, \text{BH2}, 0, \text{BH2}] \right) \right) - \right. \right. \\
& \quad \left. 2 \left( \text{BH}^2 + \left(\frac{1}{10000} + \text{BH}\right)^2 \right) \text{BH2} \left( -\frac{\text{Alfa B0i}[d\text{bb0}, \text{BH2}, 0, \text{BH2}]}{\pi} - \frac{1}{2 \pi} \right. \right. \\
& \quad \quad \left. \left. \left. \text{Alfa} \left( -\text{B0i}[d\text{bb0}, \text{BH2}, 0, \text{BH2}] - \text{B0i}[d\text{bb1}, \text{BH2}, 0, \text{BH2}] \right) \right) \right) \right) + \\
& \quad \text{A0}[\text{BH}^2] \left( -4 \text{BH}^2 \text{BH2} \left( \text{BH}^2 - \left(\frac{1}{10000} + \text{BH}\right)^2 + 2 Q2 \right) \left( -\frac{\text{Alfa B0i}[d\text{bb0}, \text{BH2}, 0, \text{BH2}]}{\pi} - \right. \right. \\
& \quad \quad \left. \left. \frac{1}{2 \pi} \text{Alfa} \left( -\text{B0i}[d\text{bb0}, \text{BH2}, 0, \text{BH2}] - \text{B0i}[d\text{bb1}, \text{BH2}, 0, \text{BH2}] \right) \right) - \right. \\
& \quad \left. 2 \text{BH2} \left( -\text{BH}^4 + \left(\frac{1}{10000} + \text{BH}\right)^4 - 6 \text{BH}^2 Q2 + 2 \left(\frac{1}{10000} + \text{BH}\right)^2 Q2 \right) \right)
\end{aligned}$$


```

$$\begin{aligned}
& \left(-\frac{\text{Alfa } B0i[dbb0, BH2, 0, BH2]}{\pi} - \frac{1}{2\pi} \right. \\
& \quad \left. \text{Alfa} (-B0i[dbb0, BH2, 0, BH2] - B0i[dbb1, BH2, 0, BH2]) \right) + \\
& B0i[bb0, Q2, BH^2, \left(\frac{1}{10000} + BH \right)^2] \left(4 BH^2 BH2 \left(\left(BH^2 - \left(\frac{1}{10000} + BH \right)^2 \right)^2 - \right. \right. \\
& \quad \left. \left. 2 \left(BH^2 + \left(\frac{1}{10000} + BH \right)^2 \right) Q2 - 2 Q2^2 \right) \left(-\frac{\text{Alfa } B0i[dbb0, BH2, 0, BH2]}{\pi} - \frac{1}{2\pi} \right. \right. \\
& \quad \left. \left. \frac{1}{2\pi} \text{Alfa} (-B0i[dbb0, BH2, 0, BH2] - B0i[dbb1, BH2, 0, BH2]) \right) - \right. \\
& \quad 2 BH2 \left(\left(BH^2 - \left(\frac{1}{10000} + BH \right)^2 \right)^2 \left(BH^2 + \left(\frac{1}{10000} + BH \right)^2 \right) + \right. \\
& \quad \left(BH^4 - 10 BH^2 \left(\frac{1}{10000} + BH \right)^2 + \left(\frac{1}{10000} + BH \right)^4 \right) Q2 - \\
& \quad \left. 2 \left(BH^2 + \left(\frac{1}{10000} + BH \right)^2 \right) Q2^2 \right) \left(-\frac{\text{Alfa } B0i[dbb0, BH2, 0, BH2]}{\pi} - \frac{1}{2\pi} \right. \\
& \quad \left. \left. \text{Alfa} (-B0i[dbb0, BH2, 0, BH2] - B0i[dbb1, BH2, 0, BH2]) \right) \right) + \\
& 2 \left(-6 BH^2 BH2 \left(-\frac{\text{Alfa } B0i[dbb0, BH2, 0, BH2]}{\pi} - \frac{1}{2\pi} \text{Alfa} \right. \right. \\
& \quad \left. \left. (-B0i[dbb0, BH2, 0, BH2] - B0i[dbb1, BH2, 0, BH2]) \right) - \right. \\
& \quad 6 \left(\frac{1}{10000} + BH \right)^2 BH2 \left(-\frac{\text{Alfa } B0i[dbb0, BH2, 0, BH2]}{\pi} - \frac{1}{2\pi} \right. \\
& \quad \left. \left. \text{Alfa} (-B0i[dbb0, BH2, 0, BH2] - B0i[dbb1, BH2, 0, BH2]) \right) + \right. \\
& \quad \left. 2 BH2 Q2 \left(-\frac{\text{Alfa } B0i[dbb0, BH2, 0, BH2]}{\pi} - \frac{1}{2\pi} \right. \right. \\
& \quad \left. \left. \text{Alfa} (-B0i[dbb0, BH2, 0, BH2] - B0i[dbb1, BH2, 0, BH2]) \right) \right) \Bigg);
\end{aligned}$$

$$\begin{aligned}
\text{metricpartDispersion}[Q2_ , BH_ , BH2_] := & \\
& \frac{1}{288 \pi^5 Q2 (BH^2 - s)} \text{I} \text{Alfa} \left(-\frac{1}{\pi^2 (-BH2 + s)} 6 BH^2 ((-BH^2 - 2 Q2 + s) A0[BH^2] + \right. \\
& (BH^2 + 2 Q2 - s) A0[s] + 2 Q2 (BH^2 - s + (2 BH^2 + Q2) B0i[bb0, Q2, BH^2, BH^2]) + \\
& (BH^4 - 2 Q2^2 - 2 Q2 s + s^2 - 2 BH^2 (Q2 + s)) B0i[bb0, Q2, BH^2, s]) \\
& \text{Im}[Alfa B0i[bb0, s, \theta, BH2]] - \frac{1}{2 \pi^2 (-BH2 + s)} (-2 Q2 (-9 BH^2 + Q2 - 3 s) (BH^2 - s) + \\
& 3 ((-BH^4 - 6 BH^2 Q2 + s (2 Q2 + s)) A0[BH^2] + (BH^2 + 2 Q2 - s) (BH^2 + s) A0[s] + \\
& 4 BH^2 Q2 (2 BH^2 + Q2) B0i[bb0, Q2, BH^2, BH^2] + (BH^6 + BH^4 (Q2 - s) + \\
& s (-2 Q2^2 + Q2 s + s^2) - BH^2 (2 Q2^2 + 10 Q2 s + s^2)) B0i[bb0, Q2, BH^2, s]) \\
& \text{Im}[Alfa (-B0i[bb0, s, \theta, BH2] - B0i[bb1, s, \theta, BH2])] - \frac{1}{Q2 ZNNLO^2} Q2^2 \\
& \left(-\frac{1}{\pi^2 (-BH2 + s)} 6 BH^2 ((BH^2 - s) A0[BH^2] - BH^2 A0[s] + s A0[s] + \right. \\
& 2 Q2 ZNNLO^2 B0i[bb0, Q2 ZNNLO, BH^2, BH^2] - BH^4 B0i[bb0, Q2 ZNNLO, BH^2, s] - \\
& 2 Q2 ZNNLO^2 B0i[bb0, Q2 ZNNLO, BH^2, s] + 2 BH^2 s B0i[bb0, Q2 ZNNLO, BH^2, s] - \\
& s^2 B0i[bb0, Q2 ZNNLO, BH^2, s] + 4 BH^2 Q2 ZNNLO^2 B0i[dbb0, Q2 ZNNLO, BH^2, BH^2] + \\
& 2 Q2 ZNNLO^3 B0i[dbb0, Q2 ZNNLO, BH^2, BH^2] + \\
& Q2 ZNNLO (BH^4 - 2 Q2 ZNNLO^2 - 2 Q2 ZNNLO s + s^2 - 2 BH^2 (Q2 ZNNLO + s)) \\
& B0i[dbb0, Q2 ZNNLO, BH^2, s]) \text{Im}[Alfa B0i[bb0, s, \theta, BH2]] - \\
& \frac{1}{2 \pi^2 (-BH2 + s)} (2 Q2 ZNNLO^2 (-BH^2 + s) + 3 (BH^4 - s^2) A0[BH^2] + \\
& 3 (-BH^4 + s^2) A0[s] + 12 BH^2 Q2 ZNNLO^2 B0i[bb0, Q2 ZNNLO, BH^2, BH^2] - \\
& 3 (2 Q2 ZNNLO^2 + (BH^2 - s)^2) (BH^2 + s) B0i[bb0, Q2 ZNNLO, BH^2, s] + \\
& 3 Q2 ZNNLO (4 BH^2 Q2 ZNNLO (2 BH^2 + Q2 ZNNLO) B0i[dbb0, Q2 ZNNLO, BH^2, BH^2] + \\
& (BH^6 + BH^4 (Q2 ZNNLO - s) + s (-2 Q2 ZNNLO^2 + Q2 ZNNLO s + s^2) - \\
& BH^2 (2 Q2 ZNNLO^2 + 10 Q2 ZNNLO s + s^2)) B0i[dbb0, Q2 ZNNLO, BH^2, s]) \\
& \left. \left. \left. \text{Im}[Alfa (-B0i[bb0, s, \theta, BH2] - B0i[bb1, s, \theta, BH2])]\right)\right)\right);
\end{aligned}$$

$$\begin{aligned}
\text{downTypeMetricpartUVREN}[Q2_ , BD_ , BD2_] := & \\
& \frac{1}{162 \left(\frac{1}{10000} + 2 BD \right) \pi^5 Q2} 625 \text{I} \text{Alfa} \left(3 \left(B0i[bb0, Q2, BD^2, \left(\frac{1}{10000} + BD \right)^2] \right. \right. \\
& \left(\frac{1}{100000000} \left(\frac{1}{10000} + 2 BD \right)^2 \left(4 BD^2 BD2 \left(-\frac{Alfa B0i[dbb0, BD2, \theta, BD2]}{\pi} - \right. \right. \right. \\
& \left. \frac{1}{2 \pi} Alfa (-B0i[dbb0, BD2, \theta, BD2] - B0i[dbb1, BD2, \theta, BD2]) \right) - 2 \\
& \left(BD^2 + \left(\frac{1}{10000} + BD \right)^2 \right) BD2 \left(-\frac{Alfa B0i[dbb0, BD2, \theta, BD2]}{\pi} - \right. \\
& \left. \frac{1}{2 \pi} Alfa (-B0i[dbb0, BD2, \theta, BD2] - B0i[dbb1, BD2, \theta, BD2]) \right) \left. \left. \right) \right) - \\
& 2 Q2^2 \left(4 BD^2 BD2 \left(-\frac{Alfa B0i[dbb0, BD2, \theta, BD2]}{\pi} - \frac{1}{2 \pi} Alfa \right. \right.
\end{aligned}$$

$$\begin{aligned}
& \left(-B\theta i[dbb0, BD2, 0, BD2] - B\theta i[dbb1, BD2, 0, BD2] \right) - \\
& 2 \left(BD^2 + \left(\frac{1}{10000} + BD \right)^2 \right) BD2 \left(-\frac{Alfa B\theta i[dbb0, BD2, 0, BD2]}{\pi} - \right. \\
& \quad \left. \frac{1}{2\pi} Alfa (-B\theta i[dbb0, BD2, 0, BD2] - B\theta i[dbb1, BD2, 0, BD2]) \right) + \\
& Q2 \left(-8 BD^2 \left(BD^2 + \left(\frac{1}{10000} + BD \right)^2 \right) BD2 \left(-\frac{Alfa B\theta i[dbb0, BD2, 0, BD2]}{\pi} - \right. \right. \\
& \quad \left. \frac{1}{2\pi} Alfa (-B\theta i[dbb0, BD2, 0, BD2] - B\theta i[dbb1, BD2, 0, BD2]) \right) - \\
& 2 \left(BD^4 - 10 BD^2 \left(\frac{1}{10000} + BD \right)^2 + \left(\frac{1}{10000} + BD \right)^4 \right) BD2 \\
& \left(-\frac{Alfa B\theta i[dbb0, BD2, 0, BD2]}{\pi} - \frac{1}{2\pi} Alfa (-B\theta i[dbb0, BD2, 0, BD2] - \right. \\
& \quad \left. B\theta i[dbb1, BD2, 0, BD2]) \right) + \left(BD^2 - \left(\frac{1}{10000} + BD \right)^2 + 2 Q2 \right) \\
& A0 \left[\left(\frac{1}{10000} + BD \right)^2 \right] \left(4 BD^2 BD2 \left(-\frac{Alfa B\theta i[dbb0, BD2, 0, BD2]}{\pi} - \frac{1}{2\pi} \right. \right. \\
& \quad \left. Alfa (-B\theta i[dbb0, BD2, 0, BD2] - B\theta i[dbb1, BD2, 0, BD2]) \right) - \\
& 2 \left(BD^2 + \left(\frac{1}{10000} + BD \right)^2 \right) BD2 \left(-\frac{Alfa B\theta i[dbb0, BD2, 0, BD2]}{\pi} - \frac{1}{2\pi} \right. \\
& \quad \left. Alfa (-B\theta i[dbb0, BD2, 0, BD2] - B\theta i[dbb1, BD2, 0, BD2]) \right) + \\
& A0[BD^2] \left(-2 BD^4 BD2 \left(-\frac{Alfa B\theta i[dbb0, BD2, 0, BD2]}{\pi} - \frac{1}{2\pi} \right. \right. \\
& \quad \left. Alfa (-B\theta i[dbb0, BD2, 0, BD2] - B\theta i[dbb1, BD2, 0, BD2]) \right) + \\
& 4 BD^2 BD2 \left(\left(\frac{1}{10000} + BD \right)^2 - 2 Q2 \right) \left(-\frac{Alfa B\theta i[dbb0, BD2, 0, BD2]}{\pi} - \right. \\
& \quad \left. \frac{1}{2\pi} Alfa (-B\theta i[dbb0, BD2, 0, BD2] - B\theta i[dbb1, BD2, 0, BD2]) \right) + \\
& 12 BD^2 BD2 Q2 \left(-\frac{Alfa B\theta i[dbb0, BD2, 0, BD2]}{\pi} - \frac{1}{2\pi} \right. \\
& \quad \left. Alfa (-B\theta i[dbb0, BD2, 0, BD2] - B\theta i[dbb1, BD2, 0, BD2]) \right) - \\
& 2 \left(\frac{1}{10000} + BD \right)^2 BD2 \left(\left(\frac{1}{10000} + BD \right)^2 + 2 Q2 \right) \left(-\frac{Alfa B\theta i[dbb0, BD2, 0, BD2]}{\pi} - \right. \\
& \quad \left. \frac{1}{2\pi} Alfa (-B\theta i[dbb0, BD2, 0, BD2] - B\theta i[dbb1, BD2, 0, BD2]) \right) - \\
& \frac{1}{5000} \left(\frac{1}{10000} + 2 BD \right) Q2 \left(-6 BD^2 BD2 \left(-\frac{Alfa B\theta i[dbb0, BD2, 0, BD2]}{\pi} - \frac{1}{2\pi} \right. \right. \\
& \quad \left. Alfa (-B\theta i[dbb0, BD2, 0, BD2] - B\theta i[dbb1, BD2, 0, BD2]) \right) - \\
& 6 \left(\frac{1}{10000} + BD \right)^2 BD2 \left(-\frac{Alfa B\theta i[dbb0, BD2, 0, BD2]}{\pi} - \frac{1}{2\pi} \right. \\
& \quad \left. Alfa (-B\theta i[dbb0, BD2, 0, BD2] - B\theta i[dbb1, BD2, 0, BD2]) \right) +
\end{aligned}$$

$$\begin{aligned} & 2 \text{ BD}^2 \text{ Q}^2 \left(-\frac{\text{Alfa } \text{B}0\text{i}[\text{dbb}0, \text{BD}2, 0, \text{BD}2]}{\pi} - \frac{1}{2\pi} \right. \\ & \quad \left. \text{Alfa}(-\text{B}0\text{i}[\text{dbb}0, \text{BD}2, 0, \text{BD}2] - \text{B}0\text{i}[\text{dbb}1, \text{BD}2, 0, \text{BD}2]) \right) \Bigg) + \\ & \frac{1}{\text{DownUv}^2} \text{Q}^2 \left(3 \left(\text{Q}^2 \text{ZDownUv } \text{B}0\text{i}[\text{dbb}0, \text{Q}^2 \text{ZDownUv}, \text{BD}^2, \left(\frac{1}{10000} + \text{BD} \right)^2] \right. \right. \\ & \quad \left(-\frac{1}{100000000} \left(\frac{1}{10000} + 2 \text{BD} \right)^2 \left(4 \text{BD}^2 \text{BD}^2 \left(-\frac{\text{Alfa } \text{B}0\text{i}[\text{dbb}0, \text{BD}2, 0, \text{BD}2]}{\pi} - \right. \right. \right. \\ & \quad \left. \left. \left. \frac{1}{2\pi} \text{Alfa}(-\text{B}0\text{i}[\text{dbb}0, \text{BD}2, 0, \text{BD}2] - \text{B}0\text{i}[\text{dbb}1, \text{BD}2, 0, \text{BD}2]) \right) \right) - \right. \\ & \quad \left. 2 \left(\text{BD}^2 + \left(\frac{1}{10000} + \text{BD} \right)^2 \right) \text{BD}^2 \left(-\frac{\text{Alfa } \text{B}0\text{i}[\text{dbb}0, \text{BD}2, 0, \text{BD}2]}{\pi} - \right. \right. \\ & \quad \left. \left. \frac{1}{2\pi} \text{Alfa}(-\text{B}0\text{i}[\text{dbb}0, \text{BD}2, 0, \text{BD}2] - \text{B}0\text{i}[\text{dbb}1, \text{BD}2, 0, \text{BD}2]) \right) \right) \Bigg) + \\ & 2 \text{Q}^2 \text{ZDownUv}^2 \left(4 \text{BD}^2 \text{BD}^2 \left(-\frac{\text{Alfa } \text{B}0\text{i}[\text{dbb}0, \text{BD}2, 0, \text{BD}2]}{\pi} - \right. \right. \\ & \quad \left. \frac{1}{2\pi} \text{Alfa}(-\text{B}0\text{i}[\text{dbb}0, \text{BD}2, 0, \text{BD}2] - \text{B}0\text{i}[\text{dbb}1, \text{BD}2, 0, \text{BD}2]) \right) \Bigg) - \\ & 2 \left(\text{BD}^2 + \left(\frac{1}{10000} + \text{BD} \right)^2 \right) \text{BD}^2 \left(-\frac{\text{Alfa } \text{B}0\text{i}[\text{dbb}0, \text{BD}2, 0, \text{BD}2]}{\pi} - \right. \\ & \quad \left. \frac{1}{2\pi} \text{Alfa}(-\text{B}0\text{i}[\text{dbb}0, \text{BD}2, 0, \text{BD}2] - \text{B}0\text{i}[\text{dbb}1, \text{BD}2, 0, \text{BD}2]) \right) \Bigg) + \\ & \text{Q}^2 \text{ZDownUv} \left(8 \text{BD}^2 \left(\text{BD}^2 + \left(\frac{1}{10000} + \text{BD} \right)^2 \right) \text{BD}^2 \left(-\frac{\text{Alfa } \text{B}0\text{i}[\text{dbb}0, \text{BD}2, 0, \text{BD}2]}{\pi} - \right. \right. \\ & \quad \left. \frac{1}{2\pi} \text{Alfa}(-\text{B}0\text{i}[\text{dbb}0, \text{BD}2, 0, \text{BD}2] - \text{B}0\text{i}[\text{dbb}1, \text{BD}2, 0, \text{BD}2]) \right) \Bigg) + \\ & 2 \left(\text{BD}^4 - 10 \text{BD}^2 \left(\frac{1}{10000} + \text{BD} \right)^2 + \left(\frac{1}{10000} + \text{BD} \right)^4 \right) \text{BD}^2 \\ & \quad \left(-\frac{\text{Alfa } \text{B}0\text{i}[\text{dbb}0, \text{BD}2, 0, \text{BD}2]}{\pi} - \right. \\ & \quad \left. \frac{1}{2\pi} \text{Alfa}(-\text{B}0\text{i}[\text{dbb}0, \text{BD}2, 0, \text{BD}2] - \text{B}0\text{i}[\text{dbb}1, \text{BD}2, 0, \text{BD}2]) \right) \Bigg) \Bigg) + \\ & \left(\left(\text{BD}^2 - \left(\frac{1}{10000} + \text{BD} \right)^2 \right)^2 + 2 \text{Q}^2 \text{ZDownUv}^2 \right) \text{B}0\text{i}[\text{bb}0, \text{Q}^2 \text{ZDownUv}, \text{BD}^2, \\ & \quad \left(\frac{1}{10000} + \text{BD} \right)^2] \left(4 \text{BD}^2 \text{BD}^2 \left(-\frac{\text{Alfa } \text{B}0\text{i}[\text{dbb}0, \text{BD}2, 0, \text{BD}2]}{\pi} - \right. \right. \\ & \quad \left. \frac{1}{2\pi} \text{Alfa}(-\text{B}0\text{i}[\text{dbb}0, \text{BD}2, 0, \text{BD}2] - \text{B}0\text{i}[\text{dbb}1, \text{BD}2, 0, \text{BD}2]) \right) \Bigg) - \\ & 2 \left(\text{BD}^2 + \left(\frac{1}{10000} + \text{BD} \right)^2 \right) \text{BD}^2 \left(-\frac{\text{Alfa } \text{B}0\text{i}[\text{dbb}0, \text{BD}2, 0, \text{BD}2]}{\pi} - \right. \\ & \quad \left. \frac{1}{2\pi} \text{Alfa}(-\text{B}0\text{i}[\text{dbb}0, \text{BD}2, 0, \text{BD}2] - \text{B}0\text{i}[\text{dbb}1, \text{BD}2, 0, \text{BD}2]) \right) \Bigg) \Bigg) + \\ & \frac{1}{10000} 3 \left(\frac{1}{10000} + 2 \text{BD} \right) \text{A}0[\text{BD}^2] \left(4 \text{BD}^2 \text{BD}^2 \left(-\frac{\text{Alfa } \text{B}0\text{i}[\text{dbb}0, \text{BD}2, 0, \text{BD}2]}{\pi} - \right. \right. \\ & \quad \left. \frac{1}{2\pi} \text{Alfa}(-\text{B}0\text{i}[\text{dbb}0, \text{BD}2, 0, \text{BD}2] - \text{B}0\text{i}[\text{dbb}1, \text{BD}2, 0, \text{BD}2]) \right) \Bigg) - \end{aligned}$$

$$\begin{aligned}
& 2 \left(BD^2 + \left(\frac{1}{10000} + BD \right)^2 \right) BD2 \left(-\frac{\text{Alfa } B\theta i[\text{dbb}\theta, BD2, \theta, BD2]}{\pi} - \frac{1}{2\pi} \text{Alfa} \right. \\
& \quad \left. (-B\theta i[\text{dbb}\theta, BD2, \theta, BD2] - B\theta i[\text{dbb}1, BD2, \theta, BD2]) \right) - \frac{1}{10000} \\
& 3 \left(\frac{1}{10000} + 2 BD \right) A\theta \left[\left(\frac{1}{10000} + BD \right)^2 \right] \left(4 BD^2 BD2 \left(-\frac{\text{Alfa } B\theta i[\text{dbb}\theta, BD2, \theta, BD2]}{\pi} - \right. \right. \\
& \quad \left. \frac{1}{2\pi} \text{Alfa} (-B\theta i[\text{dbb}\theta, BD2, \theta, BD2] - B\theta i[\text{dbb}1, BD2, \theta, BD2]) \right) - \\
& \quad 2 \left(BD^2 + \left(\frac{1}{10000} + BD \right)^2 \right) BD2 \left(-\frac{\text{Alfa } B\theta i[\text{dbb}\theta, BD2, \theta, BD2]}{\pi} - \frac{1}{2\pi} \right. \\
& \quad \left. \text{Alfa} (-B\theta i[\text{dbb}\theta, BD2, \theta, BD2] - B\theta i[\text{dbb}1, BD2, \theta, BD2]) \right) \Big) + \\
& \frac{1}{2500} \left(\frac{1}{10000} + 2 BD \right) BD2 Q2 ZDownUv^2 \left(-\frac{\text{Alfa } B\theta i[\text{dbb}\theta, BD2, \theta, BD2]}{\pi} - \right. \\
& \quad \left. \frac{1}{2\pi} \text{Alfa} (-B\theta i[\text{dbb}\theta, BD2, \theta, BD2] - B\theta i[\text{dbb}1, BD2, \theta, BD2]) \right) \Big) \Big); \\
\text{In}[6] := & \text{upTypeMetricpartUVREN}[Q2_, BU_, BU2_] := \\
& \frac{1}{81 \left(\frac{1}{10000} + 2 BU \right) \pi^5 Q2} 1250 \text{Alfa} \left(3 \left(\left(BU^2 - \left(\frac{1}{10000} + BU \right)^2 + 2 Q2 \right) \right. \right. \\
& \quad A\theta \left[\left(\frac{1}{10000} + BU \right)^2 \right] \left(4 BU^2 BU2 \left(-\frac{\text{Alfa } B\theta i[\text{dbb}\theta, BU2, \theta, BU2]}{\pi} - \frac{1}{2\pi} \right. \right. \\
& \quad \left. \left. \text{Alfa} (-B\theta i[\text{dbb}\theta, BU2, \theta, BU2] - B\theta i[\text{dbb}1, BU2, \theta, BU2]) \right) - \right. \\
& \quad \left. 2 \left(BU^2 + \left(\frac{1}{10000} + BU \right)^2 \right) BU2 \left(-\frac{\text{Alfa } B\theta i[\text{dbb}\theta, BU2, \theta, BU2]}{\pi} - \frac{1}{2\pi} \right. \right. \\
& \quad \left. \left. \text{Alfa} (-B\theta i[\text{dbb}\theta, BU2, \theta, BU2] - B\theta i[\text{dbb}1, BU2, \theta, BU2]) \right) \right) \Big) + \\
& A\theta[BU^2] \left(-4 BU^2 BU2 \left(BU^2 - \left(\frac{1}{10000} + BU \right)^2 + 2 Q2 \right) \left(-\frac{\text{Alfa } B\theta i[\text{dbb}\theta, BU2, \theta, BU2]}{\pi} - \right. \right. \\
& \quad \left. \frac{1}{2\pi} \text{Alfa} (-B\theta i[\text{dbb}\theta, BU2, \theta, BU2] - B\theta i[\text{dbb}1, BU2, \theta, BU2]) \right) - \\
& 2 BU2 \left(-BU^4 + \left(\frac{1}{10000} + BU \right)^4 - 6 BU^2 Q2 + 2 \left(\frac{1}{10000} + BU \right)^2 Q2 \right) \\
& \left(-\frac{\text{Alfa } B\theta i[\text{dbb}\theta, BU2, \theta, BU2]}{\pi} - \frac{1}{2\pi} \right. \\
& \quad \left. \text{Alfa} (-B\theta i[\text{dbb}\theta, BU2, \theta, BU2] - B\theta i[\text{dbb}1, BU2, \theta, BU2]) \right) \Big) + \\
& B\theta i[\text{bb}\theta, Q2, BU^2, \left(\frac{1}{10000} + BU \right)^2] \left(4 BU^2 BU2 \left(\left(BU^2 - \left(\frac{1}{10000} + BU \right)^2 \right)^2 - \right. \right. \\
& \quad \left. 2 \left(BU^2 + \left(\frac{1}{10000} + BU \right)^2 \right) Q2 - 2 Q2^2 \right) \left(-\frac{\text{Alfa } B\theta i[\text{dbb}\theta, BU2, \theta, BU2]}{\pi} - \right. \\
& \quad \left. \frac{1}{2\pi} \text{Alfa} (-B\theta i[\text{dbb}\theta, BU2, \theta, BU2] - B\theta i[\text{dbb}1, BU2, \theta, BU2]) \right) - \\
& 2 BU2 \left(\left(BU^2 - \left(\frac{1}{10000} + BU \right)^2 \right)^2 \left(BU^2 + \left(\frac{1}{10000} + BU \right)^2 \right) + \right.
\end{aligned}$$

$$\begin{aligned}
& \left(\text{BU}^4 - 10 \text{BU}^2 \left(\frac{1}{10000} + \text{BU} \right)^2 + \left(\frac{1}{10000} + \text{BU} \right)^4 \right) \text{Q2} - \\
& 2 \left(\text{BU}^2 + \left(\frac{1}{10000} + \text{BU} \right)^2 \right) \text{Q2}^2 \left(-\frac{\text{Alfa B0i}[\text{dbb0}, \text{BU2}, 0, \text{BU2}]}{\pi} - \frac{1}{2\pi} \right. \\
& \quad \left. \text{Alfa}(-\text{B0i}[\text{dbb0}, \text{BU2}, 0, \text{BU2}] - \text{B0i}[\text{dbb1}, \text{BU2}, 0, \text{BU2}]) \right) \left. \right) \left. \right) - \\
& \frac{1}{5000} \left(\frac{1}{10000} + 2 \text{BU} \right) \text{Q2} \left(-6 \text{BU}^2 \text{BU2} \left(-\frac{\text{Alfa B0i}[\text{dbb0}, \text{BU2}, 0, \text{BU2}]}{\pi} - \frac{1}{2\pi} \right. \right. \\
& \quad \left. \left. \text{Alfa}(-\text{B0i}[\text{dbb0}, \text{BU2}, 0, \text{BU2}] - \text{B0i}[\text{dbb1}, \text{BU2}, 0, \text{BU2}]) \right) - \right. \\
& \quad 6 \left(\frac{1}{10000} + \text{BU} \right)^2 \text{BU2} \left(-\frac{\text{Alfa B0i}[\text{dbb0}, \text{BU2}, 0, \text{BU2}]}{\pi} - \frac{1}{2\pi} \right. \\
& \quad \left. \left. \text{Alfa}(-\text{B0i}[\text{dbb0}, \text{BU2}, 0, \text{BU2}] - \text{B0i}[\text{dbb1}, \text{BU2}, 0, \text{BU2}]) \right) \right) + \\
& \quad 2 \text{BU2} \text{Q2} \left(-\frac{\text{Alfa B0i}[\text{dbb0}, \text{BU2}, 0, \text{BU2}]}{\pi} - \frac{1}{2\pi} \right. \\
& \quad \left. \left. \text{Alfa}(-\text{B0i}[\text{dbb0}, \text{BU2}, 0, \text{BU2}] - \text{B0i}[\text{dbb1}, \text{BU2}, 0, \text{BU2}]) \right) \right) + \\
& \frac{1}{\text{Q2ZUpUv}^2} \text{Q2}^2 \left(3 \left(\left(\left(\text{BU}^2 - \left(\frac{1}{10000} + \text{BU} \right)^2 \right)^2 + 2 \text{Q2ZUpUv}^2 \right) \text{B0i}[\text{bb0}, \text{Q2ZUpUv}, \right. \right. \\
& \quad \left. \left. \text{BU}^2, \left(\frac{1}{10000} + \text{BU} \right)^2 \right] \left(4 \text{BU}^2 \text{BU2} \left(-\frac{\text{Alfa B0i}[\text{dbb0}, \text{BU2}, 0, \text{BU2}]}{\pi} - \right. \right. \right. \\
& \quad \left. \left. \left. \frac{1}{2\pi} \text{Alfa}(-\text{B0i}[\text{dbb0}, \text{BU2}, 0, \text{BU2}] - \text{B0i}[\text{dbb1}, \text{BU2}, 0, \text{BU2}]) \right) \right) - \right. \right. \\
& \quad \left. 2 \left(\text{BU}^2 + \left(\frac{1}{10000} + \text{BU} \right)^2 \right) \text{BU2} \left(-\frac{\text{Alfa B0i}[\text{dbb0}, \text{BU2}, 0, \text{BU2}]}{\pi} - \right. \right. \\
& \quad \left. \left. \left. \frac{1}{2\pi} \text{Alfa}(-\text{B0i}[\text{dbb0}, \text{BU2}, 0, \text{BU2}] - \text{B0i}[\text{dbb1}, \text{BU2}, 0, \text{BU2}]) \right) \right) \right) + \\
& \quad \text{Q2ZUpUv B0i}[\text{dbb0}, \text{Q2ZUpUv}, \text{BU}^2, \left(\frac{1}{10000} + \text{BU} \right)^2] \\
& \quad \left(-4 \text{BU}^2 \text{BU2} \left(\left(\text{BU}^2 - \left(\frac{1}{10000} + \text{BU} \right)^2 \right)^2 - 2 \left(\text{BU}^2 + \left(\frac{1}{10000} + \text{BU} \right)^2 \right) \text{Q2ZUpUv} - \right. \right. \\
& \quad \left. \left. 2 \text{Q2ZUpUv}^2 \right) \left(-\frac{\text{Alfa B0i}[\text{dbb0}, \text{BU2}, 0, \text{BU2}]}{\pi} - \right. \right. \\
& \quad \left. \left. \frac{1}{2\pi} \text{Alfa}(-\text{B0i}[\text{dbb0}, \text{BU2}, 0, \text{BU2}] - \text{B0i}[\text{dbb1}, \text{BU2}, 0, \text{BU2}]) \right) \right) + \\
& \quad 2 \text{BU2} \left(\left(\text{BU}^2 - \left(\frac{1}{10000} + \text{BU} \right)^2 \right)^2 \left(\text{BU}^2 + \left(\frac{1}{10000} + \text{BU} \right)^2 \right) + \right. \\
& \quad \left(\text{BU}^4 - 10 \text{BU}^2 \left(\frac{1}{10000} + \text{BU} \right)^2 + \left(\frac{1}{10000} + \text{BU} \right)^4 \right) \text{Q2ZUpUv} - \\
& \quad 2 \left(\text{BU}^2 + \left(\frac{1}{10000} + \text{BU} \right)^2 \right) \text{Q2ZUpUv}^2 \left(-\frac{\text{Alfa B0i}[\text{dbb0}, \text{BU2}, 0, \text{BU2}]}{\pi} - \right. \\
& \quad \left. \left. \frac{1}{2\pi} \text{Alfa}(-\text{B0i}[\text{dbb0}, \text{BU2}, 0, \text{BU2}] - \text{B0i}[\text{dbb1}, \text{BU2}, 0, \text{BU2}]) \right) \right) \left. \right) + \\
& \frac{1}{10000} 3 \left(\frac{1}{10000} + 2 \text{BU} \right) \text{A0}[\text{BU}^2] \left(4 \text{BU}^2 \text{BU2} \left(-\frac{\text{Alfa B0i}[\text{dbb0}, \text{BU2}, 0, \text{BU2}]}{\pi} - \right. \right.
\end{aligned}$$

$$\begin{aligned}
& \frac{1}{2\pi} \text{Alfa} \left(-\text{B}\theta\text{i}[\text{dbb}\theta, \text{BU2}, \theta, \text{BU2}] - \text{B}\theta\text{i}[\text{dbb}1, \text{BU2}, \theta, \text{BU2}] \right) - \\
& 2 \left(\text{BU}^2 + \left(\frac{1}{10\theta\theta\theta} + \text{BU} \right)^2 \right) \text{BU2} \left(-\frac{\text{Alfa B}\theta\text{i}[\text{dbb}\theta, \text{BU2}, \theta, \text{BU2}]}{\pi} - \frac{1}{2\pi} \text{Alfa} \right. \\
& \quad \left. \left(-\text{B}\theta\text{i}[\text{dbb}\theta, \text{BU2}, \theta, \text{BU2}] - \text{B}\theta\text{i}[\text{dbb}1, \text{BU2}, \theta, \text{BU2}] \right) \right) - \frac{1}{10\theta\theta\theta} \\
& 3 \left(\frac{1}{10\theta\theta\theta} + 2\text{BU} \right) \text{A}\theta \left[\left(\frac{1}{10\theta\theta\theta} + \text{BU} \right)^2 \right] \left(4\text{BU}^2 \text{BU2} \left(-\frac{\text{Alfa B}\theta\text{i}[\text{dbb}\theta, \text{BU2}, \theta, \text{BU2}]}{\pi} - \right. \right. \\
& \quad \left. \left. \frac{1}{2\pi} \text{Alfa} \left(-\text{B}\theta\text{i}[\text{dbb}\theta, \text{BU2}, \theta, \text{BU2}] - \text{B}\theta\text{i}[\text{dbb}1, \text{BU2}, \theta, \text{BU2}] \right) \right) - \right. \\
& \quad \left. 2 \left(\text{BU}^2 + \left(\frac{1}{10\theta\theta\theta} + \text{BU} \right)^2 \right) \text{BU2} \left(-\frac{\text{Alfa B}\theta\text{i}[\text{dbb}\theta, \text{BU2}, \theta, \text{BU2}]}{\pi} - \frac{1}{2\pi} \right. \right. \\
& \quad \left. \left. \text{Alfa} \left(-\text{B}\theta\text{i}[\text{dbb}\theta, \text{BU2}, \theta, \text{BU2}] - \text{B}\theta\text{i}[\text{dbb}1, \text{BU2}, \theta, \text{BU2}] \right) \right) \right) + \\
& \frac{1}{25\theta\theta} \left(\frac{1}{10\theta\theta\theta} + 2\text{BU} \right) \text{BU2 Q2ZUpUv}^2 \left(-\frac{\text{Alfa B}\theta\text{i}[\text{dbb}\theta, \text{BU2}, \theta, \text{BU2}]}{\pi} - \frac{1}{2\pi} \right. \\
& \quad \left. \left. \text{Alfa} \left(-\text{B}\theta\text{i}[\text{dbb}\theta, \text{BU2}, \theta, \text{BU2}] - \text{B}\theta\text{i}[\text{dbb}1, \text{BU2}, \theta, \text{BU2}] \right) \right) \right) \Bigg);
\end{aligned}$$

```

In[*]:= upTypeMetricpartDisREN[Q2_, BU_, BU2_] :=
- 
$$\frac{1}{648 \pi^5 Q2 (BU^2 - s)} \operatorname{Im} \left[ \operatorname{Alfa} \left( \frac{1}{\pi^2 (-BU2 + s)} 6 BU^2 ((-BU^2 - 2 Q2 + s) A0[BU^2] + \right. \right.$$


$$(BU^2 + 2 Q2 - s) A0[s] + 2 Q2 (BU^2 - s + (2 BU^2 + Q2) B0i[bb0, Q2, BU^2, BU^2]) +$$


$$(BU^4 - 2 Q2^2 - 2 Q2 s + s^2 - 2 BU^2 (Q2 + s)) B0i[bb0, Q2, BU^2, s])$$


$$\operatorname{Im} \left[ \operatorname{Alfa} \left( \frac{1}{2} - B0i[bb0, s, 0, BU2] \right) \right] - \frac{1}{\pi^2 (-BU2 + s)} (-2 Q2 (-9 BU^2 + Q2 - 3 s) (BU^2 - s) +$$


$$3 ((-BU^4 - 6 BU^2 Q2 + s (2 Q2 + s)) A0[BU^2] + (BU^2 + 2 Q2 - s) (BU^2 + s) A0[s] +$$


$$4 BU^2 Q2 (2 BU^2 + Q2) B0i[bb0, Q2, BU^2, BU^2] + (BU^6 + BU^4 (Q2 - s) +$$


$$s (-2 Q2^2 + Q2 s + s^2) - BU^2 (2 Q2^2 + 10 Q2 s + s^2)) B0i[bb0, Q2, BU^2, s])$$


$$\operatorname{Im} \left[ \operatorname{Alfa} \left( \frac{1}{4} + \frac{1}{2} (-B0i[bb0, s, 0, BU2] - B0i[bb1, s, 0, BU2]) \right) \right] -$$


$$\frac{1}{Q2ZUpDis^2} Q2^2 \left( \frac{1}{\pi^2 (-BU2 + s)} 6 BU^2 ((BU^2 - s) A0[BU^2] - BU^2 A0[s] + s A0[s] +$$


$$2 Q2ZUpDis^2 B0i[bb0, Q2ZUpDis, BU^2, BU^2] - BU^4 B0i[bb0, Q2ZUpDis, BU^2, s] -$$


$$2 Q2ZUpDis^2 B0i[bb0, Q2ZUpDis, BU^2, s] + 2 BU^2 s B0i[bb0, Q2ZUpDis, BU^2, s] -$$


$$s^2 B0i[bb0, Q2ZUpDis, BU^2, s] + 4 BU^2 Q2ZUpDis^2$$


$$B0i[dbb0, Q2ZUpDis, BU^2, BU^2] + 2 Q2ZUpDis^3 B0i[dbb0, Q2ZUpDis, BU^2, BU^2] +$$


$$Q2ZUpDis (BU^4 - 2 Q2ZUpDis^2 - 2 Q2ZUpDis s + s^2 - 2 BU^2 (Q2ZUpDis + s))$$


$$B0i[dbb0, Q2ZUpDis, BU^2, s]) \operatorname{Im} \left[ \operatorname{Alfa} \left( \frac{1}{2} - B0i[bb0, s, 0, BU2] \right) \right] -$$


$$\frac{1}{\pi^2 (-BU2 + s)} (2 Q2ZUpDis^2 (-BU^2 + s) + 3 (BU^4 - s^2) A0[BU^2] +$$


$$3 (-BU^4 + s^2) A0[s] + 12 BU^2 Q2ZUpDis^2 B0i[bb0, Q2ZUpDis, BU^2, BU^2] -$$


$$3 (2 Q2ZUpDis^2 + (BU^2 - s)^2) (BU^2 + s) B0i[bb0, Q2ZUpDis, BU^2, s] +$$


$$3 Q2ZUpDis (4 BU^2 Q2ZUpDis (2 BU^2 + Q2ZUpDis) B0i[dbb0, Q2ZUpDis, BU^2, BU^2] +$$


$$(BU^6 + BU^4 (Q2ZUpDis - s) + s (-2 Q2ZUpDis^2 + Q2ZUpDis s + s^2) -$$


$$BU^2 (2 Q2ZUpDis^2 + 10 Q2ZUpDis s + s^2)) B0i[dbb0, Q2ZUpDis, BU^2, s])$$


$$\operatorname{Im} \left[ \operatorname{Alfa} \left( \frac{1}{4} + \frac{1}{2} (-B0i[bb0, s, 0, BU2] - B0i[bb1, s, 0, BU2]) \right) \right] \Bigg);$$

```

$$\begin{aligned}
& \text{downTypeMetricpartDisREN}[Q2_ , BD_ , BD2_] := \\
& - \frac{1}{2592 \pi^5 Q2 (BD^2 - s)} \text{I} \left[\text{Alfa} \left(\frac{1}{\pi^2 (-BD2 + s)} 6 BD^2 ((-BD^2 - 2 Q2 + s) A0[BD^2] + \right. \right. \\
& \quad (BD^2 + 2 Q2 - s) A0[s] + 2 Q2 (BD^2 - s + (2 BD^2 + Q2) B0i[bb0, Q2, BD^2, BD^2]) + \\
& \quad (BD^4 - 2 Q2^2 - 2 Q2 s + s^2 - 2 BD^2 (Q2 + s)) B0i[bb0, Q2, BD^2, s]) \text{Im} \left[\right. \\
& \quad \left. \left. \text{Alfa} \left(\frac{1}{2} - B0i[bb0, s, 0, BD2] \right) \right] - \frac{1}{\pi^2 (-BD2 + s)} (-2 Q2 (-9 BD^2 + Q2 - 3 s) (BD^2 - s) + \right. \\
& \quad 3 ((-BD^4 - 6 BD^2 Q2 + s (2 Q2 + s)) A0[BD^2] + (BD^2 + 2 Q2 - s) (BD^2 + s) A0[s] + \\
& \quad 4 BD^2 Q2 (2 BD^2 + Q2) B0i[bb0, Q2, BD^2, BD^2] + (BD^6 + BD^4 (Q2 - s) + s \\
& \quad (-2 Q2^2 + Q2 s + s^2) - BD^2 (2 Q2^2 + 10 Q2 s + s^2)) B0i[bb0, Q2, BD^2, s]) \text{Im} \left[\right. \\
& \quad \left. \left. \text{Alfa} \left(\frac{1}{4} + \frac{1}{2} (-B0i[bb0, s, 0, BD2] - B0i[bb1, s, 0, BD2]) \right) \right] \right] - \\
& \frac{1}{Q2ZDownDis^2} Q2^2 \left(\frac{1}{\pi^2 (-BD2 + s)} 6 BD^2 ((BD^2 - s) A0[BD^2] - BD^2 A0[s] + s A0[s] + \right. \\
& \quad 2 Q2ZDownDis^2 B0i[bb0, Q2ZDownDis, BD^2, BD^2] - BD^4 B0i[bb0, \\
& \quad Q2ZDownDis, BD^2, s] - 2 Q2ZDownDis^2 B0i[bb0, Q2ZDownDis, BD^2, s] + \\
& \quad 2 BD^2 s B0i[bb0, Q2ZDownDis, BD^2, s] - s^2 B0i[bb0, Q2ZDownDis, BD^2, s] + \\
& \quad 4 BD^2 Q2ZDownDis^2 B0i[dbb0, Q2ZDownDis, BD^2, BD^2] + \\
& \quad 2 Q2ZDownDis^3 B0i[dbb0, Q2ZDownDis, BD^2, BD^2] + \\
& \quad Q2ZDownDis (BD^4 - 2 Q2ZDownDis^2 - 2 Q2ZDownDis s + s^2 - 2 BD^2 (Q2ZDownDis + s)) \\
& \quad \left. B0i[dbb0, Q2ZDownDis, BD^2, s]) \text{Im} \left[\text{Alfa} \left(\frac{1}{2} - B0i[bb0, s, 0, BD2] \right) \right] \right] - \\
& \frac{1}{\pi^2 (-BD2 + s)} \left(2 Q2ZDownDis^2 (-BD^2 + s) + 3 (BD^4 - s^2) A0[BD^2] + \right. \\
& \quad 3 (-BD^4 + s^2) A0[s] + 12 BD^2 Q2ZDownDis^2 B0i[bb0, Q2ZDownDis, BD^2, BD^2] - \\
& \quad 3 (2 Q2ZDownDis^2 + (BD^2 - s)^2) (BD^2 + s) B0i[bb0, Q2ZDownDis, BD^2, s] + \\
& \quad 3 Q2ZDownDis (4 BD^2 Q2ZDownDis (2 BD^2 + Q2ZDownDis) \\
& \quad B0i[dbb0, Q2ZDownDis, BD^2, BD^2] + (BD^6 + BD^4 (Q2ZDownDis - s) + \\
& \quad s (-2 Q2ZDownDis^2 + Q2ZDownDis s + s^2) - BD^2 (2 Q2ZDownDis^2 + \\
& \quad 10 Q2ZDownDis s + s^2)) B0i[dbb0, Q2ZDownDis, BD^2, s]) \text{Im} \left[\text{Alfa} \left(\frac{1}{4} + \frac{1}{2} \right. \right. \\
& \quad \left. \left. (-B0i[bb0, s, 0, BD2] - B0i[bb1, s, 0, BD2]) \right) \right] \right];
\end{aligned}$$

```

In[*]:= triangleMetricREN[Q2_] :=
Alfa (7.663384192618505`*^-8 MB2 - 2.4496111124551734`*^-6 MC2 +
7.663206852672925`*^-8 MD2 + 6.207326462516705`*^-6 ME2 +
6.204067243946839`*^-6 ML2 + 6.207040176437114`*^-6 MM2 +
7.662866108136267`*^-8 MS2 - 1.434334376161842`*^-6 MT2 -
2.4522262058924886`*^-6 MU2 - 7.663384192618505`*^-8 A0[MB2] +
2.4496111124551734`*^-6 A0[MC2] - 7.663206852672925`*^-8 A0[MD2] -
6.207326462516705`*^-6 A0[ME2] - 6.204067243946839`*^-6 A0[ML2] -
6.207040176437114`*^-6 A0[MM2] - 7.662866108136267`*^-8 A0[MS2] +
1.434334376161842`*^-6 A0[MT2] + 2.4522262058924878`*^-6 A0[MU2] +
(7.663384192618505`*^-8 MB2 + 3.831692096309253`*^-8 Q2) B0i[bb0, Q2, MB2, MB2] +
(-2.4496111124551734`*^-6 MC2 - 1.2248055562275867`*^-6 Q2)
B0i[bb0, Q2, MC2, MC2] + 7.663206852672925`*^-8 MD2 B0i[bb0, Q2, MD2, MD2] +
6.207326462516705`*^-6 ME2 B0i[bb0, Q2, ME2, ME2] + 6.204067243946839`*^-6
ML2 B0i[bb0, Q2, ML2, ML2] + 6.207040176437114`*^-6 MM2 B0i[bb0, Q2, MM2, MM2] +
7.662866108136267`*^-8 MS2 B0i[bb0, Q2, MS2, MS2] - 1.434334376161842`*^-6
MT2 B0i[bb0, Q2, MT2, MT2] - 2.4522262058924878`*^-6 MU2 B0i[bb0, Q2, MU2, MU2] +
Q2 (3.831603426336463`*^-8 B0i[bb0, Q2, MD2, MD2] + 3.1036632312583524`*^-6
B0i[bb0, Q2, ME2, ME2] + 3.1020336219734196`*^-6 B0i[bb0, Q2, ML2, ML2] +
3.103520088218557`*^-6 B0i[bb0, Q2, MM2, MM2] + 3.8314330540681334`*^-8
B0i[bb0, Q2, MS2, MS2] - 7.17167188080921`*^-7 B0i[bb0, Q2, MT2, MT2] -
1.2261131029462439`*^-6 B0i[bb0, Q2, MU2, MU2] - 3.831692096309253`*^-8
B0i[bb0, Q2ZV, MB2, MB2] + 1.2248055562275867`*^-6 B0i[bb0, Q2ZV, MC2, MC2] -
3.831603426336463`*^-8 B0i[bb0, Q2ZV, MD2, MD2] - 3.1036632312583524`*^-6
B0i[bb0, Q2ZV, ME2, ME2] - 3.1020336219734196`*^-6 B0i[bb0, Q2ZV, ML2, ML2] -
3.103520088218557`*^-6 B0i[bb0, Q2ZV, MM2, MM2] - 3.8314330540681334`*^-8
B0i[bb0, Q2ZV, MS2, MS2] + 7.17167188080921`*^-7 B0i[bb0, Q2ZV, MT2, MT2] +
1.2261131029462439`*^-6 B0i[bb0, Q2ZV, MU2, MU2] +
(-7.663384192618505`*^-8 MB2 - 3.831692096309253`*^-8 Q2ZV) B0i[dbb0, Q2ZV,
MB2, MB2] + (2.4496111124551734`*^-6 MC2 + 1.2248055562275867`*^-6 Q2ZV) B0i[
dbb0, Q2ZV, MC2, MC2] - 7.663206852672925`*^-8 MD2 B0i[dbb0, Q2ZV, MD2, MD2] -
6.207326462516705`*^-6 ME2 B0i[dbb0, Q2ZV, ME2, ME2] -
6.204067243946839`*^-6 ML2 B0i[dbb0, Q2ZV, ML2, ML2] -
6.207040176437114`*^-6 MM2 B0i[dbb0, Q2ZV, MM2, MM2] -
7.662866108136267`*^-8 MS2 B0i[dbb0, Q2ZV, MS2, MS2] +
1.434334376161842`*^-6 MT2 B0i[dbb0, Q2ZV, MT2, MT2] +
Q2ZV (-3.831603426336463`*^-8 B0i[dbb0, Q2ZV, MD2, MD2] -
3.1036632312583524`*^-6 B0i[dbb0, Q2ZV, ME2, ME2] -
3.1020336219734196`*^-6 B0i[dbb0, Q2ZV, ML2, ML2] -
3.103520088218557`*^-6 B0i[dbb0, Q2ZV, MM2, MM2] - 3.8314330540681334`*^-8
B0i[dbb0, Q2ZV, MS2, MS2] + 7.17167188080921`*^-7 B0i[dbb0, Q2ZV,
MT2, MT2] + 1.2261131029462439`*^-6 B0i[dbb0, Q2ZV, MU2, MU2]) +
2.4522262058924878`*^-6 MU2 B0i[dbb0, Q2ZV, MU2, MU2]))

```



```

In[*]:= uvFiniteCont2Loop[Q2_, BH_, BH2_] =
  (2 *  $\pi$ )4 *  $\frac{\text{Re}[\text{metricpartUVREN}[Q2, BH, BH2] \text{ // } Q2Zuv \rightarrow 10^{-1}]}{Q2}$ ;

In[*]:= downTypeUVCont[Q2_, BD_, BD2_] =
  (2 *  $\pi$ )4 *  $\frac{1}{Q2} \text{Re}[\text{downTypeMetricpartUVREN}[Q2, BD, BD2] \text{ // } Q2ZDownUv \rightarrow 10^{-1}]$ ;


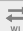
In[*]:= upTypeUVCont[Q2_, BU_, BU2_] =
  (2 *  $\pi$ )4 *  $\frac{1}{Q2} \text{Re}[\text{upTypeMetricpartUVREN}[Q2, BU, BU2] \text{ // } Q2ZUpUv \rightarrow 10^{-1}]$ ;

In[*]:= dispersionCont2Loop[Q2_, BH_, BH2_] :=
  (2 *  $\pi$ )4 * NIntegrate[ $\text{Re}[\frac{\text{metricpartDispersion}[Q2, BH, BH2]}{Q2} \text{ // } Q2ZNNLO \rightarrow 10^{-8}]$ ,
    {s, BH2, BH2, 108 * BH2}, MaxRecursion → 30,
    WorkingPrecision → 10, Method → "PrincipalValue"];

In[*]:= upTypeDisCont[Q2_, BU_, BU2_] :=
  (2 *  $\pi$ )4 * NIntegrate[ $\text{Re}[\frac{\text{upTypeMetricpartDisREN}[Q2, BU, BU2]}{Q2} \text{ // } Q2ZUpDis \rightarrow 10^{-8}]$ ,
    {s, BU2, BU2, 108 * BU2}, MaxRecursion → 30,
    WorkingPrecision → 10, Method → "PrincipalValue"];

In[*]:= downTypeDisCont[Q2_, BD_, BD2_] := (2 *  $\pi$ )4 *
  NIntegrate[ $\text{Re}[\frac{\text{downTypeMetricpartDisREN}[Q2, BD, BD2]}{Q2} \text{ // } Q2ZDownDis \rightarrow 10^{-8}]$ ,
    {s, BD2, BD2, 108 * BD2}, MaxRecursion → 30,
    WorkingPrecision → 10, Method → "PrincipalValue"];

In[*]:= Install["LoopTools"]

Out[*]:= LinkObject[  Name: '/home/reefat/packages1/LoopTools-2.14/x86_64-Linux/bin/LoopTools'
  Link mode: Listen ]

```

```

In[*]:= Alfa := 1/137.0359895;
Alfa2 := Alfa * Alfa;
ME := 0.510998928 * 10-3;
MZ := 91.1876;
MN := 0.939565379;
MW := 80.385;
ME := 0.510998928 * 10-3;
MN2 := MN * MN;
MU := 0.06983;
MD := 0.06984;
MM := 105.6583715 * 10-3;
ML := 1776.82 * 10-3;
MC := 1.275;
MB := 4.18;
MT := 173.5;
MS := 0.125;
MH := 125.0;
ME2 := ME * ME;
MH2 := MH * MH;
MM2 := MM * MM;
ML2 := ML * ML;
MC2 := MC * MC;
MB2 := MB * MB;
MT2 := MT * MT;
MS2 := MS * MS;
MD2 := MD * MD;
MU2 := MU * MU;
ME2 := ME * ME;
MW2 := MW * MW;
MZ2 := MZ * MZ

In[*]:= SetLambda[10-18]
SetDelta[0 * 103]
SetMudim[100]

In[*]:= q21 = 0.001;
q22 = 0.100;
q23 = 10.0;
q24 = 1000;
q25 = 105;
q26 = 106;

In[*]:= NLOCorrection[Q2_] := Re[ $\frac{\text{metricpartNLOREN}[Q2] \ /. \ Q2Z \rightarrow 10^{-10}}{Q2}$ ]

```

```
In[*]:= oneLoopTable =
Grid[{{"k12/GeV2", "One-loop vaccum polarization"}, {q21, NLOCorrection[q21]},
{q22, NLOCorrection[q22]}, {q23, NLOCorrection[q23]}, {q24, NLOCorrection[q24]},
{q25, NLOCorrection[q25]}, {q26, NLOCorrection[q26]}}, Frame -> All]
```

k_1^2/GeV^2	One-loop vaccum polarization
0.001	0.00502497599303168
0.1	0.00936715960871928
10.	0.0229472685075054
1000	0.0480222028387869
100 000	0.0706036886459294
1 000 000	0.0854264484453274

```
In[*]:= uvFiniteCont2LoopTableME = Grid[{{"k12/GeV2", "UV-Finite Contributions(e)"},
{q21, uvFiniteCont2Loop[q21, ME, ME2]},
{q22, uvFiniteCont2Loop[q22, ME, ME2]}, {q23, uvFiniteCont2Loop[q23, ME, ME2]},
{q24, uvFiniteCont2Loop[q24, ME, ME2]}, {q25, uvFiniteCont2Loop[q25, ME, ME2]},
{q26, uvFiniteCont2Loop[q26, ME, ME2]}, Frame -> All]
```

k_1^2/GeV^2	UV-Finite Contributions(e)
0.001	0.0000714290678792285
0.1	0.0000714410066800723
10.	0.0000714411257164574
1000	0.0000714411269067862
100 000	0.0000714411269186895
1 000 000	0.0000714411269187977

```
In[*]:= uvFiniteCont2LoopTableML = Grid[{{"k12/GeV2", "UV-Finite Contributions( $\tau$ )"},
{q21, uvFiniteCont2Loop[q21, ML, ML2]},
{q22, uvFiniteCont2Loop[q22, ML, ML2]}, {q23, uvFiniteCont2Loop[q23, ML, ML2]},
{q24, uvFiniteCont2Loop[q24, ML, ML2]}, {q25, uvFiniteCont2Loop[q25, ML, ML2]},
{q26, uvFiniteCont2Loop[q26, ML, ML2]}, Frame -> All]
```

k_1^2/GeV^2	UV-Finite Contributions(τ)
0.001	0.
0.1	0.
10.	0.
1000	0.000117505109686222
100 000	0.000117512228808099
1 000 000	0.000117512230068204

```

In[*]:= uvFiniteCont2LoopTableMM = Grid[{{"k12/GeV2", "UV-Finite Contributions( $\mu$ )"},
      {q21, uvFiniteCont2Loop[q21, MM, MM2]},
      {q22, uvFiniteCont2Loop[q22, MM, MM2]}, {q23, uvFiniteCont2Loop[q23, MM, MM2]},
      {q24, uvFiniteCont2Loop[q24, MM, MM2]}, {q25, uvFiniteCont2Loop[q25, MM, MM2]},
      {q26, uvFiniteCont2Loop[q26, MM, MM2]}, Frame -> All]

```

k_1^2/GeV^2	UV-Finite Contributions(μ)
0.001	0.
0.1	0.0000923860161032114
10.	0.000101564349550255
1000	0.000101565429671561
100 000	0.000101565432936296
1 000 000	0.000101565432965283

```

In[*]:= uvFiniteCont2LoopTableUP = Grid[
      {"k12/GeV2", "UV-Finite Contributions(UP)"}, {q21, upTypeUVCont[q21, MU, MU2]},
      {q22, upTypeUVCont[q22, MU, MU2]}, {q23, upTypeUVCont[q23, MU, MU2]},
      {q24, upTypeUVCont[q24, MU, MU2]}, {q25, upTypeUVCont[q25, MU, MU2]},
      {q26, upTypeUVCont[q26, MU, MU2]}, Frame -> All]

```

k_1^2/GeV^2	UV-Finite Contributions(UP)
0.001	-0.0000448287189485694
0.1	$-1.41406087835672 \times 10^{-6}$
10.	$-7.28678495881824 \times 10^{-7}$
1000	$-7.28523927968602 \times 10^{-7}$
100 000	$-7.28523006402142 \times 10^{-7}$
1 000 000	$-7.28522998077492 \times 10^{-7}$

```

In[*]:= uvFiniteCont2LoopTableCHARM =
      Grid[{"k12/GeV2", "UV-Finite Contributions(CHARM)"},
      {q21, upTypeUVCont[q21, MC, MC2]}, {q22, upTypeUVCont[q22, MC, MC2]},
      {q23, upTypeUVCont[q23, MC, MC2]}, {q24, upTypeUVCont[q24, MC, MC2]}, {q25,
      upTypeUVCont[q25, MC, MC2]}, {q26, upTypeUVCont[q26, MC, MC2]}, Frame -> All]

```

k_1^2/GeV^2	UV-Finite Contributions(CHARM)
0.001	0.
0.1	0.
10.	0.000040273039315184
1000	0.0000513934148293354
100 000	0.0000513942509516129
1 000 000	0.0000513942512093566

```

In[*]:= uvFiniteCont2LoopTableTOP = Grid[
  {"k12/GeV2", "UV-Finite Contributions (TOP)", {q21, upTypeUVCont[q21, MT, MT2]},
  {q22, upTypeUVCont[q22, MT, MT2]}, {q23, upTypeUVCont[q23, MT, MT2]},
  {q24, upTypeUVCont[q24, MT, MT2]}, {q25, upTypeUVCont[q25, MT, MT2]},
  {q26, upTypeUVCont[q26, MT, MT2]}, Frame -> All]

```

	k ₁ ² /GeV ²	UV-Finite Contributions (TOP)
	0.001	0.
	0.1	0.
Out[*]=	10.	0.
	1000	0.
	100 000	0.
	1 000 000	0.0000633707979624905

```

In[*]:= uvFiniteCont2LoopTableDOWN = Grid[{"k12/GeV2", "UV-Finite Contributions (DOWN)",
  {q21, downTypeUVCont[q21, MD, MD2]},
  {q22, downTypeUVCont[q22, MD, MD2]}, {q23, downTypeUVCont[q23, MD, MD2]},
  {q24, downTypeUVCont[q24, MD, MD2]}, {q25, downTypeUVCont[q25, MD, MD2]},
  {q26, downTypeUVCont[q26, MD, MD2]}, Frame -> All]

```

	k ₁ ² /GeV ²	UV-Finite Contributions (DOWN)
	0.001	-0.0000112073839046431
	0.1	-3.53731793015015 × 10 ⁻⁷
Out[*]=	10.	-1.82283907386001 × 10 ⁻⁷
	1000	-1.82245252789368 × 10 ⁻⁷
	100 000	-1.82245022361001 × 10 ⁻⁷
	1 000 000	-1.82245020280369 × 10 ⁻⁷

```

In[*]:= uvFiniteCont2LoopTableSTR =
  Grid[{"k12/GeV2", "UV-Finite Contributions (STRANGE)",
  {q21, downTypeUVCont[q21, MS, MS2]},
  {q22, downTypeUVCont[q22, MS, MS2]}, {q23, downTypeUVCont[q23, MS, MS2]},
  {q24, downTypeUVCont[q24, MS, MS2]}, {q25, downTypeUVCont[q25, MS, MS2]},
  {q26, downTypeUVCont[q26, MS, MS2]}, Frame -> All]

```

	k ₁ ² /GeV ²	UV-Finite Contributions (STRANGE)
	0.001	-0.0000146103092918533
	0.1	-5.46223531967491 × 10 ⁻⁶
Out[*]=	10.	-3.21993736906405 × 10 ⁻⁶
	1000	-3.21972774407794 × 10 ⁻⁶
	100 000	-3.21972730433597 × 10 ⁻⁶
	1 000 000	-3.21972730048846 × 10 ⁻⁶

```

In[*]:= uvFiniteCont2LoopTableBT = Grid[{"k12/GeV2", "UV-Finite Contributions(BOTTOM)"},
  {q21, downTypeUVCont[q21, MB, MB2]},
  {q22, downTypeUVCont[q22, MB, MB2]}, {q23, downTypeUVCont[q23, MB, MB2]},
  {q24, downTypeUVCont[q24, MB, MB2]}, {q25, downTypeUVCont[q25, MB, MB2]},
  {q26, downTypeUVCont[q26, MB, MB2]}, Frame -> All]

```

k_1^2/GeV^2	UV-Finite Contributions(BOTTOM)
0.001	0.
0.1	0.
10.	0.
1000	0.0000135684614343902
100 000	0.0000135939806784566
1 000 000	0.0000135939832976403

```

In[*]:= dispersionCont2LoopTableME =
  Grid[{"k12/GeV2", "Dispersion Contributions(e)"}, {q21,
    dispersionCont2Loop[q21, ME, ME2]}, {q22, dispersionCont2Loop[q22, ME, ME2]},
    {q23, dispersionCont2Loop[q23, ME, ME2]}, {q24,
    dispersionCont2Loop[q24, ME, ME2]}, {q25, dispersionCont2Loop[q25, ME, ME2]},
    {q26, dispersionCont2Loop[q26, ME, ME2]}, Frame -> All]

```

k_1^2/GeV^2	Dispersion Contributions(e)
0.001	-0.00001118783406
0.1	-0.00001768821866
10.	-0.00002419317221
1000	-0.00002737709363
100 000	-0.00002743186237
1 000 000	-0.00002743236031

```

In[*]:= dispersionCont2LoopTableML =
  Grid[{"k12/GeV2", "Dispersion Contributions( $\tau$ )"}, {q21,
    dispersionCont2Loop[q21, ML, ML2]}, {q22, dispersionCont2Loop[q22, ML, ML2]},
    {q23, dispersionCont2Loop[q23, ML, ML2]}, {q24,
    dispersionCont2Loop[q24, ML, ML2]}, {q25, dispersionCont2Loop[q25, ML, ML2]},
    {q26, dispersionCont2Loop[q26, ML, ML2]}, Frame -> All]

```

k_1^2/GeV^2	Dispersion Contributions(τ)
0.001	$3.903650759 \times 10^{-31}$
0.1	$3.903650758 \times 10^{-31}$
10.	$3.903650758 \times 10^{-31}$
1000	$-7.718033238 \times 10^{-6}$
100 000	-0.00001416824731
1 000 000	-0.00001742019076

```

In[*]:= dispersionCont2LoopTableMM =
  Grid[{{"k12/GeV2", "Dispersion Contributions( $\mu$ )"}, {q21,
    dispersionCont2Loop[q21, MM, MM2]}, {q22, dispersionCont2Loop[q22, MM, MM2]},
    {q23, dispersionCont2Loop[q23, MM, MM2]}, {q24,
    dispersionCont2Loop[q24, MM, MM2]}, {q25, dispersionCont2Loop[q25, MM, MM2]},
    {q26, dispersionCont2Loop[q26, MM, MM2]}}], Frame -> All]

```

k_1^2/GeV^2	Dispersion Contributions(μ)
0.001	$4.881045794 \times 10^{-36}$
0.1	$-5.523194678 \times 10^{-6}$
10.	$-9.150293264 \times 10^{-6}$
1000	-0.00001563634429
100 000	-0.00002214117717
1 000 000	-0.00002539351202

```

In[*]:= disCont2LoopTableUP = Grid[{{"k12/GeV2", "Dispersion Contributions(UP)"},
  {q21, upTypeDisCont[q21, MU, MU2]},
  {q22, upTypeDisCont[q22, MU, MU2]}, {q23, upTypeDisCont[q23, MU, MU2]},
  {q24, upTypeDisCont[q24, MU, MU2]}, {q25, upTypeDisCont[q25, MU, MU2]},
  {q26, upTypeDisCont[q26, MU, MU2]}}], Frame -> All]

```

k_1^2/GeV^2	Dispersion Contributions(UP)
0.001	$-4.138880582 \times 10^{-37}$
0.1	$2.166794682 \times 10^{-6}$
10.	$4.581935054 \times 10^{-6}$
1000	$7.469235405 \times 10^{-6}$
100 000	0.00001036048567
1 000 000	0.00001174512634

```

In[*]:= disCont2LoopTableCHARM = Grid[{{"k12/GeV2", "Dispersion Contributions(CHARM)"},
  {q21, upTypeDisCont[q21, MC, MC2]},
  {q22, upTypeDisCont[q22, MC, MC2]}, {q23, upTypeDisCont[q23, MC, MC2]},
  {q24, upTypeDisCont[q24, MC, MC2]}, {q25, upTypeDisCont[q25, MC, MC2]},
  {q26, upTypeDisCont[q26, MC, MC2]}}], Frame -> All]

```

k_1^2/GeV^2	Dispersion Contributions(CHARM)
0.001	$-4.599974683 \times 10^{-32}$
0.1	$-4.599974682 \times 10^{-32}$
10.	$2.916723348 \times 10^{-6}$
1000	$3.835012161 \times 10^{-6}$
100 000	$6.713689401 \times 10^{-6}$
1 000 000	$8.159005679 \times 10^{-6}$

```
In[*]:= disCont2LoopTableTOP = Grid[{"k12/GeV2", "Dispersion Contributions(TOP)"},
  {q21, upTypeDisCont[q21, MT, MT2]},
  {q22, upTypeDisCont[q22, MT, MT2]}, {q23, upTypeDisCont[q23, MT, MT2]},
  {q24, upTypeDisCont[q24, MT, MT2]}, {q25, upTypeDisCont[q25, MT, MT2]},
  {q26, upTypeDisCont[q26, MT, MT2]}, Frame -> All]
```

k_1^2/GeV^2	Dispersion Contributions(TOP)
0.001	$-1.577293882 \times 10^{-23}$
0.1	$-1.577293882 \times 10^{-23}$
10.	$-1.577293882 \times 10^{-23}$
1000	$-1.577293882 \times 10^{-23}$
100 000	$-1.577293882 \times 10^{-23}$
1 000 000	$2.265344250 \times 10^{-6}$

```
In[*]:= disCont2LoopTableDOWN = Grid[{"k12/GeV2", "Dispersion Contributions(DOWN)"},
  {q21, downTypeDisCont[q21, MD, MD2]},
  {q22, downTypeDisCont[q22, MD, MD2]}, {q23, downTypeDisCont[q23, MD, MD2]},
  {q24, downTypeDisCont[q24, MD, MD2]}, {q25, downTypeDisCont[q25, MD, MD2]},
  {q26, downTypeDisCont[q26, MD, MD2]}, Frame -> All]
```

k_1^2/GeV^2	Dispersion Contributions(DOWN)
0.001	$-1.035312981 \times 10^{-37}$
0.1	$5.416936588 \times 10^{-7}$
10.	$1.145438574 \times 10^{-6}$
1000	$1.867264525 \times 10^{-6}$
100 000	$2.590076386 \times 10^{-6}$
1 000 000	$2.936251310 \times 10^{-6}$

```
In[*]:= disCont2LoopTableSTR = Grid[{"k12/GeV2", "Dispersion Contributions(STRANGE)"},
  {q21, downTypeDisCont[q21, MS, MS2]},
  {q22, downTypeDisCont[q22, MS, MS2]}, {q23, downTypeDisCont[q23, MS, MS2]},
  {q24, downTypeDisCont[q24, MS, MS2]}, {q25, downTypeDisCont[q25, MS, MS2]},
  {q26, downTypeDisCont[q26, MS, MS2]}, Frame -> All]
```

k_1^2/GeV^2	Dispersion Contributions(STRANGE)
0.001	$-1.062416412 \times 10^{-36}$
0.1	$7.147532346 \times 10^{-7}$
10.	$9.648070079 \times 10^{-7}$
1000	$1.684591697 \times 10^{-6}$
100 000	$2.407349731 \times 10^{-6}$
1 000 000	$2.768736575 \times 10^{-6}$


```

In[ ]:= disCont2LoopTableBT = Grid[{"k12/GeV2", "Dispersion Contributions(BOTTOM)"},
  {q21, downTypeDisCont[q21, MB, MB2]},
  {q22, downTypeDisCont[q22, MB, MB2]}, {q23, downTypeDisCont[q23, MB, MB2]},
  {q24, downTypeDisCont[q24, MB, MB2]}, {q25, downTypeDisCont[q25, MB, MB2]},
  {q26, downTypeDisCont[q26, MB, MB2]}, Frame -> All]

```

k_1^2/GeV^2	Dispersion Contributions(BOTTOM)
0.001	$-1.328494736 \times 10^{-30}$
0.1	$-1.328494736 \times 10^{-30}$
10.	$-1.328494736 \times 10^{-30}$
1000	$6.204472690 \times 10^{-7}$
100 000	$1.305978847 \times 10^{-6}$
1 000 000	$1.667095734 \times 10^{-6}$

```

In[*]:= twoLoopTable = Grid[{"k12/GeV2", "Two Loop Contribution (LEPTONS)"},
  {q21, 2 * (uvFiniteCont2LoopTableME[[1]][[2]][[2]] +
    uvFiniteCont2LoopTableML[[1]][[2]][[2]] +
    uvFiniteCont2LoopTableMM[[1]][[2]][[2]] + dispersionCont2LoopTableME[[1]][[
      2]][[2]] + dispersionCont2LoopTableML[[1]][[2]][[2]] +
    dispersionCont2LoopTableMM[[1]][[2]][[2]])},
  {q22, 2 * (uvFiniteCont2LoopTableME[[1]][[3]][[2]] +
    uvFiniteCont2LoopTableML[[1]][[3]][[2]] +
    uvFiniteCont2LoopTableMM[[1]][[3]][[2]] + dispersionCont2LoopTableME[[1]][[
      3]][[2]] + dispersionCont2LoopTableML[[1]][[3]][[2]] +
    dispersionCont2LoopTableMM[[1]][[3]][[2]])},
  {q23, 2 * (uvFiniteCont2LoopTableME[[1]][[4]][[2]] +
    uvFiniteCont2LoopTableML[[1]][[4]][[2]] +
    uvFiniteCont2LoopTableMM[[1]][[4]][[2]] +
    dispersionCont2LoopTableME[[1]][[4]][[2]] +
    dispersionCont2LoopTableML[[1]][[4]][[2]] +
    dispersionCont2LoopTableMM[[1]][[4]][[2]])},
  {q24, 2 * (uvFiniteCont2LoopTableME[[1]][[5]][[2]] +
    uvFiniteCont2LoopTableML[[1]][[5]][[2]] +
    uvFiniteCont2LoopTableMM[[1]][[5]][[2]] +
    dispersionCont2LoopTableME[[1]][[5]][[2]] +
    dispersionCont2LoopTableML[[1]][[5]][[2]] +
    dispersionCont2LoopTableMM[[1]][[5]][[2]])},
  {q25, 2 * (uvFiniteCont2LoopTableME[[1]][[6]][[2]] +
    uvFiniteCont2LoopTableML[[1]][[6]][[2]] +
    uvFiniteCont2LoopTableMM[[1]][[6]][[2]] +
    dispersionCont2LoopTableME[[1]][[6]][[2]] +
    dispersionCont2LoopTableML[[1]][[6]][[2]] +
    dispersionCont2LoopTableMM[[1]][[6]][[2]])},
  {q26, 2 * (uvFiniteCont2LoopTableME[[1]][[7]][[2]] +
    uvFiniteCont2LoopTableML[[1]][[7]][[2]] +
    uvFiniteCont2LoopTableMM[[1]][[7]][[2]] +
    dispersionCont2LoopTableME[[1]][[7]][[2]] +
    dispersionCont2LoopTableML[[1]][[7]][[2]] +
    dispersionCont2LoopTableMM[[1]][[7]][[2]])}], Frame -> All]

```

k ₁ ² /GeV ²	Two Loop Contribution (LEPTONS)
0.001	0.000120482467634885
0.1	0.0002812312188941
10.	0.000279324019577548
1000	0.00047956039021742
100000	0.000453555003615108
1000000	0.000440545453731408

```

In[*]:= twoLoopTable1 =
  Grid[{"k12/GeV2", "Vacuum Polarization Two-loop Contribution (LEP+QUARKS)"},

```

```

{q21, 2 * (uvFiniteCont2LoopTableME[1][2][2] +
uvFiniteCont2LoopTableML[1][2][2] +
uvFiniteCont2LoopTableMM[1][2][2] + uvFiniteCont2LoopTableUP[1][[
2]][2] + uvFiniteCont2LoopTableCHARM[1][2][2] +
uvFiniteCont2LoopTableTOP[1][2][2] + uvFiniteCont2LoopTableDOWN[1][[
2]][2] + uvFiniteCont2LoopTableSTR[1][2][2] +
uvFiniteCont2LoopTableBT[1][2][2] + dispersionCont2LoopTableME[1][[
2]][2] + dispersionCont2LoopTableML[1][2][2] +
dispersionCont2LoopTableMM[1][2][2] +
disCont2LoopTableUP[1][2][2] + disCont2LoopTableCHARM[1][2][2] +
disCont2LoopTableTOP[1][2][2] + disCont2LoopTableDOWN[1][2][2] +
disCont2LoopTableSTR[1][2][2] + disCont2LoopTableBT[1][2][2])},
{q22, 2 * (uvFiniteCont2LoopTableME[1][3][2] +
uvFiniteCont2LoopTableML[1][3][2] +
uvFiniteCont2LoopTableMM[1][3][2] +
uvFiniteCont2LoopTableUP[1][3][2] +
uvFiniteCont2LoopTableCHARM[1][3][2] +
uvFiniteCont2LoopTableTOP[1][3][2] +
uvFiniteCont2LoopTableDOWN[1][3][2] +
uvFiniteCont2LoopTableSTR[1][3][2] +
uvFiniteCont2LoopTableBT[1][3][2] +
dispersionCont2LoopTableME[1][3][2] +
dispersionCont2LoopTableML[1][3][2] +
dispersionCont2LoopTableMM[1][3][2] +
disCont2LoopTableUP[1][3][2] + disCont2LoopTableCHARM[1][3][2] +
disCont2LoopTableTOP[1][3][2] + disCont2LoopTableDOWN[1][3][2] +
disCont2LoopTableSTR[1][3][2] + disCont2LoopTableBT[1][3][2])},
{q23, 2 * (uvFiniteCont2LoopTableME[1][4][2] +
uvFiniteCont2LoopTableML[1][4][2] +
uvFiniteCont2LoopTableMM[1][4][2] +
uvFiniteCont2LoopTableUP[1][4][2] +
uvFiniteCont2LoopTableCHARM[1][4][2] +
uvFiniteCont2LoopTableTOP[1][4][2] +
uvFiniteCont2LoopTableDOWN[1][4][2] +
uvFiniteCont2LoopTableSTR[1][4][2] +
uvFiniteCont2LoopTableBT[1][4][2] +
dispersionCont2LoopTableME[1][4][2] +
dispersionCont2LoopTableML[1][4][2] +
dispersionCont2LoopTableMM[1][4][2] +
disCont2LoopTableUP[1][4][2] + disCont2LoopTableCHARM[1][4][2] +
disCont2LoopTableTOP[1][4][2] + disCont2LoopTableDOWN[1][4][2] +
disCont2LoopTableSTR[1][4][2] + disCont2LoopTableBT[1][4][2])},
{q24, 2 * (uvFiniteCont2LoopTableME[1][5][2] +
uvFiniteCont2LoopTableML[1][5][2] +
uvFiniteCont2LoopTableMM[1][5][2] +

```

```

uvFiniteCont2LoopTableUP[[1]][[5]][[2]] +
uvFiniteCont2LoopTableCHARM[[1]][[5]][[2]] +
uvFiniteCont2LoopTableTOP[[1]][[5]][[2]] +
uvFiniteCont2LoopTableDOWN[[1]][[5]][[2]] +
uvFiniteCont2LoopTableSTR[[1]][[5]][[2]] +
uvFiniteCont2LoopTableBT[[1]][[5]][[2]] +
dispersionCont2LoopTableME[[1]][[5]][[2]] +
dispersionCont2LoopTableML[[1]][[5]][[2]] +
dispersionCont2LoopTableMM[[1]][[5]][[2]] +
disCont2LoopTableUP[[1]][[5]][[2]] + disCont2LoopTableCHARM[[1]][[5]][[2]] +
disCont2LoopTableTOP[[1]][[5]][[2]] + disCont2LoopTableDOWN[[1]][[5]][[2]] +
disCont2LoopTableSTR[[1]][[5]][[2]] + disCont2LoopTableBT[[1]][[5]][[2]]},
{q25, 2 * (uvFiniteCont2LoopTableME[[1]][[6]][[2]] +
uvFiniteCont2LoopTableML[[1]][[6]][[2]] +
uvFiniteCont2LoopTableMM[[1]][[6]][[2]] +
uvFiniteCont2LoopTableUP[[1]][[6]][[2]] +
uvFiniteCont2LoopTableCHARM[[1]][[6]][[2]] +
uvFiniteCont2LoopTableTOP[[1]][[6]][[2]] +
uvFiniteCont2LoopTableDOWN[[1]][[6]][[2]] +
uvFiniteCont2LoopTableSTR[[1]][[6]][[2]] +
uvFiniteCont2LoopTableBT[[1]][[6]][[2]] +
dispersionCont2LoopTableME[[1]][[6]][[2]] +
dispersionCont2LoopTableML[[1]][[6]][[2]] +
dispersionCont2LoopTableMM[[1]][[6]][[2]] +
disCont2LoopTableUP[[1]][[6]][[2]] + disCont2LoopTableCHARM[[1]][[6]][[2]] +
disCont2LoopTableTOP[[1]][[6]][[2]] + disCont2LoopTableDOWN[[1]][[6]][[2]] +
disCont2LoopTableSTR[[1]][[6]][[2]] + disCont2LoopTableBT[[1]][[6]][[2]]},
{q26, 2 * (uvFiniteCont2LoopTableME[[1]][[7]][[2]] +
uvFiniteCont2LoopTableML[[1]][[7]][[2]] +
uvFiniteCont2LoopTableMM[[1]][[7]][[2]] +
uvFiniteCont2LoopTableUP[[1]][[7]][[2]] +
uvFiniteCont2LoopTableCHARM[[1]][[7]][[2]] +
uvFiniteCont2LoopTableTOP[[1]][[7]][[2]] +
uvFiniteCont2LoopTableDOWN[[1]][[7]][[2]] +
uvFiniteCont2LoopTableSTR[[1]][[7]][[2]] +
uvFiniteCont2LoopTableBT[[1]][[7]][[2]] +
dispersionCont2LoopTableME[[1]][[7]][[2]] +
dispersionCont2LoopTableML[[1]][[7]][[2]] +
dispersionCont2LoopTableMM[[1]][[7]][[2]] +
disCont2LoopTableUP[[1]][[7]][[2]] + disCont2LoopTableCHARM[[1]][[7]][[2]] +
disCont2LoopTableTOP[[1]][[7]][[2]] +
disCont2LoopTableDOWN[[1]][[7]][[2]] + disCont2LoopTableSTR[[1]][[7]][[2]] +
disCont2LoopTableBT[[1]][[7]][[2]])}, Frame -> All]

```

k_1^2/GeV^2	Vacuum Polarization Two-loop Contribution (LEP+QUARKS)
0.001	-0.0000208103566552471
0.1	0.000273617646062098
10.	0.000370826106630867
1000	0.000632176251010665
100 000	0.000622025636270523
1 000 000	0.000748085647805046

$\text{In}[*]:= \text{triangleCorrection}[Q2_]:= \text{Re}\left[\frac{\text{triangleMetricREN}[Q2] \text{ /. } Q2ZV \rightarrow 10^{-10}}{Q2}\right];$

$\text{triangleTable} =$
 $\text{Grid}[\{\{"k_1^2/\text{GeV}^2", "Triangle Contribution"\}, \{q21, \text{triangleCorrection}[q21]\},$
 $\{q22, \text{triangleCorrection}[q22]\}, \{q23, \text{triangleCorrection}[q23]\},$
 $\{q24, \text{triangleCorrection}[q24]\}, \{q25, \text{triangleCorrection}[q25]\},$
 $\{q26, \text{triangleCorrection}[q26]\}\}, \text{Frame} \rightarrow \text{All}]$

k_1^2/GeV^2	Triangle Contribution
0.001	$-1.49032676451433 \times 10^{-7}$
0.1	$-2.36001274748313 \times 10^{-7}$
10.	$-4.098581514546 \times 10^{-7}$
1000	$-6.44010378813779 \times 10^{-7}$
100 000	$-8.85032585361598 \times 10^{-7}$
1 000 000	$-9.8731834532708 \times 10^{-7}$

$\text{In}[*]:= \text{twoLoopTable2} = \text{Grid}[\{\{"k_1^2/\text{GeV}^2",$
 $"Vacuum Polarization Two-loop Contribution (LEP+QUARKS+TRIANGLES)" \},$
 $\{q21, 2 * (\text{uvFiniteCont2LoopTableME}[[1]][[2]][[2]] +$
 $\text{uvFiniteCont2LoopTableML}[[1]][[2]][[2]] +$
 $\text{uvFiniteCont2LoopTableMM}[[1]][[2]][[2]] + \text{uvFiniteCont2LoopTableUP}[[1]][[$
 $2]][[2]] + \text{uvFiniteCont2LoopTableCHARM}[[1]][[2]][[2]] +$
 $\text{uvFiniteCont2LoopTableTOP}[[1]][[2]][[2]] + \text{uvFiniteCont2LoopTableDOWN}[[$
 $1]][[2]][[2]] + \text{uvFiniteCont2LoopTableSTR}[[1]][[2]][[2]] +$
 $\text{uvFiniteCont2LoopTableBT}[[1]][[2]][[2]] + \text{dispersionCont2LoopTableME}[[$
 $1]][[2]][[2]] + \text{dispersionCont2LoopTableML}[[1]][[2]][[2]] +$
 $\text{dispersionCont2LoopTableMM}[[1]][[2]][[2]] + \text{disCont2LoopTableUP}[[1]][[$
 $2]][[2]] + \text{disCont2LoopTableCHARM}[[1]][[2]][[2]] +$
 $\text{disCont2LoopTableTOP}[[1]][[2]][[2]] + \text{disCont2LoopTableDOWN}[[1]][[2]][[$
 $2]] + \text{disCont2LoopTableSTR}[[1]][[2]][[2]] +$
 $\text{disCont2LoopTableBT}[[1]][[2]][[2]] + \text{triangleTable}[[1]][[2]][[2]]\},$
 $\{q22, 2 * (\text{uvFiniteCont2LoopTableME}[[1]][[3]][[2]] +$
 $\text{uvFiniteCont2LoopTableML}[[1]][[3]][[2]] +$
 $\text{uvFiniteCont2LoopTableMM}[[1]][[3]][[2]] +$
 $\text{uvFiniteCont2LoopTableUP}[[1]][[3]][[2]] +$
 $\text{uvFiniteCont2LoopTableCHARM}[[1]][[3]][[2]] +$
 $\text{uvFiniteCont2LoopTableTOP}[[1]][[3]][[2]] +$
 $\text{uvFiniteCont2LoopTableDOWN}[[1]][[3]][[2]] +$
 $\text{uvFiniteCont2LoopTableSTR}[[1]][[3]][[2]] +$

```

uvFiniteCont2LoopTableBT[[1]][[3]][[2]] +
dispersionCont2LoopTableME[[1]][[3]][[2]] +
dispersionCont2LoopTableML[[1]][[3]][[2]] +
dispersionCont2LoopTableMM[[1]][[3]][[2]] +
disCont2LoopTableUP[[1]][[3]][[2]] + disCont2LoopTableCHARM[[1]][[3]][[
2]] + disCont2LoopTableTOP[[1]][[3]][[2]] +
disCont2LoopTableDOWN[[1]][[3]][[2]] + disCont2LoopTableSTR[[1]][[3]][[
2]] + disCont2LoopTableBT[[1]][[3]][[2]] + triangleTable[[1]][[3]][[2]]},
{q23, 2 * (uvFiniteCont2LoopTableME[[1]][[4]][[2]] +
uvFiniteCont2LoopTableML[[1]][[4]][[2]] +
uvFiniteCont2LoopTableMM[[1]][[4]][[2]] +
uvFiniteCont2LoopTableUP[[1]][[4]][[2]] +
uvFiniteCont2LoopTableCHARM[[1]][[4]][[2]] +
uvFiniteCont2LoopTableTOP[[1]][[4]][[2]] +
uvFiniteCont2LoopTableDOWN[[1]][[4]][[2]] +
uvFiniteCont2LoopTableSTR[[1]][[4]][[2]] +
uvFiniteCont2LoopTableBT[[1]][[4]][[2]] +
dispersionCont2LoopTableME[[1]][[4]][[2]] +
dispersionCont2LoopTableML[[1]][[4]][[2]] +
dispersionCont2LoopTableMM[[1]][[4]][[2]] +
disCont2LoopTableUP[[1]][[4]][[2]] + disCont2LoopTableCHARM[[1]][[4]][[
2]] + disCont2LoopTableTOP[[1]][[4]][[2]] +
disCont2LoopTableDOWN[[1]][[4]][[2]] + disCont2LoopTableSTR[[1]][[4]][[
2]] + disCont2LoopTableBT[[1]][[4]][[2]] + triangleTable[[1]][[4]][[2]]},
{q24, 2 * (uvFiniteCont2LoopTableME[[1]][[5]][[2]] +
uvFiniteCont2LoopTableML[[1]][[5]][[2]] +
uvFiniteCont2LoopTableMM[[1]][[5]][[2]] +
uvFiniteCont2LoopTableUP[[1]][[5]][[2]] +
uvFiniteCont2LoopTableCHARM[[1]][[5]][[2]] +
uvFiniteCont2LoopTableTOP[[1]][[5]][[2]] +
uvFiniteCont2LoopTableDOWN[[1]][[5]][[2]] +
uvFiniteCont2LoopTableSTR[[1]][[5]][[2]] +
uvFiniteCont2LoopTableBT[[1]][[5]][[2]] +
dispersionCont2LoopTableME[[1]][[5]][[2]] +
dispersionCont2LoopTableML[[1]][[5]][[2]] +
dispersionCont2LoopTableMM[[1]][[5]][[2]] +
disCont2LoopTableUP[[1]][[5]][[2]] + disCont2LoopTableCHARM[[1]][[5]][[
2]] + disCont2LoopTableTOP[[1]][[5]][[2]] +
disCont2LoopTableDOWN[[1]][[5]][[2]] + disCont2LoopTableSTR[[1]][[5]][[
2]] + disCont2LoopTableBT[[1]][[5]][[2]] + triangleTable[[1]][[5]][[2]]},
{q25, 2 * (uvFiniteCont2LoopTableME[[1]][[6]][[2]] +
uvFiniteCont2LoopTableML[[1]][[6]][[2]] +
uvFiniteCont2LoopTableMM[[1]][[6]][[2]] +
uvFiniteCont2LoopTableUP[[1]][[6]][[2]] +
uvFiniteCont2LoopTableCHARM[[1]][[6]][[2]] +

```

```

uvFiniteCont2LoopTableTOP[[1]][[6]][[2]] +
uvFiniteCont2LoopTableDOWN[[1]][[6]][[2]] +
uvFiniteCont2LoopTableSTR[[1]][[6]][[2]] +
uvFiniteCont2LoopTableBT[[1]][[6]][[2]] +
dispersionCont2LoopTableME[[1]][[6]][[2]] +
dispersionCont2LoopTableML[[1]][[6]][[2]] +
dispersionCont2LoopTableMM[[1]][[6]][[2]] +
disCont2LoopTableUP[[1]][[6]][[2]] + disCont2LoopTableCHARM[[1]][[6]][[
2]] + disCont2LoopTableTOP[[1]][[6]][[2]] +
disCont2LoopTableDOWN[[1]][[6]][[2]] + disCont2LoopTableSTR[[1]][[6]][[
2]] + disCont2LoopTableBT[[1]][[6]][[2]] + triangleTable[[1]][[6]][[2]]},
{q26, 2 * (uvFiniteCont2LoopTableME[[1]][[7]][[2]] +
uvFiniteCont2LoopTableML[[1]][[7]][[2]] +
uvFiniteCont2LoopTableMM[[1]][[7]][[2]] +
uvFiniteCont2LoopTableUP[[1]][[7]][[2]] +
uvFiniteCont2LoopTableCHARM[[1]][[7]][[2]] +
uvFiniteCont2LoopTableTOP[[1]][[7]][[2]] +
uvFiniteCont2LoopTableDOWN[[1]][[7]][[2]] +
uvFiniteCont2LoopTableSTR[[1]][[7]][[2]] +
uvFiniteCont2LoopTableBT[[1]][[7]][[2]] +
dispersionCont2LoopTableME[[1]][[7]][[2]] +
dispersionCont2LoopTableML[[1]][[7]][[2]] +
dispersionCont2LoopTableMM[[1]][[7]][[2]] +
disCont2LoopTableUP[[1]][[7]][[2]] +
disCont2LoopTableCHARM[[1]][[7]][[2]] + disCont2LoopTableTOP[[1]][[7]][[
2]] + disCont2LoopTableDOWN[[1]][[7]][[2]] +
disCont2LoopTableSTR[[1]][[7]][[2]] + disCont2LoopTableBT[[1]][[7]][[2]] +
triangleTable[[1]][[7]][[2]]}, Frame -> All]

```

k_T^2/GeV^2	Vacuum Polarization Two-loop Contribution (LEP+QUARKS+TRIANGLES)
0.001	-0.0000209593893316985
0.1	0.00027338164478735
10.	0.000370416248479413
1000	0.000631532240631851
100 000	0.000621140603685161
1 000 000	0.000747098329459719

Out[4]=

```

In[*]:= NNLOCorrectionTable =
  Grid[{"k12/GeV2", "Vacuum Polarization Contribution (NLO+NNLO)"},
    {q21, oneLoopTable[[1]][[2]][[2]] + twoLoopTable2[[1]][[2]][[2]]},
    {q22, oneLoopTable[[1]][[3]][[2]] + twoLoopTable2[[1]][[3]][[2]]},
    {q23, oneLoopTable[[1]][[4]][[2]] + twoLoopTable2[[1]][[4]][[2]]},
    {q24, oneLoopTable[[1]][[5]][[2]] + twoLoopTable2[[1]][[5]][[2]]},
    {q25, oneLoopTable[[1]][[6]][[2]] + twoLoopTable2[[1]][[6]][[2]]}, {q26,
      oneLoopTable[[1]][[7]][[2]] + twoLoopTable2[[1]][[7]][[2]]}], Frame -> All]

```

k_1^2/GeV^2	Vacuum Polarization Contribution (NLO+NNLO)
0.001	0.00500401660369998
0.1	0.00964054125350663
10.	0.0233176847559848
1000	0.0486537350794188
100000	0.0712248292496145
1000000	0.0861735467747872

```

In[*]:=

```

```

In[*]:= (*denCorrection is the addition of all the Vacuum Polarization function*)

```

```

In[*]:= denCorrection[Q2_] :=
  2 * (uvFiniteCont2Loop[Q2, ME, ME2] + dispersionCont2Loop[Q2, ME, ME2] +
    uvFiniteCont2Loop[Q2, ML, ML2] + dispersionCont2Loop[Q2, ML, ML2] +
    uvFiniteCont2Loop[Q2, MM, MM2] + dispersionCont2Loop[Q2, MM, MM2] +
    downTypeUVCont[Q2, MD, MD2] + downTypeDisCont[Q2, MD, MD2] +
    downTypeUVCont[Q2, MS, MS2] + downTypeDisCont[Q2, MS, MS2] +
    downTypeUVCont[Q2, MB, MB2] + downTypeDisCont[Q2, MB, MB2] +
    upTypeUVCont[Q2, MU, MU2] + upTypeDisCont[Q2, MU, MU2] +
    upTypeUVCont[Q2, MC, MC2] + upTypeDisCont[Q2, MC, MC2] +
    upTypeUVCont[Q2, MT, MT2] + upTypeDisCont[Q2, MT, MT2]) +
  NNLOCorrection[Q2] + triangleCorrection[Q2];

```



```

In[*]:= ComparisonTable = Grid[{{"k12/GeV2", " $\frac{\alpha_{\text{upto 2-loops}} - \alpha_{\text{upto 1-loops}}}{\alpha_{\text{tree level}}} * 100$ "},
  {q21,  $\left(\frac{1}{1 - \text{denCorrection}[q21]} - \frac{1}{1 - \text{NL0Correction}[q21]}\right) * 100$ },
  {q22,  $\left(\frac{1}{1 - \text{denCorrection}[q22]} - \frac{1}{1 - \text{NL0Correction}[q22]}\right) * 100$ },
  {q23,  $\left(\frac{1}{1 - \text{denCorrection}[q23]} - \frac{1}{1 - \text{NL0Correction}[q23]}\right) * 100$ },
  {q24,  $\left(\frac{1}{1 - \text{denCorrection}[q24]} - \frac{1}{1 - \text{NL0Correction}[q24]}\right) * 100$ },
  {q25,  $\left(\frac{1}{1 - \text{denCorrection}[q25]} - \frac{1}{1 - \text{NL0Correction}[q25]}\right) * 100$ },
  {q26,  $\left(\frac{1}{1 - \text{denCorrection}[q26]} - \frac{1}{1 - \text{NL0Correction}[q26]}\right) * 100$ }}, Frame -> All]

```

Out[*]=

k ₁ ² /GeV ²	$\frac{\alpha_{\text{upto 2-loops}} - \alpha_{\text{upto 1-loops}}}{\alpha_{\text{tree level}}} * 100$
0.001	-0.00211711826145766
0.1	0.0278653034695431
10.	0.0388167080995761
1000	0.069731673795892
100 000	0.0719578831070988
1 000 000	0.0893913305579863

```

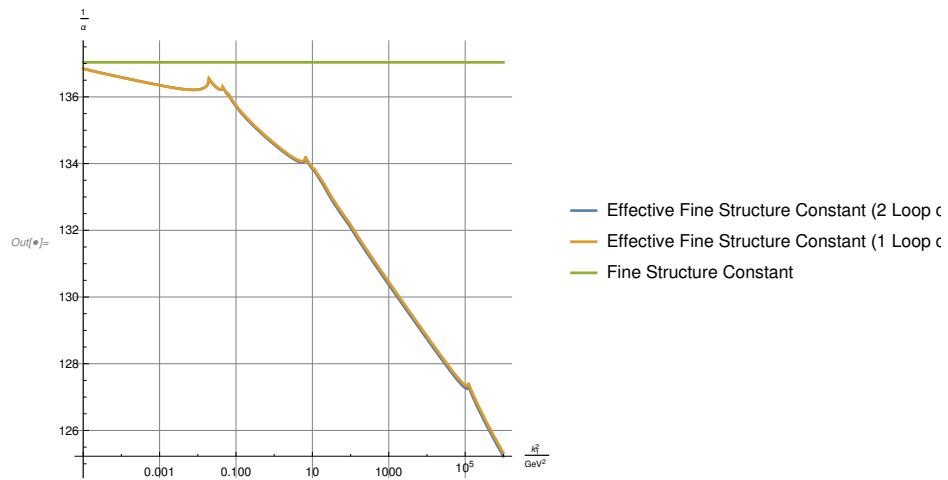
In[*]:= EffectiveAlfaTwoLoop := Alfa  $\left(\frac{1}{1 - \text{denCorrection}[Q2]}\right)$ ;

```

```

In[*]:= LogLinearPlot[{EffectiveAlfaTwoLoop^-1, (Alfa (1/(1 - NLOCorrection[Q2]))^-1, Alfa^-1},
  {Q2, 10^-5, 10^6}, AxesLabel -> {k1^2 / GeV^2, 1/alpha},
  (*PlotRange->{1/125, 1/145}, *)PlotRange -> All,
  PlotLegends -> {"Effective Fine Structure Constant (2 Loop correction)",
    "Effective Fine Structure Constant (1 Loop correction)",
    "Fine Structure Constant"},
  AspectRatio -> 1 / 1, GridLines -> Automatic, PlotStyle -> Thick]

```



Bibliography

- [1] A. Aleksejevs. Dispersion approach in two-loop calculations. *Phys. Rev. D*, 98:036021, Aug 2018.
- [2] A. G. Aleksejevs, S. G. Barkanova, Yu. M. Bystritskiy, E. A. Kuraev, and V. A. Zykunov. Two-loop electroweak vertex corrections for polarized Møller scattering. *Phys. Part. Nucl. Lett.*, 13(3):310–317, 2016.
- [3] Laurie M. Brown. The idea of the neutrino. *Phys. Today*, Volume 31, September 1978.
- [4] C. L. Cowan, Jr., F. Reines, F. B. Harrison, H. W. Kruse, and A. D. McGuire. Detection of the Free Neutrino: A Confirmation. *Science*, 124:103–104, July 1956.
- [5] Rohini Godbole. The heart of matter, June 2010.
- [6] David Griffiths. *Introduction to elementary particles*. Wiley-VCH, Weinheim Germany, 2008.
- [7] Thomas Hahn. Feynman Diagram Calculations with FeynArts, FormCalc, and LoopTools. *PoS*, ACAT2010:078, 2010.
- [8] Thomas Hahn. Feynman diagram calculations with feynarts, formcalc, and loop-tools. 2010.

- [9] Thomas Hahn. Feynman diagram calculations with feynarts, formcalc, and loop-tools. 2010.
- [10] Vakhtang Kartvelishvili. Particle physics discovery raises hope for a theory of everything, May 2015.
- [11] Dirk Kreimer. Unitarity, dispersion relations, cutkosky’s cutting rules, April 2012.
- [12] University of Oxford. Dark matter dark energy, January 2019.
- [13] G. Passarino and M. J. G. Veltman. One-loop corrections for e^+e^- annihilation into $\mu^+\mu^-$ in the Weinberg model. *Nucl. Phys.*, B160, 1979.
- [14] Hiren Patel. Package-x: A mathematica package for the analytic calculation of one-loop integrals. 2015.
- [15] Michael Peskin. *An introduction to quantum field theory*. Addison-Wesley, Reading, Mass, 1995.
- [16] Matthew Robinson. *Symmetry and the standard model mathematics and particle physics*. Springer, New York, 2011.
- [17] Matthew D. Schwartz. *Quantum Field Theory and the Standard Model*. Cambridge University Press, Cambridge, United Kingdom, 2014.
- [18] Gerard ’t Hooft and M. J. G. Veltman. Scalar One Loop Integrals. *Nucl. Phys.*, B153:365–401, 1979.